Title
Biochemical, functional, and structural characterization of human [gamma]-tubulin

Author
Aldaz, Hector

Publication Date
2005

Peer reviewed|Thesis/dissertation

Biochemical, Functional, and Structural Characterization of Human γ-Tubulin

by

Hector Aldaz

DISSERTATION

Submitted in partial satisfaction of the requirements for the degree of

DOCTOR OF PHILOSOPHY

in

Biophysics

in the

GRADUATE DIVISION

of the

UNIVERSITY OF CALIFORNIA, SAN FRANCISCO

Acknowledgements

A large part of the work presented here is the result of a very rewarding collaboration with Michelle Moritz and Luke Rice. I thank them both for their scientific insight and for their friendship. I also thank Steve Murphy and Tim Stearns for providing the γ-tubulin baculovirus and for early advice on how to purify the protein.

The Agard lab as a whole has been a great place to work. In particular, I'd like to acknowledge the support (both personal and scientific) of John Lyle, Stephanie Truhlar, Erin Cunningham, Matt Trammell, Seth Harris, and Andy Shiau.

Thanks to Julie Ransom, the administrator for the Graduate Group in Biophysics, for her support.

My thesis committee members were the ones who kept things rolling, always reminding me that there actually is an end to graduate school. I'd like to thank Ron Vale and Robert Fletterick, for encouragement and for helping me to keep focused. And I'd like to thank David Agard, my thesis committee chair and advisor, for his support and insight. I would also like to thank David for fostering such a great lab environment as well as for understanding the importance of life outside of lab.

Friends outside of lab were an amazing source of support, both moral and at times financial. In particular I'd like to thank Mike Temkin, Juliana Liu, Jon and Jane Kuo Paris, Bobby and Anita Gupta, and my classmate Erik Hom.

Family has always been central to me. Thanks to my parents and to my sister Patti for their love and encouragement. I was also fortunate enough to marry into a great

family (the Ignacios) who provided unconditional support as if I were their own son. Thanks also to my own little family. Thanks to my sons, Gaby, Mateo, and Emilio, for inspiration and for reminding me of the great things that exist outside of lab.

And finally, thanks to Gladys, my wife. Her boundless support and faith allowed me to complete this work while also keeping our family strong. I doubt I would have finished without her.

Biochemical, Functional, and Structural Characterization of Human γ-Tubulin

Hector Aldaz

Microtubules are hollow polymers of αβ-tubulin whose assembly in vivo is initiated at the centrosome through the action of γ-tubulin, in the form of the γ-Tubulin Ring Complex. Decades of research have yielded a near-atomic resolution understanding of αβ-tubulin, yet similar insight into γ-tubulin has been lacking because of its relative scarcity. In response, here is presented the purification and molecular characterization of recombinant human γ-tubulin. Biochemical characterization of γ-tubulin revealed that it is very similar to β-tubulin in nucleotide binding properties, but very different in oligomeric properties, capable of existing as monomers, tetramers, filaments, and possibly tubes. Functional characterization was carried out by first demonstrating that pure γ-tubulin can nucleate microtubule assembly. A kinetic analysis of the assembly data revealed that the mechanism by which γ-tubulin initiates microtubule assembly differs as a function of oligomeric state, with larger oligomers being more efficient nucleators than smaller ones. Finally, the x-ray crystal structure of human γ-tubulin bound to GTPγS was solved to 2.7Å resolution. The structure was observed to be in a 'curved' conformation, a state previously attributed exclusively to tubulin-GDP. One of the crystal contacts both used conserved residues and bore a striking resemblance to lateral contacts found in a microtubule, suggesting that it is a physiologically relevant interaction. Based on similarities between α-, β-, and γ-tubulin, these findings were extended to develop a new model for microtubule assembly in which nucleotide acts not by promoting a switch between conformers, but by modulating the strength of longitudinal interactions.

Table of Contents

List of Figures and Tables

Introduction

The microtubule cytoskeleton provides a framework for the trafficking of cargo during interphase and for spindle assembly during mitosis and meiosis in eukaryotic cells. This framework is composed of microtubules, dynamic, hollow polymers of αβ-tubulin heterodimers. Under appropriate conditions, microtubules can self-assemble in vitro. Microtubule assembly in vivo, however, generally requires γ-tubulin, a centrosomal component and another member of the tubulin superfamily. Decades of research have resulted in a near-atomic resolution model of αβ-tubulin function. In contrast, the relative scarcity of γ-tubulin has hindered progress toward a molecular understanding of this essential molecule.

αβ-Tubulin

αβ-Tubulin was first isolated through its affinity for colchicine, an anti-mitotic drug which was known to target spindles [1]. It was determined that this colchicine-binding protein was composed of 2 polypeptides with a total molecular weight of ~110 kDa, or ~55 kDa per polypeptide. The dimer was recovered with two moles of guanine triphosphate, though only one of the two binding sites was exchangeable. The discovery that αβ-tubulin could self-assemble above a certain critical concentration and in buffers containing calcium chelators and GTP marked the beginning of the molecular characterization of microtubule assembly[2]. Electron microscopy studies of negatively stained samples revealed that microtubules are approximately 25 nm in diameter and are composed of 10-15 parallel protofilaments arranged in a helical 3-start helix[3], in which αβ-tubulin are arranged in a head-to tail fashion to create each protofilament. Further

biochemical characterization of αβ-tubulin led to the insight that the polar nature of microtubules is reflected in the assembly dynamics, with one end (the plus end) growing faster than the other end (the minus end), and that GTP hydrolysis promotes depolymerization, rather than polymerization of microtubules[4].

Based on an analysis of microtubule length distributions in fixed samples, a mechanism for microtubule assembly, called dynamic instability, was proposed[5]. In this model, microtubules undergo stages of polymerization and depolymerization, never reaching a steady state. The conversion from polymerization to depolymerization was termed a "catastrophe" and the opposite was termed a "rescue". It has been proposed that such a phenomenon is an efficient way to search three-dimensional space, as required when a microtubule needs to attach to a kinetochore during spindle assembly[6]. The relative infrequency of catastrophes led to a proposal that a cap of GTP-tubulin that has not yet hydrolyzed stabilizes the plus end of a microtubule. Whether or not a GTP cap exists, localization studies did determine that the plus end is crowned by β-tubulin [7] and the minus end is crowned by α-tubulin [8].

Cryo-EM structural analyses of growing microtubules revealed a two-dimensional sheet at the plus end of microtubules that closes during growth [9]. During catastrophes, it was observed that protofilaments curl and peel off microtubules [10]. GDP-tubulin had also been known to form double ring structures [11]. These and other biochemical and structural studies [12-14], led to the model that tubulin exists in two conformational states: a curved, GDP state and a straight GTP state. In this model, straight GTP-tubulin assembles into microtubules and, once in the microtubule lattice, undergoes hydrolysis

into GDP-tubulin. GDP-tubulin prefers to be curved and hence introduces strain in the lattice. This strain is relieved only after depolymerization occurs (Figure 1).

High-resolution structural analysis of tubulin has been difficult because of the difficulty in preparing the samples for study. αβ-Tubulin tends to polymerize at higher concentrations and is very labile, making the growth of three-dimensional crystals suitable for x-ray diffraction so far unsuccessful. Further more, αβ-tubulin has yet to be produced recombinantly in a soluble form, making the search for a more appropriate construct through mutagenesis an unviable option. However, the discovery that αβ-tubulin assembles into two-dimensional sheets in the presence of zinc ions [15] made it possible to study tubulin structure with EM crystallographic methods[16].

After advances in sample preparation and cryo-EM methodology, 2D electron crystallography of taxol-stabilized, zinc-induced sheets led to a 3.7A resolution model of αβ-tubulin [17], which was followed by a 3.5Å refined structure[18](Figure 2). The heterodimer is constructed from two tubulin chains (α- and β-tubulin) related to one another by translational symmetry. The two are basically identical, though α-tubulin is bound to GTP and β-tubulin is bound to GDP and taxol. Each tubulin monomer forms a compact structure, and has been divided into an N-terminal domain, an intermediate domain, and a C-terminal domain. The N-terminal domain is the nucleotide binding domain and forms a Rossmann fold. It is comprised of six parallel β strands with alternating helices. The loops connecting each strand with the beginning of the following helix are directly involved in binding nucleotide. The intermediate domain is smaller and is formed by three helices and a mixed beta sheet, while the C-terminal domain is made up of two anti-parallel helices that cross over the other two domains. One of the

differences between the two structures is found in the taxol-binding pocket of β-tubulin. The analogous site in α-tubulin is occluded by an extra loop which makes contacts with the pocket very similar to those that taxol makes with β-tubulin.

The GTP bound to α-tubulin is buried at the monomer-monomer interface and the β-tubulin bound nucleotide is exposed. The zinc sheets themselves are arranged as anti-parallel protofilaments, thereby giving insight into longitudinal interactions within a microtubule. These interactions are very similar between interdimer and intradimer interfaces. Upon longitudinal assembly, about 3000Å^2 of surface area is buried between heterodimers, including the β-tubulin bound nucleotide. Hydrolysis is thought to be promoted by microtubule assembly through juxtaposition of a glutamic acid residue from α-tubulin with the nucleotide bound to β-tubulin, completing the β-tubulin GTPase active site. Indeed, mutation of this glutamic acid to an alanine in budding yeast resulted in a dominant lethal phenotype [18]. The structure of αβ-tubulin also bears a striking resemblance to that of FtsZ, a bacterial cell division protein which also hydrolyzes GTP but possesses little primary sequence homology[19]. Within the nucleotide binding pocket, both proteins are more similar to glyceraldehydes-3-phosphate dehydrogenase than to classical GTP binding proteins such as EF-Tu, suggesting that the tubulins constitute a distinct family of GTPases[20].

Three dimensional reconstructions of intact microtubules have been determined to sufficient resolution to allow the docking of the crystal structure of αβ-tubulin, yielding a model near atomic resolution model of the microtubule lattice [21, 22](Figure 3). Though resolution limits have hindered a detailed understanding of lateral interactions, some clues as to the nature of this interaction have been revealed. For example, it was found

that the so-called M-loop is flexible enough to mediate lateral interactions in both zinc sheets (anti-parallel protofilaments) and microtubules (parallel protofilaments). The M-loop is also a critical part of the taxol binding pocket, giving insight into the mode of action of this anti-mitotic compound.

High resolution insight into the structure of the curved form of αβ-tubulin has come from x-ray crystallography of αβ-tubulin bound to colchicine and the stathmin-like domain of RB3, a tubulin sequestering factor [23, 24](Figure 4). This 3.6Å structure was composed of two heterodimers (β-tubulin bound to GDP, α-tubulin bound to GTP) arranged head-to-tail and bound by a long α-helix which caps one end of the complex. Within the complex, tubulin was found to be kinked, both within and between each subunit. The curvature within each subunit has been attributed to changes within the intermediate domain, with the N-terminal and C-terminal domains behaving as rigid blocks. These changes result in secondary structural element movements, such as in helix 10, which disrupt protofilament-like longitudinal interactions, leading to a kinking at the tubulin-tubulin interface as well as within each tubulin subunit. Colchicine was observed to bind at this kinked interface, explaining how this drug might prevent microtubule assembly. Because β-tubulin was GDP-bound and the curvature of the complex is consistent with the curvature of GDP rings, this structure is thought to represent a curved form of tubulin induced by GDP. It was hypothesized that the binding of GDP by β-tubulin both creates the kink within β-tubulin and transmits this curvature to the adjacent α-tubulin.

Though the biochemical and structural details of microtubule assembly are numerous, several fundamental aspects of microtubule assembly remain poorly

understood. Resolution limits have hindered better understanding of microtubules, especially at the lateral interface. Also, if the stathmin-bound complex does represent the curved form of tubulin, how does GDP transmit the "curve" signal from β-tubulin to α-tubulin? Understanding these things is critical to a proper understanding of microtubule assembly dynamics.

γ-Tubulin

γ-Tubulin was first identified in Asperilligus nidulans, during a genetic screen for suppressors of a β-tubulin mutation[25]. Based on similarities in sequence identity between α-, β, and γ-tubulin (~ 35%), γ-tubulin is thought to have diverged from an ancestral tubulin around the time α- and β-tubulin diverged from each other, making γ-tubulin a distinct member of the tubulin superfamily. Subsequent studies on γ-tubulin in A. nidulans revealed that is an essential protein and that it localizes not with microtubules but with the spindle pole body [26]. The ubiquity of γ-tubulin was demonstrated when γ-tubulin was found in such diverse organisms as H. sapiens, D. melanogaster, X. laevis, and S. pombe[27, 28]. It has since been found in a much wider range of organisms, with all γ-tubulins possessing about 70% identity with one another. S. cerevisiae and C. elegans were found to possess the most divergent γ-tubulins, but even these were found to be essential spindle pole components[29]. Localization studies revealed that γ-tubulin localized to the pericentriolar material of the centrosome, an organelle already known to possess microtubule nucleating activity [30]. A more direct role for γ-tubulin in microtubule nucleation was demonstrated first in studies using X. laevis egg extracts [31]. Here, γ-tubulin was found in a large cytoplasmic complex which was recruited from

the cytoplasm during assembly of the centrosome and could bind microtubules. Overexpression of γ-tubulin in mammalian cells, meanwhile, resulted in ectopic nucleation of microtubules not associated with the centrosome[32].

A breakthrough in understanding the role of γ-tubulin in microtubule nucleation came with the purification of the γ-Tubulin Ring Complex, or γ-TuRC[33]. The 2.2 MDa protein complex was purified from X. laevis egg extracts by antibody affinity chromatography and was found to be composed of about 5-7 different polypeptides, including 12-14 copies of γ-tubulin. This complex could both nucleate microtubule assembly and cap the minus ends of microtubules in vitro. Electron microscopy of negatively stained samples showed that it is lock-washer shaped with a diameter of about 25nm, the same diameter as microtubules. EM tomographic studies of isolated Drosophila centrosomes showed that γ-tubulin is localized to 25nm ring structures in the pericentriolar material [34](Figure 5). The essential nature of the γ-TuRC to the microtubule nucleating activity of the centrosome was demonstrated through studies in which salt-stripped centrosomes had their microtubule nucleating activity reconstituted in a γ-TuRC-dependent fashion[35].

Further biochemical analysis of the γ-TuRC revealed that high salt concentrations could break it down into a well-defined heterotetramer and several additional higher molecular weight polypeptides[36]. The heterotetramer was composed of 2 copies of γ-tubulin and 1 copy of 2 additional factors (GCP2/3 in humans, Dgrips 84/91 in Drosophila) and termed the γ-Tubulin Small Complex (γ-TuSC). A study of the nucleotide binding properties of the γ-TuSC indicates that it has a higher affinity for GDP than GTP[36, 37], though precise affinities were not determined. This ~280 KDa

complex has also been characterized in S. cerevisiae as the Tub4 complex , where it is composed of 2 copies of Tub4p and 1 copy each of Spc97p and Spc98p[38, 39]. Relative to the γ-TuRC, both the γ-TuSC and Tub4 complex possess weak microtubule nucleating activity[36, 37, 39]. It is believed that assembly of this small complex into the γ-TuRC is part of the γ-TuRC assembly pathway, though no such larger complex has yet been characterized in S. cerevisiae.

The open ring structure of the γ-TuRC led to two structural models for the mechanism of microtubule nucleation: the template model and the protofilament model [40](Figure 6). In the template model, γ-tubulin interacts with itself laterally within the γ-TuRC and interacts with α-tubulin longitudinally, forming a cap at the minus end. In the protofilament model, the γ-TuRC unwinds and becomes the first protofilament of a growing microtubule, with γ-tubulin interacting longitudinally with itself and laterally with both α-tubulin and β-tubulin. EM tomographic reconstructions of individual γ-TuRC molecules have revealed a repeating V-shaped subunit within the wall of the complex and an asymmetric cap[41]. It is hypothesized that each V-shaped subunit is a γ-TuSC and that the cap is composed of the higher molecular weight components (Figure 7). Detailed examination of the γ-TuRC bound to the minus end of microtubules revealed that it forms a cap structure and that γ-tubulin does not extend very far into the microtubule[41-43]. Furthermore, the γ-TuRC was found to be able to prevent minus end growth of microtubules[44]. Together, these results strongly favor the template model of microtubule nucleation, in which the higher molecular weight components of the γ-TuRC serve a more structural or regulatory role.

Early studies found that γ-tubulin is present at less than 1% the level of either α- or β-tubulin[27]. The relative scarcity of γ-tubulin, therefore, has made it laborious to study biochemically. Like αβ-tubulin, recombinant methods have thus far failed to yield a reliable supply of γ-tubulin, though some studies have reported the production, semi-purification, and characterization of small amounts of γ-tubulin from in vitro reticulocyte lysate translation systems [45, 46]. One of these studies demonstrated that γ-tubulin can both nucleate and cap microtubules. A kinetic model for microtubule nucleation was presented (see below), as well as evidence for a direct γ-tubulin/β-tubulin interaction, though it is unclear how such an interaction is consistent with a minus end capping protein. Another study used a SPOT-peptide technique to identify domains on α-, β-, and γ-tubulin that interact with one another, leading to the conclusion that γ-tubulin interacts with αβ-tubulin a lateral fashion [47]. Sequence analysis, with the aid of a γ-tubulin homology model, indirectly suggested that a lateral interaction between αβ-tubulin and γ-tubulin by concluding that γ-tubulin can interact with itself longitudinally[48]. Characterization of the interactions between γ-tubulin and other molecules within the γ-TuRC have been carried out both genetically [49] and biochemically[50], though a thorough understanding awaits a high resolution structural analysis of the complex.

Recently, it has been discovered that γ-tubulin mediated microtubule nucleation from cis-Golgi membranes is required for Golgi ribbon formation[51]. In addition, genetic studies of γ-tubulin have begun to implicate it in activities beyond microtubule nucleation, such as chromosome segregation and cytokinesis [52-54]. Numerous reports have also localized γ-tubulin to places other than the centrosome ,such as the mitotic spindle[55], the mammalian midbody [56], the core of the centriole[57], and along

microtubule arrays in plant cells[58]. These findings suggest that the role γ-tubulin plays in the cell is complex and yet to be fully unveiled, though some of the localization studies may be suspect due to a lack of antibody specificity.

Mechanistic detail about the most well characterized γ-tubulin function, microtubule nucleation, remains lacking. Like αβ-tubulin, a thorough understanding of the molecular properties of γ-tubulin would likely lead to more structural and mechanistic understanding of this molecule. How is γ-tubulin arranged within the γ-TuRC? How does γ-tubulin interact with a microtubule? What role does GTP play in microtubule assembly? The previously described studies have yielded insight, as well as conflicting models, into some of these questions. Future studies would benefit from a reliable source of γ-tubulin with which to pursue a more quantitative understanding of its structure and function.

Kinetic Models of Microtubule Nucleation

The earliest structures along the microtubule assembly pathway that have been detected are sheets of protofilaments [59], though the intermediates leading up to these sheets have never been directly observed. Models for the early steps of microtubule nucleation have hence relied on the analysis of kinetic data, collected by following the increase in light scattering via absorbance at 350nm as a function of time. By understanding the parameters that govern microtubule assembly, experiments could be designed to reveal how γ-tubulin and γ-tubulin complexes act as nucleators.

The formation of a microtubule from αβ-tubulin heterodimers happens in two phases [60](Figure 8). In the first phase, a small oligomer of αβ-tubulin heterodimers

forms. This is the nucleus and it is defined as the first stable species along the microtubule assembly pathway. During the second phase of assembly, the microtubule rapidly grows from the nucleus in a process known as elongation. Microtubule assembly is limited by the thermodynamically unfavorable process of nucleus assembly, manifested as a lag time before elongation. Therefore, information on the size of the nucleus can be obtained from the kinetics of assembly.

In 1984, Voter and Erickson published a series of microtubule polymerization curves collected over a range of initial αβ-tubulin concentrations[61]. Microtubule assembly was carried out in a glycerol-containing buffer to prevent depolymerization, thereby ensuring that only polymerization was being observed. The kinetic data was then interpreted using a physical model derived from the study of actin assembly [62], which assumes the nucleus is formed in a single rate-limiting step. Because sheets of αβ-tubulin had been observed in the early stages of microtubule assembly [59], the model was modified to extend polymerization from a one dimensional process (as in actin assembly) to a two dimensional process. However, even this adjusted model failed to fit the data, demonstrating that microtubule assembly is a considerably more complex process than actin assembly.

In a re-examination of the original Voter and Erickson data, Flyvbjerg and colleagues were able to develop a new kinetic model for microtubule assembly by employing a more sophisticated approach with fewer assumptions[63]. The problem was approached as an "inverse problem", in which one tries to deduce a reaction mechanism for a non-equilibrium process from the analysis of an experimental time series.

In the first step in their analysis, the authors concluded that the assembly curves could be scaled together, an important property for subsequent analyses. To determine this, the authors first normalized the amplitude of each curve with respect to the plateau of each curve. Secondly, the time of each assembly curve was normalized with respect to the time it took the curve to reach 10% of its final value, known as the characteristic time. After these transformations, all the curves looked similar enough to allow them to be superimposed on top of one another. This implied that a single mechanism was at work over all the αβ-tubulin concentrations. This in turn meant that a single function could be used to describe the mechanism of assembly.

In order to determine this function, the curves were analyzed in order to extract 1) the number of rate-limiting steps and 2) the concentration dependence of the characteristic time. The number of rate limiting steps was deduced from the fact that early growth was proportional to the fourth power of time (t^4), which implied that there are four rate-limiting steps in the assembly mechanism. The characteristic time, meanwhile, was found to be proportional to the inverse cube of the initial αβ-tubulin concentration, implying that the rate-limiting intermediates are made up of multiples of three tubulin subunits. Together, these results pointed to a model of assembly in which the nucleus forms in four steps, with three αβ-tubulin heterodimers added at each step. A nucleus size of twelve αβ-tubulin heterodimers was then deduced, with subsequent microtubule elongation occurring by repeated monomer (single αβ-tubulin heterodimer) addition. These findings were then applied to a generic set of differential equations describing the nucleation/elongation process through an undefined number of

intermediates. Both scaling and the nucleus assembly parameters simplified the equations so that individual rate constants in the assembly pathway could be calculated.

The semi-purification of recombinant human γ-tubulin led to the first kinetic analysis microtubule assembly in the presence of a nucleator[46]. The effect monomeric γ-tubulin had on the kinetics of microtubule assembly was manifested in a decrease in the lag time required for the rapid elongation stage to begin. By applying principles originally developed for actin assembly [61, 62], the authors concluded that γ-tubulin promotes microtubule assembly by decreasing the nucleus size from seven to three tubulin subunits. However, Voter and Erikson had already demonstrated that the actin assembly model does not suffice to explain the complexities of microtubule assembly. Together with the fact that the γ-tubulin used in the study was only semi-purified, this over-simplified approach left the mechanism of microtubule assembly with or without a nucleator an open question. The application of the Flybjerg method to the analysis of microtubule assembly[63] in the presence and absence of a purified nucleator could be a powerful way to gain insight into the mode of action of γ-tubulin and γ-tubulin complexes.

Specific Aims

Mechanistic understanding of γ-tubulin function has been hindered because of the limited amounts of protein available for study and the lack of a good method for understanding the details of microtubule assembly. In order to begin to understand the molecular basis of γ-tubulin function, the following specific aims will be addressed:

1.) Expression, purification and biochemical characterization of recombinant γ-tubulin. γ-Tubulin is similar to αβ-tubulin both in sequence and in the fact that both exist as oligomers in vivo. An understanding of the oligomeric and nucleotide binding properties of γ-tubulin is therefore likely to provide important clues regarding its mode of action. Such knowledge should also be useful in the design and interpretation of future experiments.

2.) A kinetic analysis of microtubule assembly in the presence and absence of γ-tubulin. Kinetic data will be gathered through light scattering assays and analyzed in the manner of Flyvbjerg, et al, both in the presence and absence of γ-tubulin. The results should lead to an understanding of the impact of γ-tubulin on the parameters of microtubule assembly, such as the nucleus assembly pathway, the nucleus size, and individual rate constants.

3.) Structure determination of γ-tubulin by x-ray crystallography. The search for crystal growth conditions will be aided by previous molecular analyses of γ-tubulin. This structure will provide a basis for the generation of future mutants in the endeavor to better understand nucleotide binding and how γ-tubulin interacts with αβ-tubulin. A structure of γ-tubulin may also provide insight into the nature of γ-tubulin/γ-tubulin interactions, supporting certain models of γ-TuRC organization and microtubule nucleation.

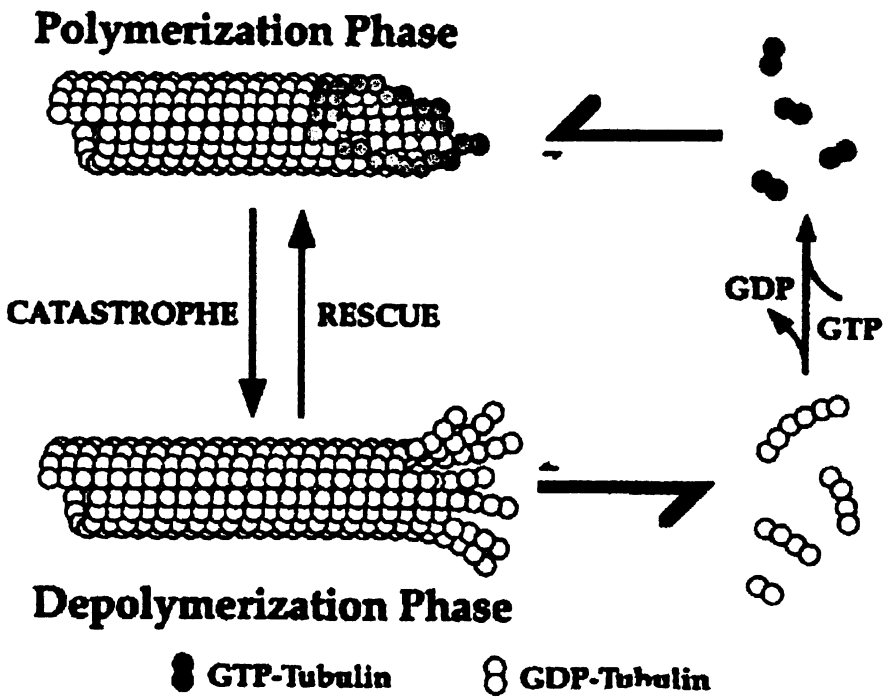

Figure 1. A model for microtubule assembly. GTP-tubulin assembles into microtubules, hydrolyzes GTP, and subsequently disassembles. In this model, tubulin toggles between two states: a straight, microtubule-compatible conformation in the presence of GTP and a curved, microtubule-incompatible conformation in the presence of GDP. Figure from [64].

Figure 2. The structure of αβ-tubulin solved to 3.5Å resolution. The top subunit is β-tubulin, the bottom is α-tubulin. β-Tubulin is bound to taxol (yellow sticks) and GDP (spacefilling). α-Tubulin is bound to GTP (spacefilling). Figure from [65]

A.

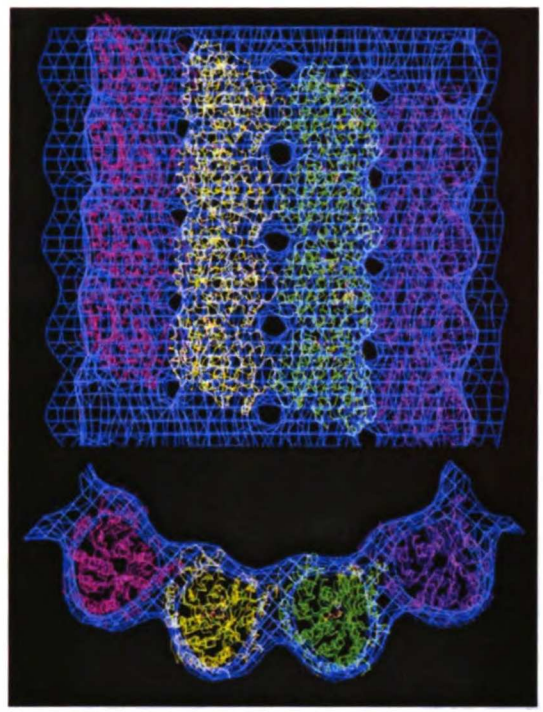

B.

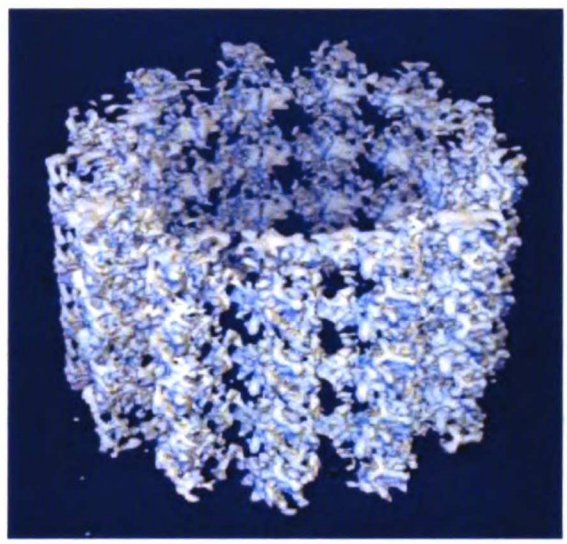

Figure 3. A.) The crystal structure of αβ-tubulin docked into a 20Å resolution reconstruction of a microtubule. Figure from [21]. B.) An 8Å resolution reconstruction of a microtubule. Figure from [22].

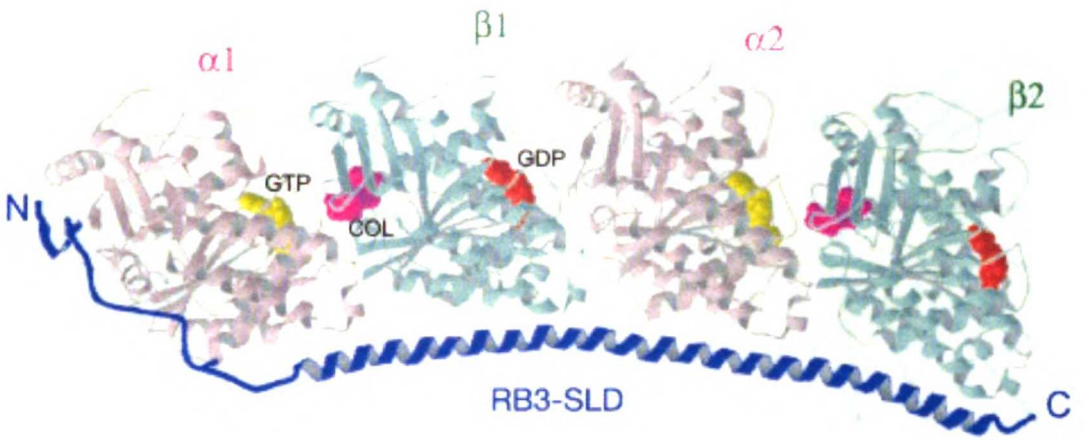

Figure 4. 3.6Å crystal structure of two αβ-tubulin heterodimers bound to colchicine and the stathmin-like domain of RB3, a tubulin sequestering factor. Figure from [24].

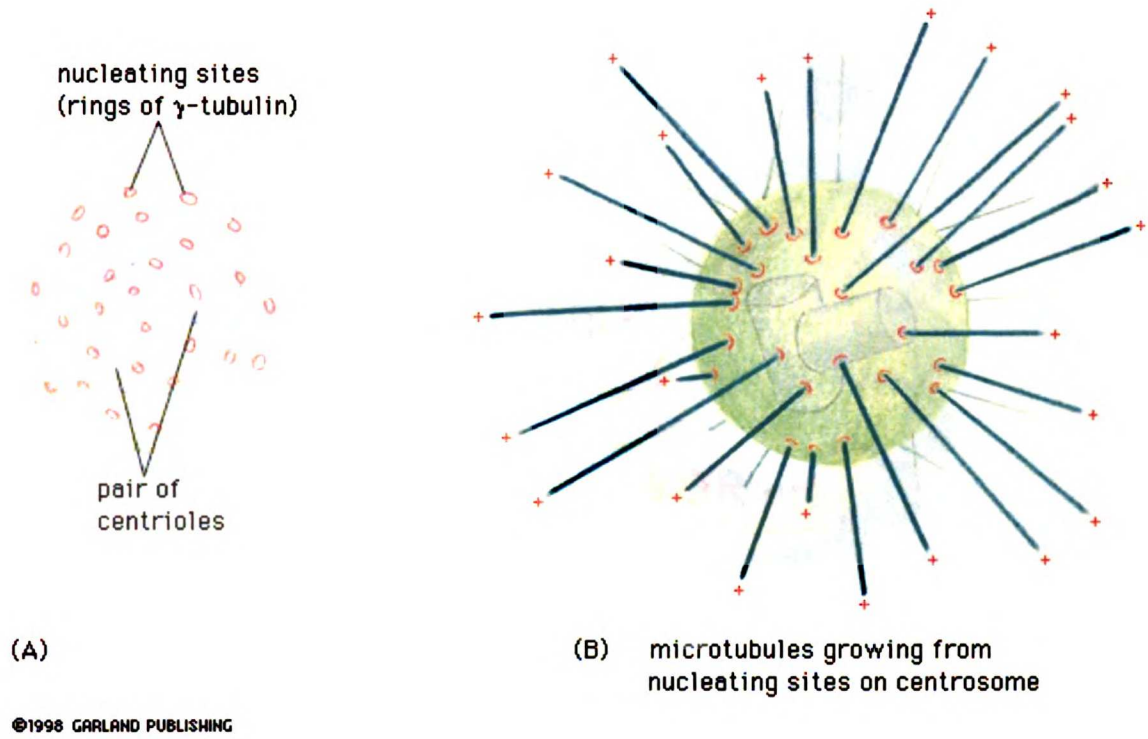

Figure 5. A.) The pericentriolar material of centrosomes is decorated with 25nm γ-tubulin rings. B.) These rings localize to the minus ends of microtubules grown from the centrosome.

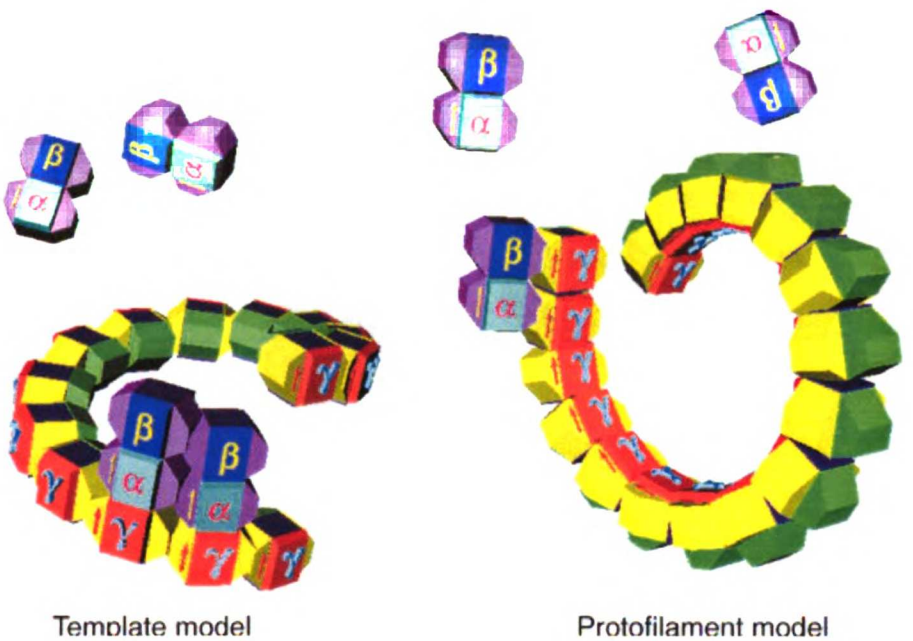

Figure 6. Two structural models for the mechanism of microtubule nucleation by the γ-Tubulin Ring Complex. The template model (left) predicts lateral interactions between γ-tubulins and longitudinal interactions between γ-tubulin and α-tubulin. The protofilament model predicts longitudinal interactions between γ-tubulins and lateral interactins between γ-tubulin and αβ-tubulin. Figure from [66].

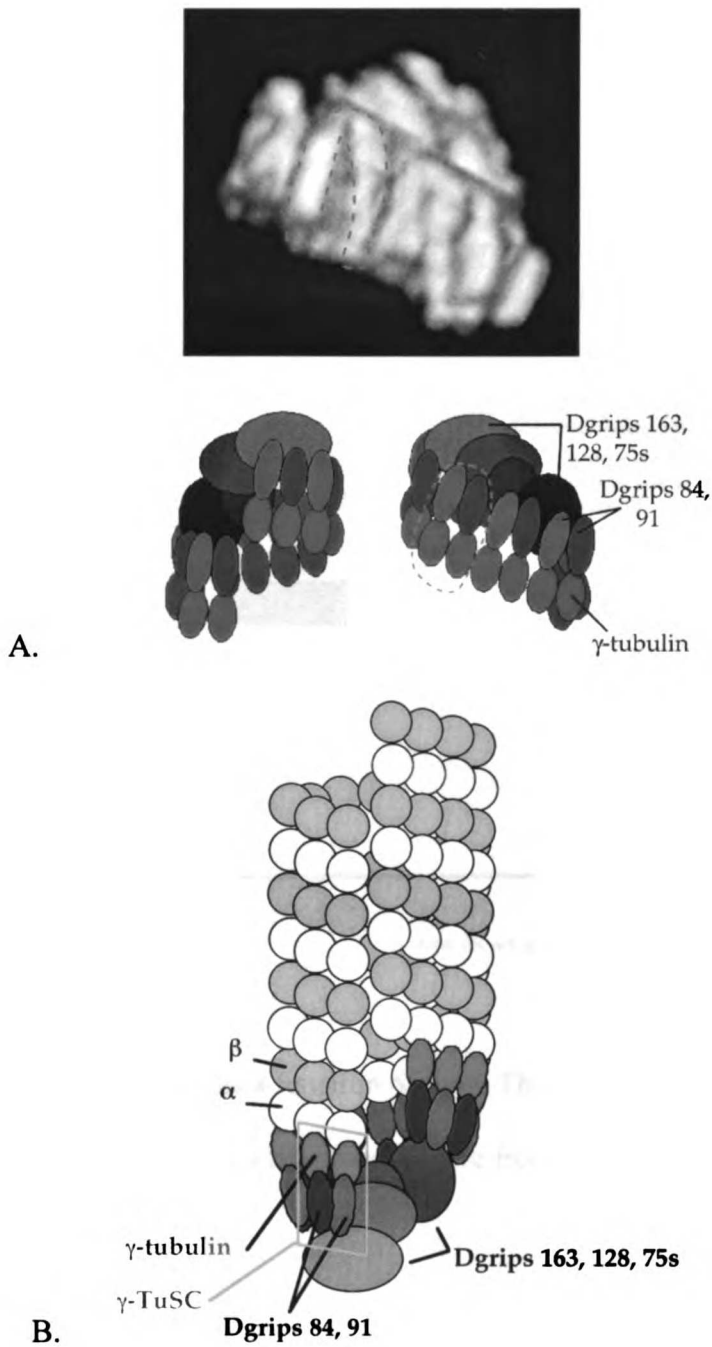

Figure 7. A.) Top: EM tomographic reconstruction of Drosophila γ-TuRC. Outlined in dotted blue is thought to be the γ-Tubulin Small Comples (γ-TuSC). Bottom: Model for protein organization within the γ-TuRC. B.) Model for how the γ-TuRC is thought to interact with a microtubule. Figure from [41].

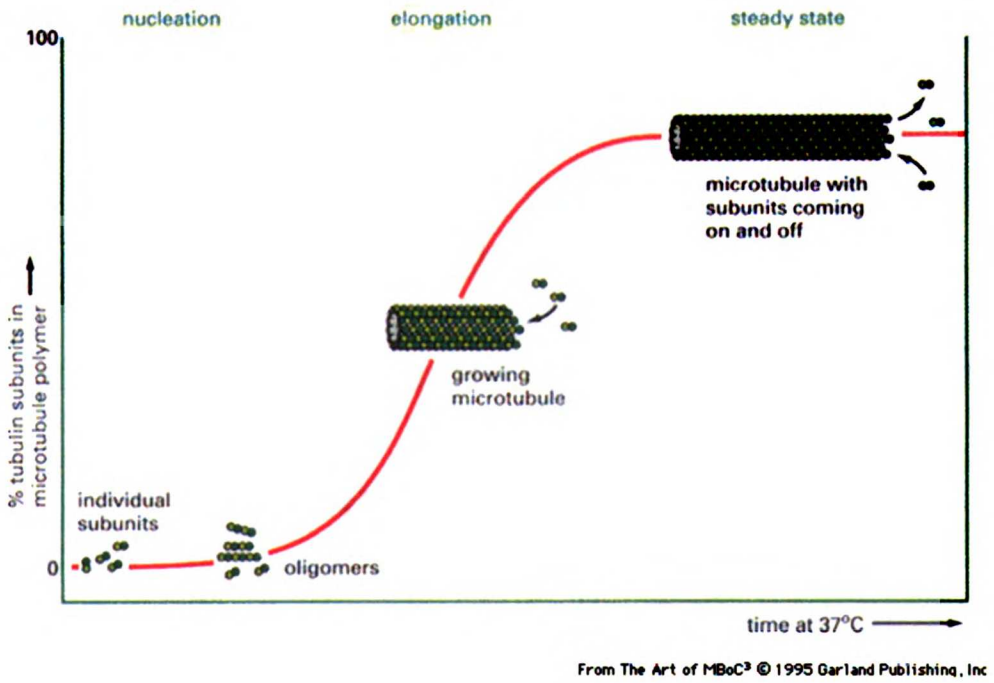

Figure 8. Microtubule assembly as a function of time. The unfavorable process of nucleus formation is manifested in a lag phase. Figure from [60]

Chapter 1:

Molecular Properties of Pure Recombinant Human γ-Tubulin

Synopsis

γ-Tubulin is the primary component of the γ-Tubulin Ring Complex, the protein complex responsible for microtubule nucleation at the centrosome. Here is reported the purification and characterization of recombinant human γ-tubulin, a significant step towards a more mechanistic understanding of γ-tubulin function. While monomeric γ-tubulin is the dominant species in high ionic strength buffers, sizing studies reveal that γ-tubulin assembles into tetramers and novel filamentous structures as a function of concentration and pH. Binding studies show that γ-tubulin possesses an exchangeable guanine nucleotide-binding site and displays a preference for GTP over GDP. Pure γ-tubulin is also shown to possess a microtubule nucleating activity that is coupled to its oligomeric state. Preliminary chemical crosslinking efforts, which may aid future attempts to map γ-tubulin/γ-tubulin and γ-tubulin/αβ-tubulin interactions, are also presented.

Introduction

Microtubules are hollow polymers of αβ-tubulin that are critical to proper cell function during both interphase and mitosis/meiosis. Microtubule assembly dynamics are regulated by an intrinsic GTPase activity as well as by a variety of microtubule regulating factors. In vivo, microtubule assembly is initiated primarily at the centrosome, through the action of another tubulin isoform, γ-tubulin, in the form of the γ-Tubuliun Ring Complex. Biochemical analysis of purified αβ-tubulin has illuminated many of the properties critical for understanding its structure and function[64, 65]. However, a mechanistic understanding of γ-tubulin function has been lacking, due primarily to the absence of a reliable supply of pure γ-tubulin in quantities sufficient for biochemical characterization.

To address this issue, we report the purification and biochemical characterization of recombinant human γ-tubulin, a first step toward a more complete structural and functional understanding of this essential molecule. Surprisingly, we find that γ-tubulin exists in a variety of oligomeric states, ranging from monomers to tetramers to filaments. The affinity of γ-tubulin for GTP suggests that the binding site is similar to β-tubulin. γ-Tubulin is also found to promote microtubule nucleation, establishing it as a simplified model system with which to understand γ-tubulin-mediated microtubule nucleation. Symmetry arguments and biochemical data together place constraints on possible models for γ-tubulin organization within the tetramer, suggesting a new mode of tubulin-tubulin interaction. Preliminary studies indicate that chemical crosslinking may be a viable approach with which to understand the nature of γ-tubulin/γ-tubulin interactions in higher

order γ-tubulin assemblies, though further work is required to identify a γ-tubulin/αβ-tubulin crosslink.

Results

Expression and purification of recombinant human γ-tubulin.

Recombinant human γ-tubulin, C-terminally labeled with a myc tag and a polyhistidine tail, was expressed in baculovirus infected sf9 cells and initially purified via Ni-NTA affintiy and ion (either anion or cation) exchange chromatography. Elution profiles and SDS-PAGE analysis of the purified product revealed a doublet, migrating on a gel as a polypeptide with a molecular weight approximately that of γ-tubulin (Figure 1A). The doublet could be resolved by gel filtration chromatography, in a buffer of high ionic strength (500 mM KCl), revealing one peak with an elution volume consistent with a monomer of approximately 54,000 Daltons and a second peak in the void volume (Figure 1B). The fraction of γ-tubulin in the void volume varied in different preparations. Biochemical characterization focused on the major monomeric γ-tubulin peak and subsequent purifications used only Ni-NTA affinity and gel filtration chromatography. SDS-PAGE and Coomassie staining of these fractions revealed a single band (Figure 1C), and this was confirmed by silver staining. A cell pellet derived from 1 liter of infected cells typically yielded 0.5-1 mg of monomeric γ-tubulin.

Pure γ-tubulin can exist as monomers, tetramers, and filaments.

Since there was some evidence of multimerization during the purification of γ-tubulin, the effects of pH, ionic strength, guanine nucleotide, and protein concentration

on the oligomerization of γ-tubulin were explored. These variables were investigated by two independent means: gel filtration chromatography and sucrose gradient velocity sedimentation, both with correlation to the migration of molecular weight standards. Early attempts at sizing via analytical ultracentrifugation failed due to the protein precipitating in the sample cell, most likely due to lack of enough care in sample handling. These experiments were only attempted in the early stage of γ-tubulin characterization, however, and warrant repeating with samples kept as cold as possible and always with GTP.

γ-Tubulin was found to exist as a monomer only at high ionic strength (pH6.6, and 0.5 M KCl) (Figures 1B, 2D). At relatively low protein concentrations (~67 nM), decreasing the ionic strength of the buffer to 100 mM KCl or lower caused the monomeric γ-tubulin to assemble into tetramers (Figures 2A, 2C). Tetramers can be returned to a primarily monomeric state by raising the ionic strength to 500 mM KCl. Additional experiments indicated that γ-tubulin remained tetrameric up to protein concentrations of at least 250nM (Figure 2E), with larger assemblies beginning to appear at protein concentrations around 500nM.

Sucrose gradient sizing experiments of γ-tubulin at pH 6.6 and low ionic strength, but at higher concentrations of γ-tubulin (~ 2 μM), revealed that most of the protein migrated to the bottom of the gradient (Figure 3A). This observation is in contrast with gel filtration results in which a similar concentration of protein was used (Figure 2A). The difference in behavior between the gel filtration experiments, which were completed in approximately 30 minutes, and the sucrose gradient experiments which required approximately 6 hours to complete, suggests that a time-dependent aggregation or

assembly process may have occurred. The nature of the pelleted γ-tubulin was investigated directly by negative-stain electron microscopy, both with and without added GTP. In both cases we observed novel filamentous structures (Figure 3B). Unlike microtubules, these γ-filaments did not require GTP or heating for their assembly. The smallest of these filaments were about 24 nm in diameter and appeared to be composed of two intertwined 12 nm-diameter fibers, whose width was defined by 2 subunits. From these measurements, a γ-tubulin diameter of ~6 nm can be deduced, in good agreement with the size expected from its sequence conservation with α and β tubulin. The filaments were observed both singly and in larger bundles.

Native PAGE analysis (0.1M Tris pH 8.8) (Pharmacia Phastgel) of pure γ-tubulin resulted in a ladder of higher molecular weight species (Figure 4A, lane 1), indicating that large oligomers had formed. This experiment also revealed for the first time that pure γ-tubulin and αβ-tubulin can interact with one another (Figure 4A, lanes 2, 3), indicating that the other components of the γ-TuRC are not required for this interaction.

To investigate the structural nature of the γ-tubulin oligomer from the native gel experiment, γ-tubulin (4 μM) was dialyzed against 0.1M Tris pH 8.8 for 1 hour at 4°C. Samples were then negative-stained and examined in the electron microscope, revealing a second form of filamentous γ-tubulin (Figure 4B). Unlike the filaments observed at pH 6.6, these had a wide range of diameters (20 to 40 nm) and enhanced density along the edges, suggesting that these structures may be tubes. Again differing from microtubules, these filaments had no apparent protofilament structure and did not require GTP, heat, or very high protein concentrations to form. Analysis of γ-tubulin on a gel filtration column as a function of pH revealed that γ-tubulin migrates as a larger species at higher pH

values (Figure 4C). These results indicate that γ-tubulin possesses assembly properties that are quite distinct from those of αβ-tubulin.

γ-Tubulin specifically binds to GTP and GDP.

One of the most conserved regions within the tubulin superfamily is the nucleotide-binding pocket. Recombinant, monomeric γ-tubulin was found to bind radiolabeled GTP in photocrosslinking experiments (Figure 5A). UV-crosslinking of radiolabeled GTP to γ-tubulin was inhibited by the presence of excess unlabeled GTP, GDP, or any of several nonhydrolyzable GTP analogs, but not by ATP or CTP (Figure 5A), indicating that γ-tubulin specifically binds only guanine nucleotides.

A photocrosslinking strategy was also used to quantify the binding of GTP to monomeric γ-tubulin, yielding a K_D of 3.9± 0.66 μM (Figure 5B). GDP binding strength was then assessed by its ability to compete with radiolabeled GTP in binding to monomeric γ-tubulin. The data are well fit by a competitive inhibition model, giving a K_I of 8.5±0.95 μM (Figure 5C). The affinity of guanine nucleotide for tetrameric γ-tubulin was also investigated. We used an identical photocrosslinking strategy, but had to work under conditions of low ionic strength (16 mM) and lower protein concentration (66 nM) in order to promote tetramer formation. The K_D for the interaction between tetrameric γ-tubulin and GTP was determined to be 58.4±12.6 nM (Figure 5D) while the affinity for GDP was 1.13±0.20 μM (Figure 5E). Thus, tetrameric γ-tubulin bound GTP nearly 70-fold more tightly and GDP approximately 8-fold more tightly than did monomeric γ-tubulin.

Pure γ-tubulin can nucleate microtubule assembly.

In order to determine the functional significance of the purified recombinant human γ-tubulin, its effect on microtubule assembly was monitored by light scattering. These experiments were performed by Michelle Moritz. Both in vitro and in vivo, rapid microtubule growth is preceded by a rate-limiting step in which a small oligomer of αβ-tubulin, known as the nucleus, must form. This assembly pathway is revealed by a clear lag phase in the kinetic curves of microtubule growth. Nucleators, by definition, promote nucleus formation and hence decrease this lag phase. Freshly cycled bovine brain αβ-tubulin was mixed with γ-tubulin or GF2 buffer. Microtubule assembly was monitored by following optical absorbance (turbidity) at 350 nm over time. Compared to the buffer control, γ-tubulin decreased the lag time in a dose-dependent manner (Figure 6A). At higher concentrations of γ-tubulin, microtubule nucleation was greatly enhanced. In order to investigate this phenomenon further, a value proportional to the rate of nucleation was calculated and plotted versus γ-tubulin concentration (Figure 6B; see figure legend). While lower concentrations of γ-tubulin (0.78-130 nM) exhibited hyperbolic saturation behavior analogous to simple Michaelis-Menten kinetics, a radical increase in nucleation activity was evident at higher γ-tubulin concentrations (260-520 nM) (Figure 6B). The sizing experiments presented previously had shown that γ-tubulin forms a tetramer at the lower concentrations tested and that the tetramer assembles into higher-order oligomers upon an increase in protein concentration (Figures 2, 3). Thus, the apparent divergence in kinetic mechanisms at high and low γ-tubulin concentrations may be attributable to the different types of γ-tubulin oligomers that predominate at different concentrations.

Chemical crosslinking as a method to understand γ-tubulin/αβ-tubulin interactions.

The demonstration that pure γ-tubulin can nucleate microtubule assembly indicates that it constitutes a simple model system with which to begin to understand the mechanism of the more complicated γ-TuRC. In particular, the architecture at the minus end of a γ-tubulin-nucleated microtubule is unknown. There is evidence for γ-tubulin interacting with α-tubulin [41-43], β-tubulin [25, 46], and both [47]. In order to begin to understand the architecture of the minus end, a chemical crosslinking strategy was employed to determine the identity of γ-tubulin binding partners. γ-Tubulin and αβ-tubulin were incubated together with 1-ethyl-3-(3-dimethylaminopropyl) carbodiimide (EDAC), a zero-length crosslinker which covalently links carboxyl groups to primary amines. The products were subsequently separated by SDS-PAGE and visualized by Western blotting in order to look for higher molecular weight species that are composed of either γ-tubulin/α-tubulin or γ-tubulin/β-tubulin, indicating a direct interaction.

Preliminary EDAC experiments showed evidence of γ-tubulin/α-tubulin interaction (Figure 7A), in the form of a ~150 kDa crosslinked species that could labelled with antibodies specific for γ-tubulin and α-tubulin, but not β-tubulin. 100 kDa species were also detected that could be labeled by all three antibodies, reflecting the complications of a crosslinking experiment such as this one where the proteins being probed tend to oligomerize and are of approximately the same size. The presence of GTP in the reaction (Figure 7A, lanes 2, 4) resulted in reduced intensity for the higher order complexes, most likely reflecting a partial quenching of the crosslinker.

Initial attempts to repeat the experiment with more controls, however, were unsuccessful, resulting in either too many or too few crosslinked species. Furthermore, the antibody used against β-tubulin was from a poorly labeled, depleted stock. In order to optimize the reaction, temperature and crosslinker concentrations were varied for samples containing γ-tubulin, αβ-tubulin, or both (Figures 7B-D). DM1β was used to probe for β-tubulin. It was found that crosslinking proceded more efficiently at room temperature than on ice. Also, conditions were identified in which γ-tubulin made higher order complexes only in the presence of αβ-tubulin. (Figure 7B, lanes 3A-C). However, analysis of α-tubulin migration yielded no clear new species in the same lane (Figure 7C, lane 3C). Furthermore, it was discovered that DM1β crossreacts with γ-tubulin (Figure 7D), making analysis of β-tubulin migration with this antibody impossible.

Ni-NTA resin was used as a means to enrich the reactions, post-crosslinking, for γ-tubulin and γ-tubulin associated proteins. A range of temperatures and crosslinker concentrations was used as before. However, western blotting with DM1α revealed α-tubulin did not crosslink to form higher order species, yet was still present in the samples even after washing (Figure 7E). Future experiments should include +/- crosslinker controls and explore different washing conditions.

As a solution to the problem of background αβ-tubulin crosslinks, γ-tubulin was conjugated to a tetraflouroaryl azide, a photoactivateable crosslinker. Subsequent UV irradiation in the presence of αβ-tubulin should result in crosslinking events only directly connected to γ-tubulin. Experiments utilizing this crosslinker revealed robust γ-tubulin/γ-tubulin crosslinks, but did not result in any shifts in αβ-tubulin (Figure 8A). The experiment was repeated using protein concentrations closer to those used during

microtubule nucleation reactions. Because of the resulting low concentration of γ-tubulin,, a TCA precipitation step was added to enrich the γ-tubulin signal. Resulting gels showed α-tubulin crosslinks even in the absence of γ-tubulin-conjugated photocrosslinker (Figure 8B). This phenomenon was seen with and without GTP, UV irradiation, and excess DTT. This may be the result of simply overloading the gel with αβ-tubulin.

Discussion

While biochemical analyses of pure αβ-tubulin have led to a detailed molecular understanding of αβ-tubulin structure and function, similar studies with γ-tubulin have been difficult due to limited protein availability. Here it is shown that useful quantities of active recombinant human γ-tubulin can be purified from baculovirus infected cells, allowing for the first time, a detailed characterization of its biochemical and functional properties.

Initial purifications using ion exchange chromatography revealed a variable population of γ-tubulin which consistently eluted as a large oligomer even in buffers of high ionic strength. This form of γ-tubulin ran as a slightly retarded species compared to the monomeric fraction, and may be the result of a post-translational modification. Though it is possible that such a modification simply resulted in non-specific aggregation of the protein, the role of post-translational modifications in γ-tubulin function is poorly understood and will require more in vivo analysis to fully understand.

Despite what sequence analysis suggests[48], the various oligomeric states observed in this study indicate that γ-tubulin is capable of associating with itself in a

manner quite unlike αβ-tubulin, forming both discrete tetramers as well as filaments and possibly tubes. The ability of γ-tubulin to form tubes is supported by a previous study of γ-tubulin overexpression in vivo[32]. γ-Tubulin tetramers and higher order oligomers both exhibit microtubule-nucleating activity, with the latter being the more potent nucleator. Therefore, γ-tubulin's innate oligomeric properties may be relevant for the assembly of higher order γ-tubulin complexes such as the Tub4 complex, the γ-TuSC, and the γ-TuRC.

The dependence of γ-tubulin-mediated microtubule nucleation on the tetramerization of γ-tubulin remains to be determined. The generation of mutants which stay monomeric under microtubule assembly conditions will be required to investigate this. Based on analysis of the crystal structure of γ-tubulin (Chapter 4), a possible region to target for mutagenesis is the minus end of the protein. This region contains residues which are highly conserved only in γ-tubulin, not α- or β-tubulin. This suggests that it makes unique contacts, possibly to the other components of the γ-TuRC. In the absence of these other components, to which it is always is bound in vivo, the minus end of γ-tubulin may be capable of non-specific binding.

If tetramerization is found to be necessary for the nucleating activity of γ-tubulin, then the organization of the γ-TuRC may be related to the organization of the tetramer. This organization may be deduced from three observations: 1.) Homotetramers must possess either a single 4-fold symmetry axis (C_4 symmetry) (Figure 9A) or three orthogonal 2-fold axes (D_2 symmetry)(Figure 9B). 2.) GTP binding by tetrameric γ-tubulin is readily exchangeable with an affinity similar to that observed for β-tubulin[67] (Chapter 4), in which the binding site is fully exposed. 3.) γ-tubulin is found as a dimer in

certain complexes, such as the γ-TuSC and the Tub4 complex from yeast[36, 38, 68]Together, these observations would indicate that the tetramer is most likely composed of a dimer of dimers in which the nucleotide binding sites are exposed (Figure 9B). Furthermore, γ-tubulins in these complexes would not be parallel, as previously assumed, but related to one another by a two-fold axis This would in turn suggest a model for functionally relevant γ-tubulin complexes quite unlike that for microtubules (see Introduction).

However, if mutational studies reveal that monomeric γ-tubulin can nucleate microtubule assembly as well as (or better than) tetrameric γ-tubulin, then tetramerization may be an artifact stemming from the absence of the other γ-TuSC/γ-TuRC components. In this case, the increase in γ-tubulin nucleating activity associated with the formation of higher order oligomers would be the sole instance of γ-tubulin assembling in a functionally relevant manner in this study. High resolution structural studies will be required to definitively understand how γ-tubulin is organized in complexes such as the γ-TuSC or the Tub4 complex, though crystallographic analysis of monomeric γ-tubulin strongly indicates a microtubule-like mode of self-assembly which uses lateral interactions (Chapter 4), a type of interaction not easily reconciled with possible architectures for a homo-tetramer (Figure 9)

While it is clear that γ-tubulin exhibits assembly and functional properties that are quite distinct from those of αβ-tubulin[64], the ability to selectively bind guanine nucleotides is conserved. A comparison of guanine nucleotide binding affinities between γ-tubulin and β-tubulin reveals that they possess nearly identical affinities for both GTP and GDP (Chapter 4). In both cases, GTP was bound approximately 20-fold tighter than

GDP. Given the critical role of GTP binding and hydrolysis in αβ-tubulin function[64], it will be interesting to explore the potential regulatory role of GTP binding and hydrolysis by γ-tubulin during γ-TuRC assembly and microtubule nucleation (see Chapter 2)

Curiously, monomeric γ-tubulin only has a 2-fold preference for GTP over GDP. However, because 1.) monomeric γ-tubulin is present only in high salt buffers of and 2.) extensive biochemical analysis of αβ-tubulin has not revealed salt to be a factor in conformational switching, this difference more likely reflects a strong ionic component to γ-phosphate binding than the existence of oligomerization-dependent conformational changes.

It has been reported that the Drosophila γ-TuSC has a preference for GDP over GTP [36], although Oegema, et. al were unable to determine binding constants. This needs to be explored more fully by a direct and quantitative comparison of the nucleotide binding affinities of purified γ-tubulin, γ-TuSC, and γ-TuRC. Another recent study reported that baculovirus-produced Drosophila γ-tubulin can be photocrosslinked to GTP only when certain γ-TuRC components are co-expressed, suggesting that these components play a role in regulating the GTP binding properties of γ-tubulin[50]. However, we have shown that human γ-tubulin specifically binds GTP with nanomolar affinity and nucleates microtubules, indicating that pure γ-tubulin can exist in a functional state in the absence of other γ-TuRC components. This discrepancy is most likely due to variations in the biochemical stability of γ-tubulin from different species. While the ability of γ-tubulin to nucleate microtubules on its own does suggest that the other components of the γ-TuRC serve a predominantly regulatory and/or structural role in

microtubule nucleation, the precise function they serve awaits a more detailed biochemical analysis.

Previous studies have reported the production and partial purification of small quantities of recombinant human γ-tubulin [45, 46, 69]. Vassilev, et. al similarly concluded that γ-tubulin is monomeric in the presence of 0.5M NaCl. However, the other reports concluded that human γ-tubulin is also monomeric under conditions of much lower ionic strength. It is evident from the present study that γ-tubulin oligomerization is extremely sensitive to changes in pH, ionic strength, and concentration. The discrepancy could be due to the very low concentrations of protein produced in the earlier studies or perhaps to their use of a gel filtration column having much lower resolution in the 50KDa-200KDa range than does the Superdex 200 column used here.

Chemical crosslinking holds promise as a means to identify γ-tubulin binding partners. Initial experiments with the zero-length crosslinker EDAC revealed 150kDa species that is reactive to α-tubulin and γ-tubulin, but not β-tubulin, antibodies. Subsequent experiments have refined the reaction conditions to improve reproducibility, though these conditions need further refinement. In particular, the identification of a β-tubulin antibody that does not cross react with γ-tubulin will be required. The use of a γ-tubulin-conjugated photocrosslinker yielded robust γ-tubulin/γ-tubulin crosslinks, but has yet to reveal a γ-tubulin /αβ-tubulin interaction. It is possible that the presence of the relatively bulky tetrafluoroaryl azide group disrupts the binding surface of γ-tubulin. Future experiments with this crosslinker should also include a denaturing pulldown step to rid the resulting western blots of background signal (Figure 8B).

Though the characterization of γ-tubulin/αβ-tubulin interactions through crosslinking methods requires more work, γ-tubulin/γ-tubulin interactions appear to be easily identified with either chemical crosslinking or photocrosslinking methods. Partially proteolyzed crosslinked species can be subjected to peptide identification by mass spectrometry in order to map protein-protein interaction surfaces. This method may aid in illuminating the organization of γ-tubulin tetramers and filaments.

It is clear from these studies that γ-tubulin is a unique member of the tubulin superfamily and that assumptions about its behavior based on sequence similarity with αβ-tubulin should be viewed critically. The purification and characterization of recombinant γ-tubulin will allow a more detailed biochemical understanding of this molecule and has already allowed us to begin to determine the detailed kinetic mechanism of γ-tubulin-mediated microtubule nucleation (Chapter 3). Understanding the molecular properties of γ-tubulin also represents a first step toward high-resolution structural analysis of this protein (Chapter 4). Such studies will be a critical element in an atomic- resolution understanding of microtubule nucleation by the centrosome.

Materials and Methods

Buffers

Lysis buffer: 50 mM KPO_4 pH 8.0, 150 mM KCl, 1 mM $MgCl_2$, 0.25 μM GTP, 5 mM βME, Complete EDTA-free Protease Inhibitor Cocktail Tablet (1 tablet/50 ml) (Roche); *Wash buffer 1*: 50 mM KPO_4 pH 8.0, 250 mM KCl, 1 mM $MgCl_2$, 10% glycerol, 25 mM imidazole, 0.25 μM GTP, 5 mM βME; *Wash buffer 2*: 50 mM K-MES pH 6.6, 500 mM KCl, 5mM $MgSO_4$, 10% glycerol, 25 mM imidazole, 0.25 μM GTP, 5

mM βME; *Elution buffer*: 50 mM K-MES pH 6.6, 500 mM KCl, 5 mM $MgSO_4$, 10% glycerol, 250 mM imidazole, 1 μM GTP, 5 mM βME; *GF buffer*: 50 mM K-MES pH 6.6, 500 mM KCl, 5mM $MgSO_4$, 1 mM K-EGTA, 1 μM GTP, 1 mM DTT, 10% glycerol; *GF2 buffer*: 50 mM K-MES pH 6.6, 500 mM KCl, 5 mM $MgSO_4$, 1 mM K-EGTA, 1 μM GTP, 1 mM DTT; *Assembly buffer*: 50 mM K-MES pH 6.6, 5 mM $MgSO_4$, 1 mM K-EGTA; *BRB80*: 80 mM K-PIPES pH 6.8, 5 mM $MgCl_2$, 1 mM K-EGTA

Expression and purification

A human γ-tubulin construct with a C-terminal myc-His_6 tag was used for the production of recombinant baculovirus as described[68]. Sf9 cells at a density $2x10^6$ cells/ml were infected with the γ-tubulin baculovirus at an MOI ~3, or in some cases optimized through small-scale infections. Cell pellets were harvested 48 hrs. post-infection, flash-frozen in liquid nitrogen, and stored at –80°C. Infections were done both in-house and at the National Cell Culture Center (Minneapolis, MN).

A cell pellet derived from 1 liter of cells was lysed on ice by manual dounce homogenization in 9 volumes of lysis buffer and centrifuged for 10 minutes at 12,000 RPM in an SS34 rotor at 4°C. Glycerol, imidazole, and KCl were added directly to the supernatant to final concentrations of 10%, 5 mM, and 500 mM, respectively. The lysate was centrifuged for 30 minutes at 35,000 RPM in a Type 45 rotor at 4°C. The resulting clarified lysate was removed and histidine-tagged protein was allowed to bind in batch to 0.5 ml Ni-NTA Superflow resin (Qiagen) for 1 hour. Beads were washed with 10 volumes wash buffer 1, 10 volumes wash buffer 2, and protein was eluted with elution buffer. Initial purifications using ion exchange chromatography used an elution buffer

having only 100mM KCl. Later purifications using gel filtration used an elution buffer with 500 mM KCl. In the latter cases, peak fractions containing recombinant γ-tubulin were pooled and loaded onto a HiLoad 16/60 Superdex 200 gel filtration column (Amersham Biosciences) pre-equilibrated with GF buffer (for freezing γ-tubulin) or GF2 buffer (for using γ-tubulin immediately). Peak fractions were identified by A_{280} and gel analysis. Protein concentrations were assessed by Bradford assays. When necessary, protein was further concentrated in Ultrafree Biomax microconcentrators (Millipore).

Analytical gel filtration

A Superdex PC 3.2/30 column (Amersham Biosciences) was used on a SMART System (Pharmacia) for analytical sizing of γ-tubulin under different buffer conditions. The column was equilibrated with the desired buffer and 50 µl protein (~2 µM) was injected, allowing buffer exchange within the column at a flow rate of 50 µl/minute. Elution times were monitored by A_{280} and standardized with Gel Filtration Standards (BioRad).

Sucrose gradients

2-16% sucrose gradients were poured in 5 x 900 µl steps (2%, 5.5%, 9%, 12.5%, 16% sucrose in desired buffer) using blunt end pipet tips. The gradients were allowed to diffuse ~17 hours before use.

γ-Tubulin was dialyzed for 2 hours against the desired buffer using Slide-A-Lyzer Mini Dialysis Units (Pierce) at 4°C. 100 µl protein solution (~2 µM) was then carefully layered on top of the sucrose gradients. The gradients were centrifuged for 4 hours at

50,000 rpm in an SW55 rotor at 4°C and manually collected from the top as 150 µl fractions using blunt end tips. The refractive index of each fraction was checked to ensure proper gradient formation and fractionation consistency.

Each 150 µl fraction was TCA precipitated by adding 5 µl 1 mg/ml BSA as carrier protein, 15 µl cold 100% TCA, incubating for 30 minutes on ice, centrifuging for 20 minutes at 4°C at 14,000 rpm in a tabletop microcentrifuge, and decanting the supernatant. 10 µl 2X SDS sample buffer was added and neutralized with NH_4OH vapor. Samples were boiled, separated on 12% SDS-PAGE, transferred onto nitrocellulose, and probed with a monoclonal anti-his_5 antibody (Qiagen) using the prescribed protocol (Qiagen). Gel Filtration Standards (BioRad) were used to determine a standard curve. Westerns were digitized and bands were quantified with ImageQuant software (Molecular Dynamics)

Electron microscopy

Carbon-coated grids were glow discharged for 30 seconds prior to use. 3 µl of dialyzed protein solution was added to each grid, allowed to sit for 60 seconds, and washed on a 1 ml drop of ddH_20. A drop of filtered 1% uranyl acetate in 50% methanol was added to the grid and allowed to sit for 30 seconds. Excess stain was wicked off with filter paper, and grids were allowed to dry at room temperature. Images were obtained on a Tecnai20 transmission electron microscope (FEI) with the use of either a 1024x1024 pixel CCD camera or a 4096x4096 pixel CCD camera (Gatan).

GTP/GDP binding experiments

To examine nucleotide binding specificity, 2 μl [α-^{32}P]GTP (400 Ci/mmol; 10mCi/ml) was mixed with 2 μl of 5 mM cold competitor nucleotide. 2 μl of the [α-^{32}P]GTP /cold competitor mix was added to 15 μl monomeric γ-tubulin (~2 μM), mixed, and incubated for 1 hour on ice. Bound nucleotide was crosslinked to γ-tubulin by pipeting the samples directly onto a Saranwrap-covered UV lamp (312nm handheld UV lamp fitted with an 8W bulb, Fisher Scientific) and illuminating for 30 seconds. Protein was separated from unbound nucleotide by 12% SDS-PAGE and ^{32}P labeling was visualized using a Phosphorimager (Storm 840, Molecular Dynamics).

Quantification of GTP binding to γ-tubulin was performed as follows: Dilution series of radiolabeled GTP ranging in concentration from 1.6 μM to 1280 μM (for the monomeric γ-tubulin experiments) and 16 nM to 4.8 μM (for the tetrameric γ-tubulin experiments) were constructed by doping unlabeled GTP with [α-^{32}P] GTP (400 Ci/mmol; 10mCi/ml). Monomeric γ-tubulin (~2 μM) was freshly prepared in GF2 buffer and distributed into a series of 30 μl aliquots. Tetrameric γ-tubulin was prepared by diluting the above protein 1:30 in 50 mM MES 6.6, 5 mM MgSO4, 1 mM EGTA (final [KCl]=16 mM KCl, final [γ-tubulin]=~66 nM) and aliquoting as before. Tetrameric γ-tubulin reaction volumes were twice the volume of the monomeric γ-tubulin reactions, in order to increase the signal:noise ratio. 2 μl (or 4 μl) of each concentration of ^{32}P-doped GTP was added to 30 μl monomeric (or 60 μl tetrameric) γ-tubulin. Final [GTP] ranged from 0.1 μM to 80 μM for the monomeric γ-tubulin experiments and from 1 nM to 300 nM for the tetrameric γ-tubulin experiments. Solutions were mixed and incubated for 1 hour on ice. UV crosslinking, TCA precipitation, SDS-PAGE, and band detection were

performed as before. Gel bands were quantified and background-corrected with ImageQuant software (Molecular Dynamics). Data was analyzed with Kaleidagraph 3.5 software (Synergy) and fit as a simple hyperbolic binding curve to obtain dissociation constants.

Quantification of GDP competing GTP off γ-tubulin was performed as follows: A dilution series of GDP ranging in concentration from 8 μM to 4800 μM was constructed. Monomeric and tetrameric γ-tubulin aliquots were made as before. 1 μl (or 2 μl) of each concentration of GDP was added to 30 μl monomeric (or 60 μl tetrameric) γ-tubulin, yielding final [GDP] ranging from 2.5 μM to 150 μM for the monomeric γ-tubulin experiments and from 0.25 μM to 25 μM for the tetrameric γ-tubulin experiments. 1 μl 12.5 μM α-^{32}P GTP was added to each monomeric γ-tubulin sample (final [GTP]=0.39 μM) and 2 μl 625 nM α-^{32}P GTP was added to each tetrameric γ-tubulin sample (final [GTP]=19.5 nM). Solutions were mixed and incubated for 1 hour on ice. Crosslinking, visualization, and quantitation were performed as before. Data was analyzed as before and fit as a competitive inhibition curve to obtain inhibition constants. All quantitative crosslinking experiments were performed in triplicate.

Microtubule nucleation assays

To study the microtubule-nucleating activity of pure, recombinant human γ-tubulin *in vitro*, polymerization of pure, bovine-brain tubulin in the presence or absence of γ-tubulin was followed in a Perkin Elmer Lambda 20 spectrometer (Perkin Elmer Instruments, Norwalk, CT) by turbidity at 350 nm basically as described previously[61, 70]. Briefly, γ-tubulin was prepared fresh in GF2 buffer, concentrated, and diluted 1:30

into freshly cycled αβ-tubulin in assembly buffer plus 1mM GTP, resulting in a final [KCl] of 16mM. A range of γ-tubulin concentrations were tested with 11 μM αβ-tubulin. The reactions were mixed at 0°C (in an ice-water slurry) and then rapidly (~30 seconds) heated to 37°C in a waterbath. They were then transferred to a pre-warmed cuvette in a 37°C peltier cell changer and recording of A_{350} was begun. Buffer control reactions were followed in parallel.

Chemical crosslinking

The initial EDAC experiment: 25 μl monomeric γ-tubulin (3.6μM) plus 25 μl αβ-tubulin (1.8 μM) were mixed and dialyzed against BRB80 (80mM K-PIPES pH 6.8, 5mM $MgCl_2$, 1 mM EGTA)+26% glycerol for 1 hour at 4°C using MINI-Dialyzers (Pierce). N-hydroxysuccinimide (NHS) was dissolved in DMSO and 0.5 ml was added to a final concentration of 1.8mM. The inclusion of NHS was to enhance the efficiency of the EDAC crosslinking reaction. The solution was mixed and 0.5μl EDAC was added, also to a final concentration of 1.8mM. The mixture was incubated for 30 minutes at room temperature and the crosslinking was quenched with 3μl 2M Tris pH 7.5.
Later EDAC experiments were similarly executed, with the following exceptions: Dialysis buffer was 50 mM K-MES pH 6.6, 16mM KCl, 5mM $MgSO_4$, 1mM EGTA. Final crosslinker concentrations varied as indicated in figure legends. Crosslinking was carried out both on ice and at room temperature. Also, DM1β was used as the antibody against β-tubulin, while the β-tubulin antibody used in the initial experiment is unknown. Ni-NTA pulldowns were performed as follows: After crosslinking and quenching as above, 30 μl of a Ni-NTA solution (1:1 in 50mM K-MES pH 6.6, 16mM KCl) was added

to each sample. The samples were agitated for 1 hour at 4°C and quickly spun down. The supernatant was removed, the beads were quickly washed with 150μl wash buffer 2 (see γ-tubulin purification), and eluted with 30μl elution buffer (see γ-tubulin purification).

Photocrosslinking was performed as follows: All manipulations prior to UV irradiation were carried out under either dim or dark conditions. Tetrafluoroarylazide succinimide (ALT, Inc.) was weighed out and dissolved in DMSO to a final concentration of 2.5mM. 5 μl of this crosslinker was added to 50μl γ-tubulin (3μM) and incubated for 30 minutes at room temperature, quenched with 3μl 2M Tris pH 7.5 and exchanged into K-MES pH6.6, 5mM $MgSO_4$, 1mM EGTA. The resulting conjugated γ-tubulin was mixed with an equimolar solution of αβ-tubulin (similarly dialyzed), allowed to incubate for 10 minutes at room temperature, and UV-crosslinked for 10 minutes. Crosslinking was carried out by exposing a 96-well plate covered with aluminum foil on the bottom to a handheld longwave UV lamp. TCA precipitations were carried out in a manner analogous to those procedures employed during GTP crosslinking (see above). All crosslinked products were analyzed by SDS-PAGE, transferred onto nitricellulose, and probed by blotting with different antibodies. Blotting with anti-his_6 antibody (Qiagen) was performed as dictated by manual. All other blotting procedures followed standard protocols.

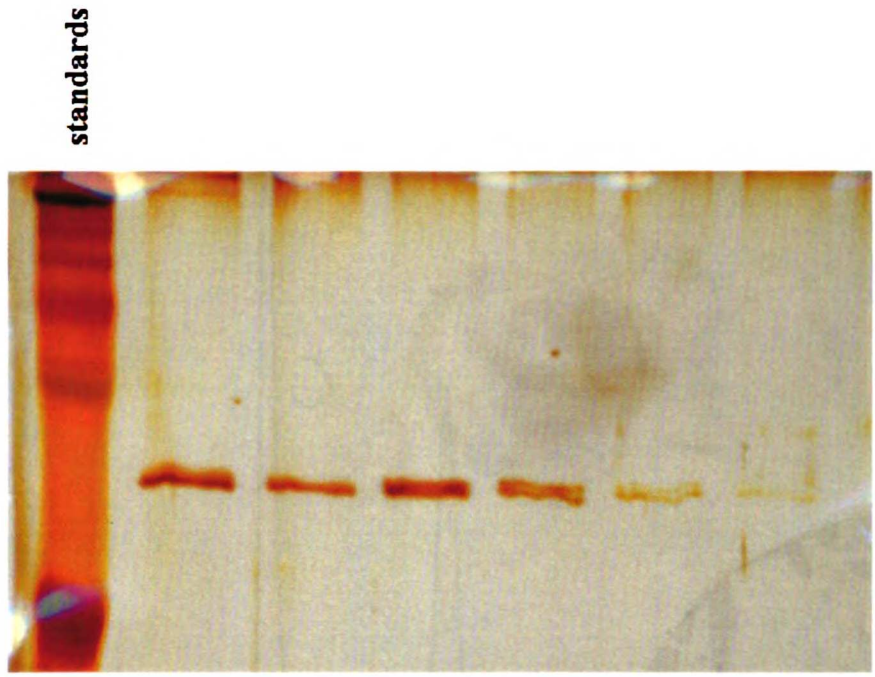

Figure 1A. Purification of recombinant human γ-tubulin. Silver stained SDS-PAGE of γ-tubulin purified by Ni-NTA affinity and ion exchange chromatography. Protein runs as a doublet.

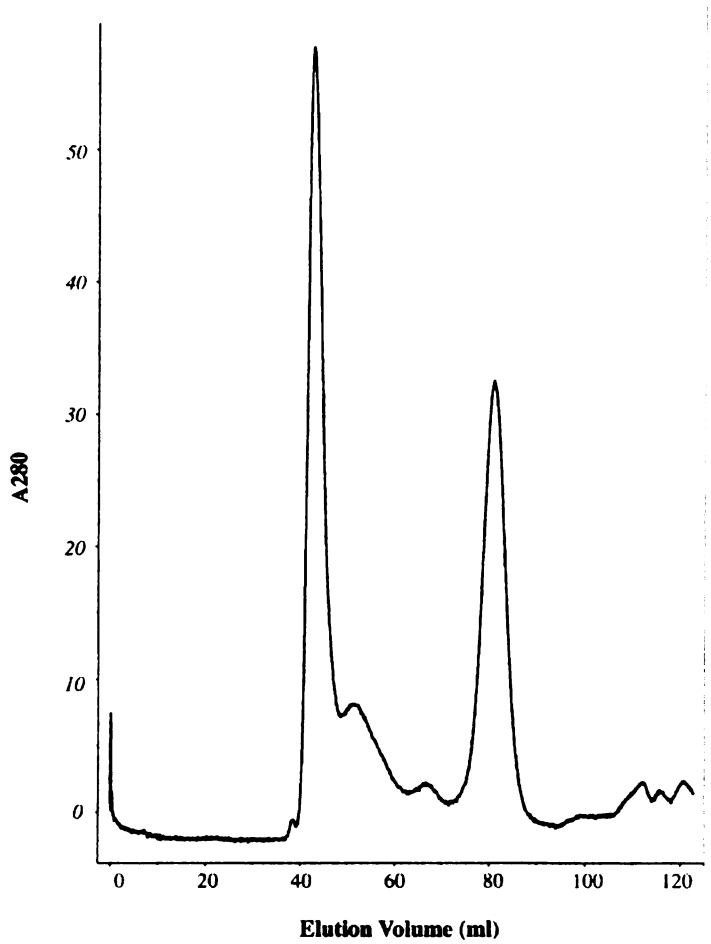

Figure 1B. Purification of recombinant human γ-tubulin. Preparative Superdex200 gel filtration profile from overexpressed/Ni-NTA affinity purified recombinant human γ-tubulin. γ-Tubulin elutes in a major peak at an elution volume consistent with that of a monomer (~80 ml) as well as in the void volume (~42 ml). Subsequent biochemical analysis focused on the monomeric γ-tubulin.

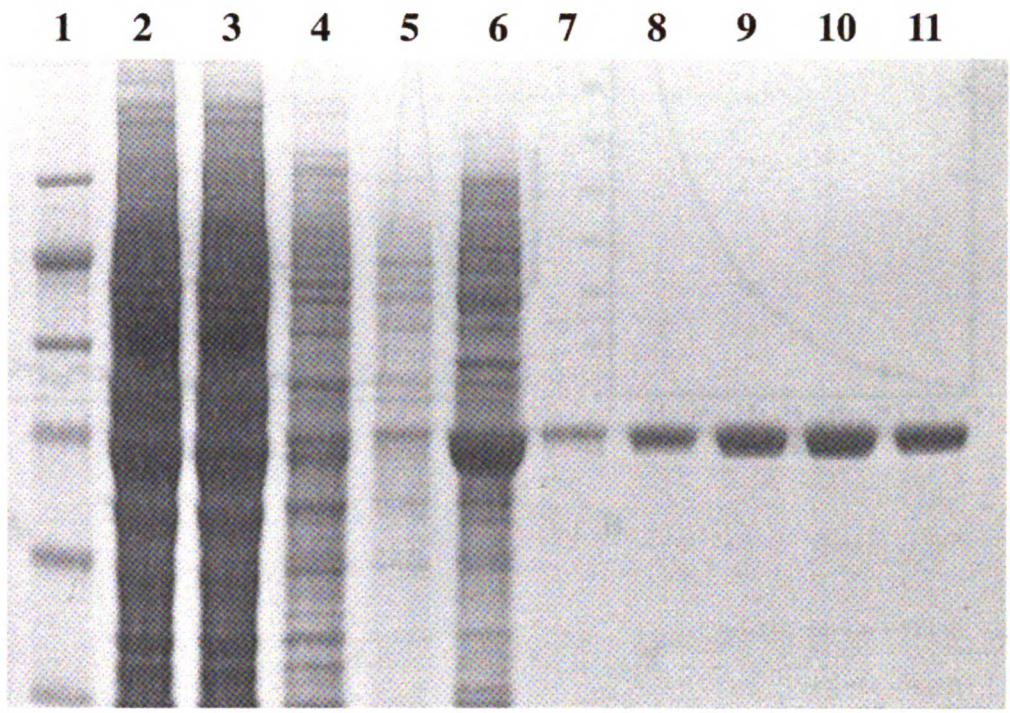

Figure 1C. Purification of recombinant human γ-tubulin. Coomassie stained SDS-PAGE of monomeric γ-tubulin purified by Ni-NTA and gel filtration chromatography. Lane 1: standards, lane 2: clarified lysate, lane 3: Ni-NTA flow-through, lane 4: Ni-NTA wash 1, lane 5: Ni-NTA wash 2, lane 6: Ni-NTA elution, lanes 7-11:Superdex200 peak elution.

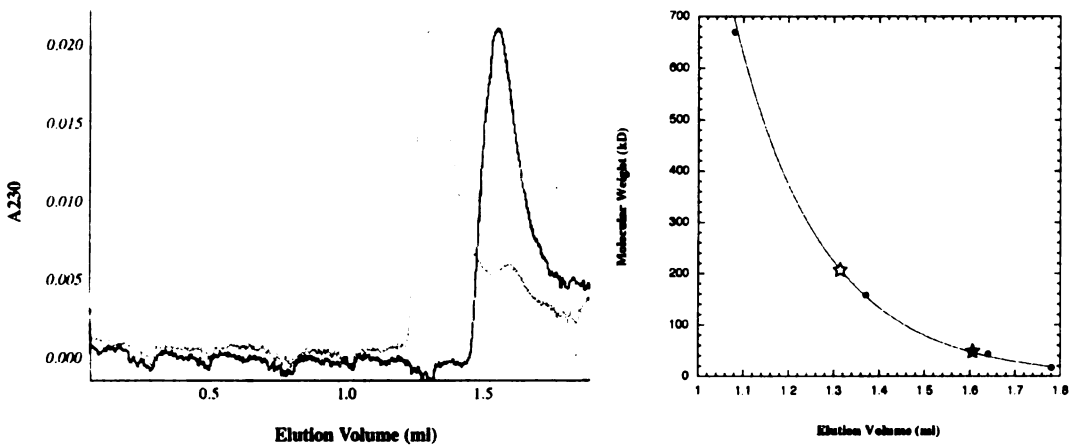

A. B.

Figure 2. γ-Tubulin oligomerization.

A.) Analytical gel filtration (Superdex 3.2/16) of γ-tubulin. γ-Tubulin (~4 μM) elutes as a monomer (black curve) in high salt buffer (50 mM MES pH 6.6, 5 mM $MgSO_4$, 1 mM EGTA, 500 mM KCl) and as a tetramer (grey curve) in a low salt buffer (50 mM MES pH 6.6, 5 mM $MgSO_4$, 1 mM EGTA, 100 mM KCl).

B.) Analytical gel filtration (Superdex 3.2/16) standard curve generated with: bovine thyroglobulin (670 kD), bovine gamma globulin (158 kD), chicken ovalbumin (44 kD), horse myoglobin (17 kD). Monomer elution position denoted by a black star, tetramer elution position denoted by a white star.

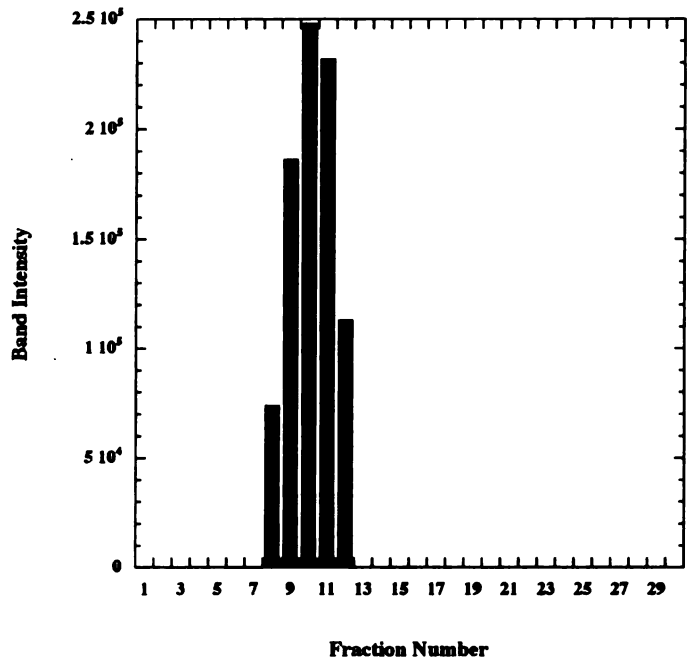

Figure 2. γ-Tubulin oligomerization.

C.) Sucrose density gradient (2-16%) sizing of γ-tubulin. Immuno-blotting results were digitized, quantified, and plotted. Gradients were loaded with 67 nM γ-tubulin in 16 mM KCl-containing buffer. γ-Tubulin migrates primarily as a tetramer. γ-Tubulin migrates in a similar fashion up to concentrations of at least 250 nM (data not shown).

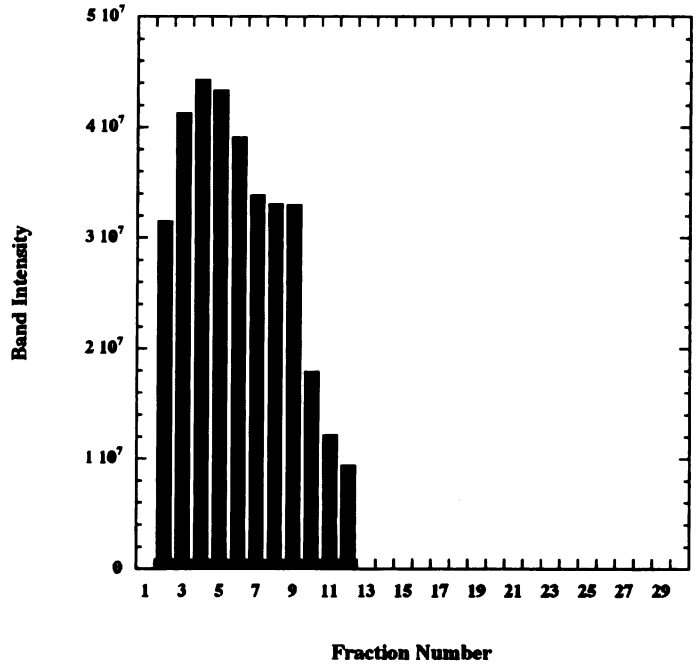

Figure 2. γ-Tubulin oligomerization.

D.) Sucrose density gradient (2-16%) sizing of 2 μM γ-tubulin in 500 mM KCl-containing buffer, showing mostly monomeric γ-tubulin.

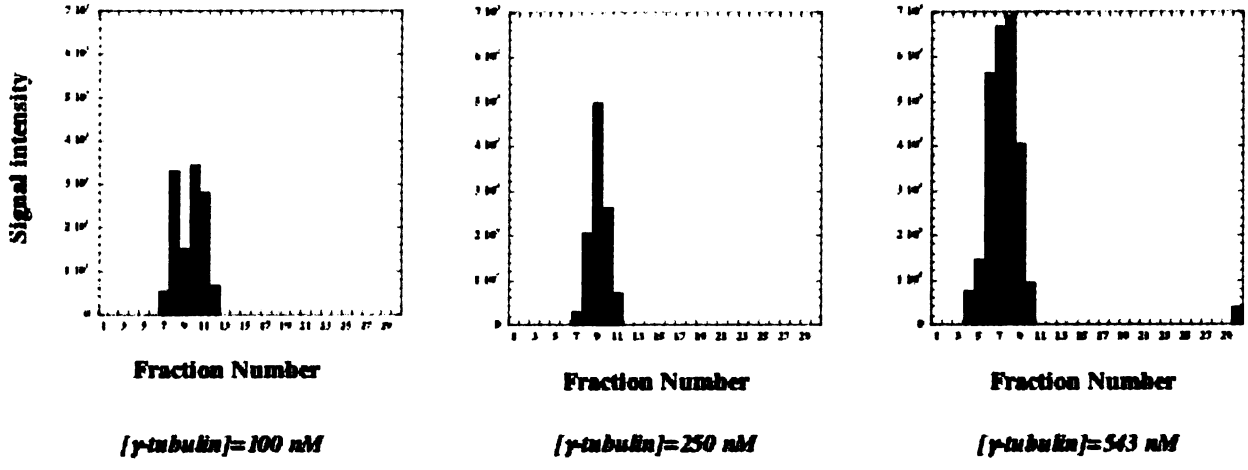

Figure 2. γ-Tubulin oligomerization.

E.) Sedimentation profiles of varying [γ-tubulin] on a 2-16% sucrose gradient in 50 mM MES pH 6.6, 16 mM KCl, 5 mM $MgSO_4$, 1 mM EGTA, 1 mM GTP. At 543 nM γ-tubulin (right panel), a fraction of γ-tubulin migrates to the bottom of the gradient appears.

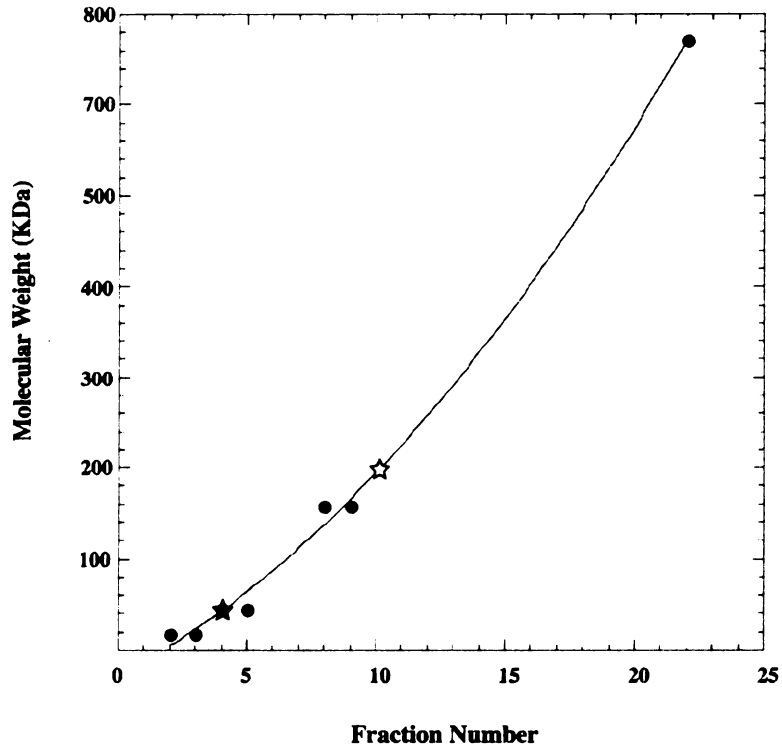

E.

Figure 2. γ-Tubulin oligomerization.

F.) Standard curve generated from parallel 2-16% sucrose gradients loaded with: bovine thyroglobulin (670 kD), bovine gamma globulin (158 kD), chicken ovalbumin (44 kD), horse myoglobin (17 kD). Monomer elution position denoted by a black star, tetramer elution position denoted by a white star.

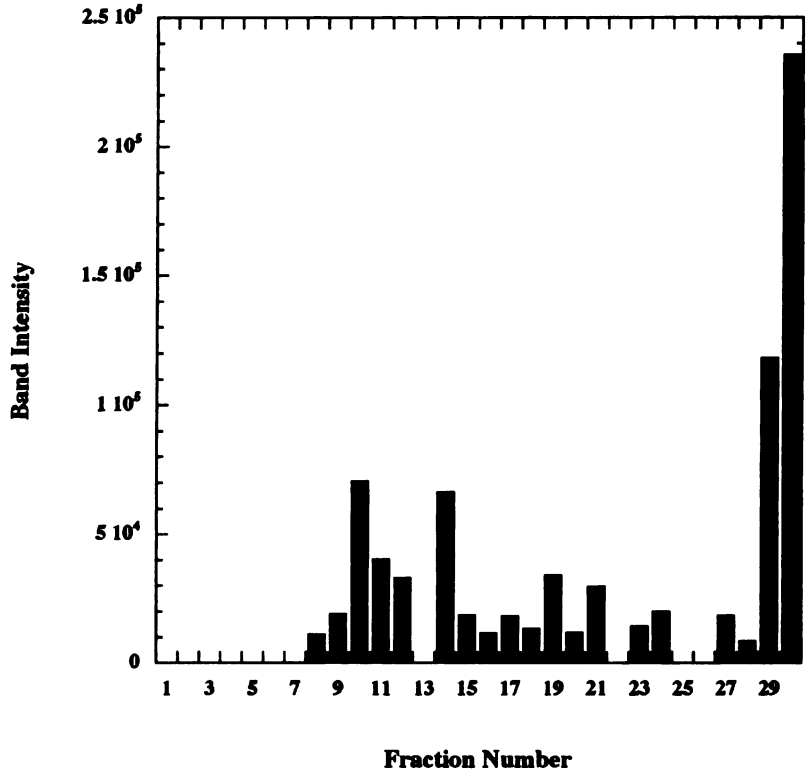

Figure 3. γ-tubulin forms higher order filamentous assemblies.

A.) Sedimentation profile of 2 μM γ-tubulin on a 2-16% sucrose gradient in 50 mM MES pH 6.6, 16 mM KCl, 5 mM $MgSO_4$, 1 mM EGTA, 1 mM GTP.

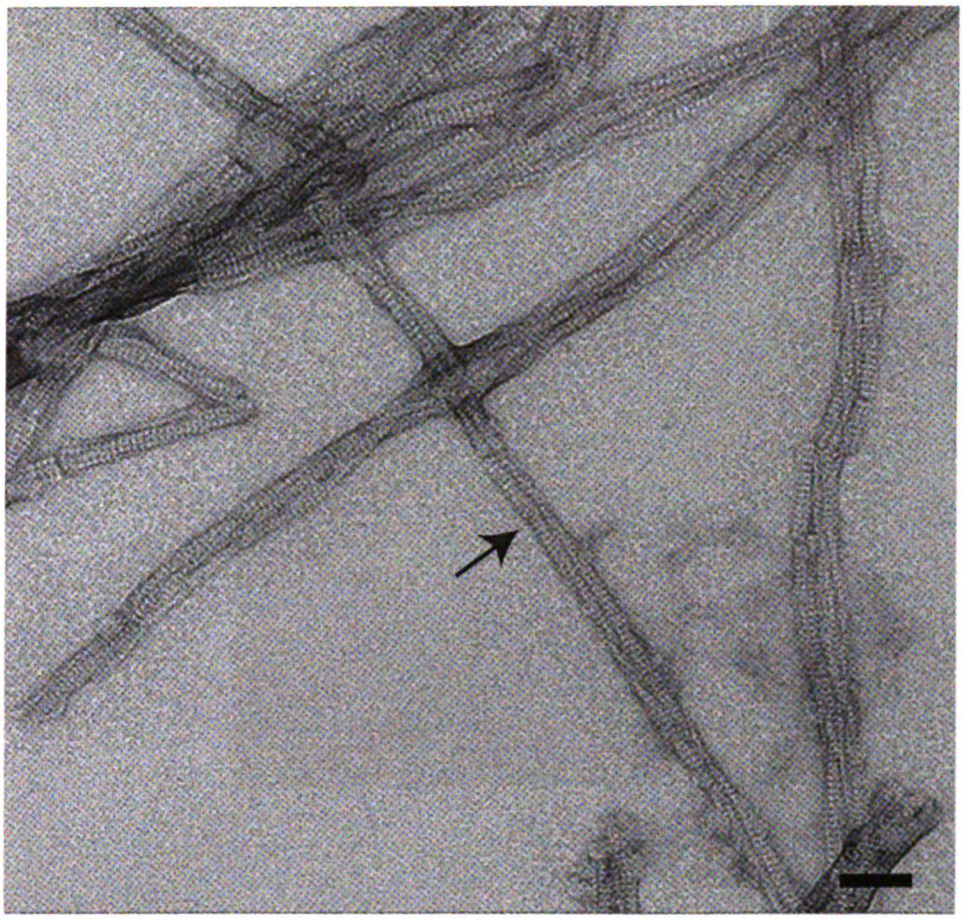

Figure 3. γ-tubulin forms higher order filamentous assemblies.

B.) Negative-stain electron microscopy of γ-tubulin (3 μM) in 50 mM MES pH 6.6, 16 mM KCl, 5 mM $MgSO_4$, 1 mM EGTA, 1 mM GTP. 62,000X magnification. Arrow indicates 24 nm filament. Bar = 55 nm.

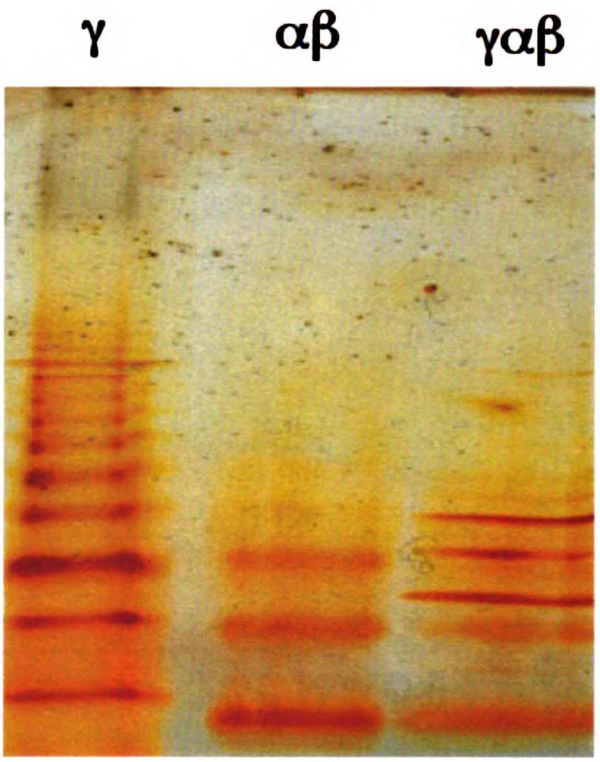

Figure 4. γ-tubulin forms higher order assemblies as a function of pH.

A.) Native PAGE analysis of pure γ-tubulin. Under native gel conditions, γ-tubulin alone appears as a ladder (left lane) and, interacts with αβ-tubulin (right lane).

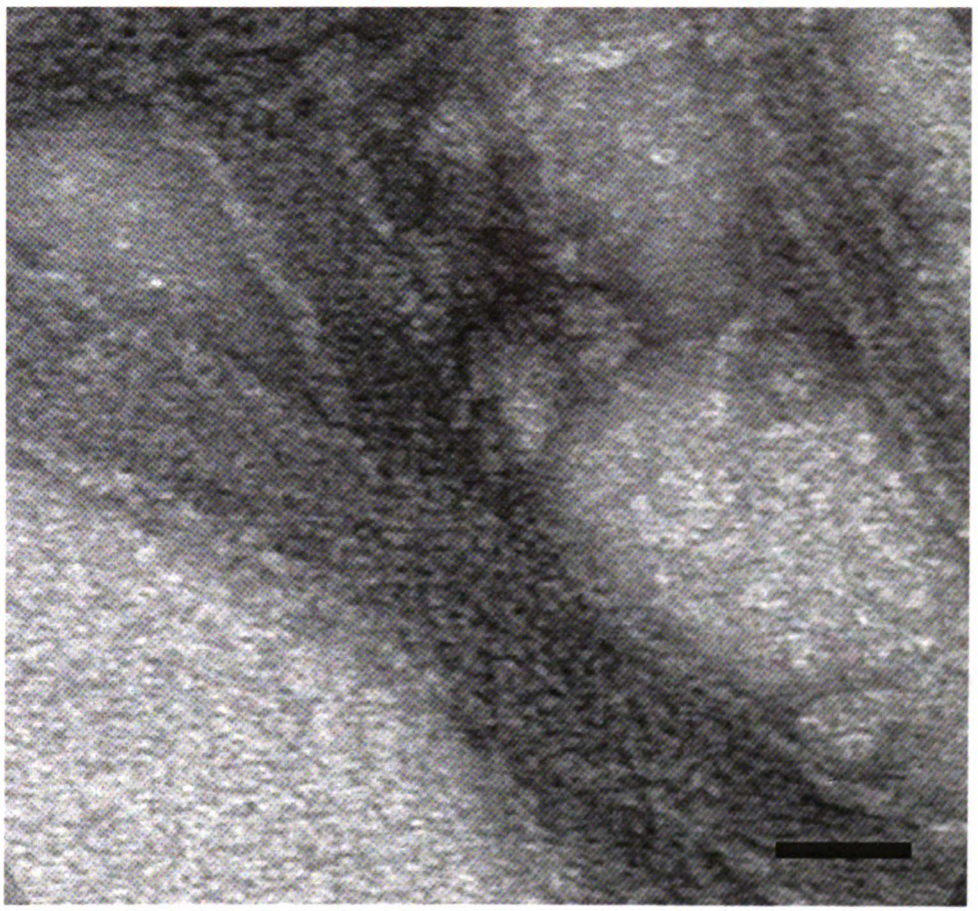

Figure 4. γ-tubulin forms higher order assemblies as a function of pH.

B.) Negative-stain electron microscopy of γ-tubulin (4 μM) in 0.1 M Tris pH 8.8. 62,000X magnification. Bar = 30 nm.

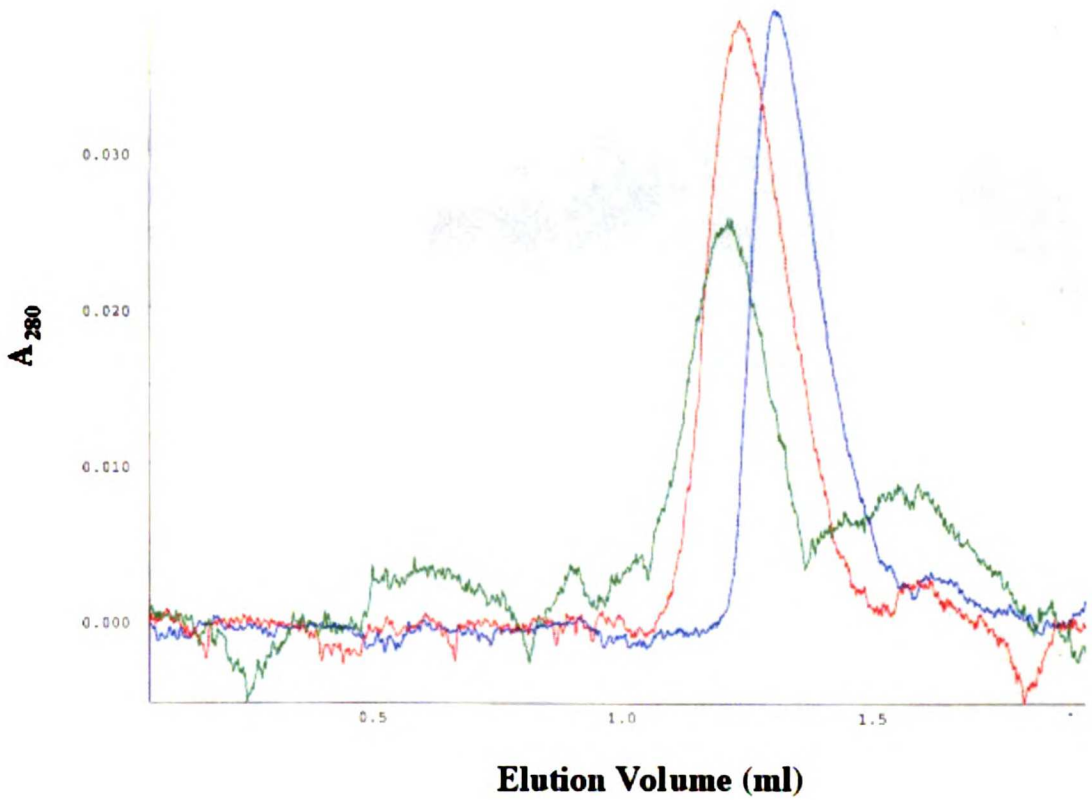

Figure 4. γ-tubulin forms higher order assemblies as a function of pH.

C.) Analytical gel filtration of γ-tubulin in: 50mM MES, pH 6.9 (blue), 50mM HEPES pH 7.4,(red), 50mM HEPES pH 8.0 (green).

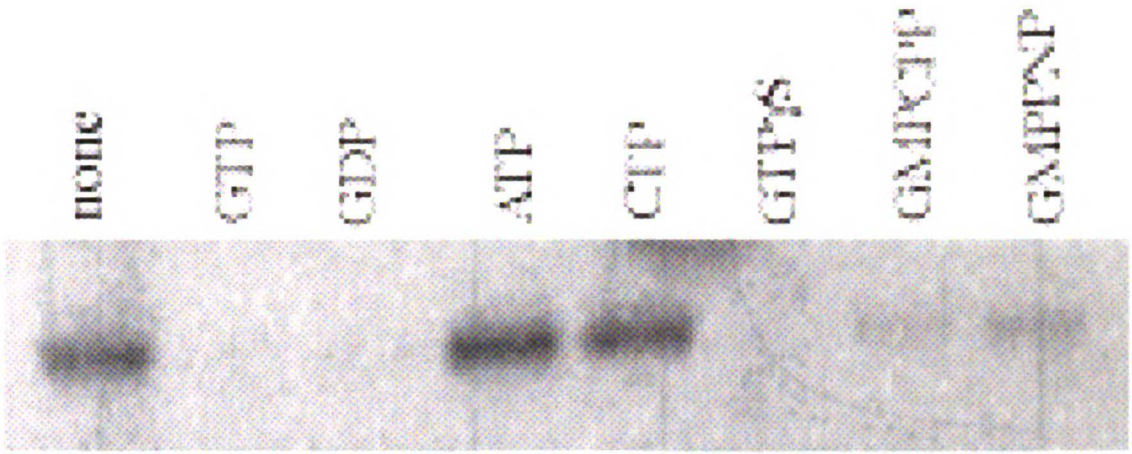

Figure 5. γ-tubulin specifically binds GTP and GDP.

A.) [α-^{32}P] GTP can be photocrosslinked to monomeric γ-tubulin. Bound [α-^{32}P]GTP can be competed off by a 200-fold excess of unlabeled GTP, GDP, or any of several GTP analogs, but not by either ATP or CTP.

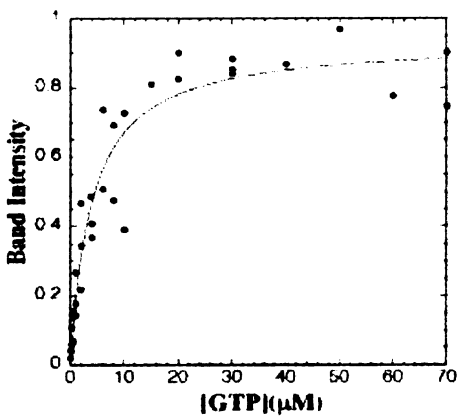

B.

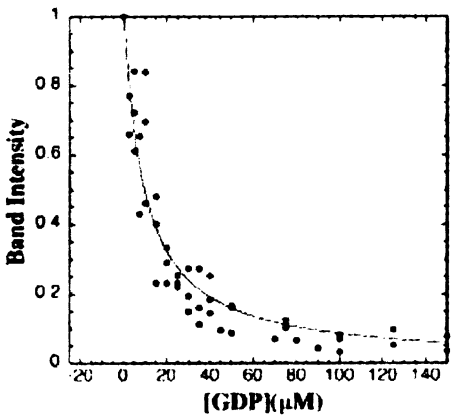

C.

Figure 5. γ-tubulin specifically binds GTP and GDP.

B.) Monomeric γ-tubulin/GTP binding curve. Increasing concentrations of radiolabeled GTP were incubated with γ-tubulin, crosslinked, separated by SDS-PAGE, visualized and quantified. Experiments were performed in triplicate. Data were fit to the following equation: $y=ax/(K_D+x)$. K_D= 3.9 μM (±0.66).

C.) Monomeric γ-tubulin/GDP inhibition curve. A constant amount of radiolabeled GTP (0.39 μM) was incubated with monomeric γ-tubulin and increasing concentrations of cold GDP. Samples were crosslinked, visualized, and quantified as described. Experiments were performed in triplicate. Data were fit to the following equation: $y=a[\gamma\text{-tubulin}]/([\gamma\text{-tubulin}]+K_{D(GTP)}(1+(x/K_I)))$. K_I= 8.55 μM (±0.95).

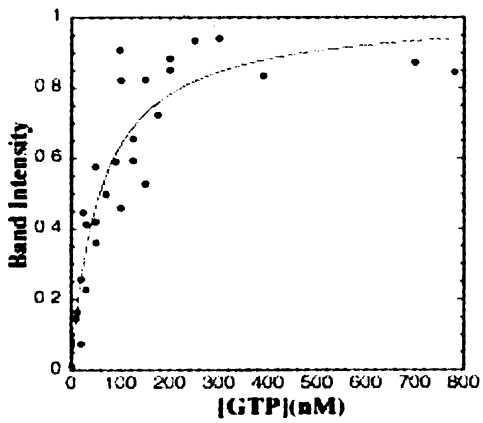

D.

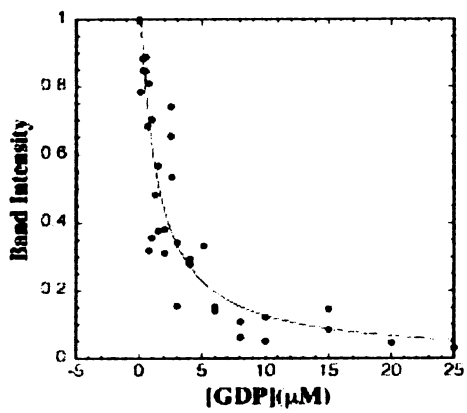

E.

Figure 5. γ-tubulin specifically binds GTP and GDP.

D.) Tetrameric γ-tubulin/GTP binding curve. Experiments were performed in triplicate. K_D= 58.4 nM (±12.6).

E.) Tetrameric γ-tubulin/GDP inhibition curve. A constant amount of radiolabeled GTP (19.5 nM) was incubated with tetrameric γ-tubulin and increasing concentrations of cold GDP. Experiments were performed in triplicate. K_I = 1.13 μM (±0.20).

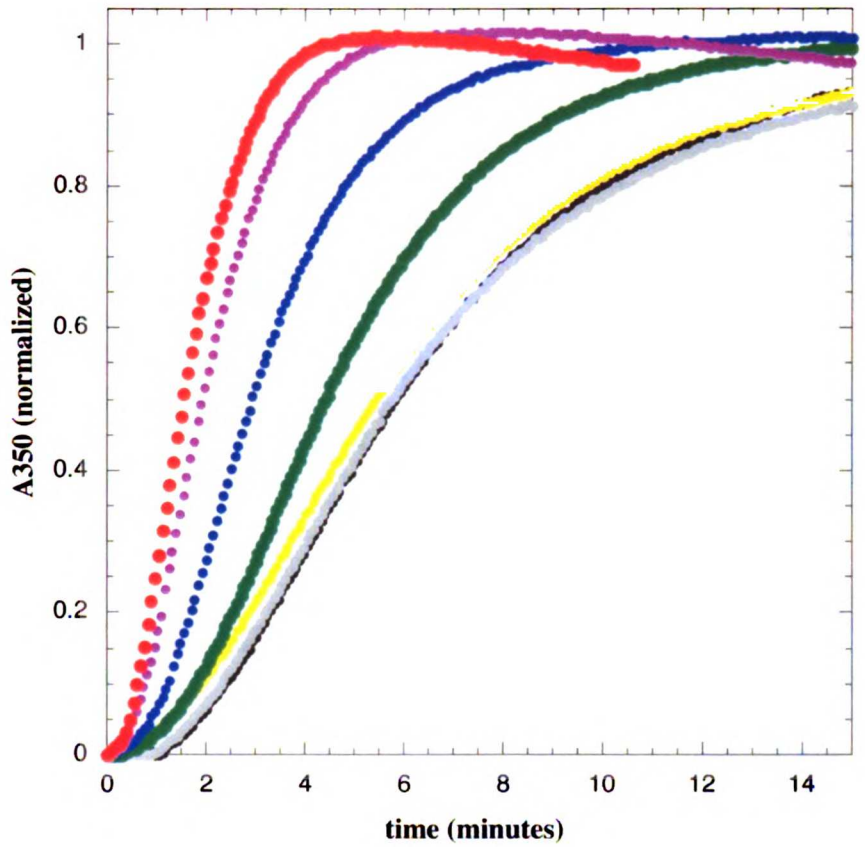

Figure 6. Pure γ-tubulin can nucleate microtubule assembly

A.) Relative to the buffer control, γ-tubulin decreases the lag time before rapid assembly of αβ-tubulin polymer. Polymerization was followed by A_{350} over time in the presence and absence of a range of concentrations of pure γ-tubulin. [αβ-Tubulin]= 11 μM. [γ-Tubulin] is color-coded: black = buffer alone, grey = 0.78nM, yellow = 26nM, green = 130nM, blue = 260nM, purple = 390nM, red = 520nM.

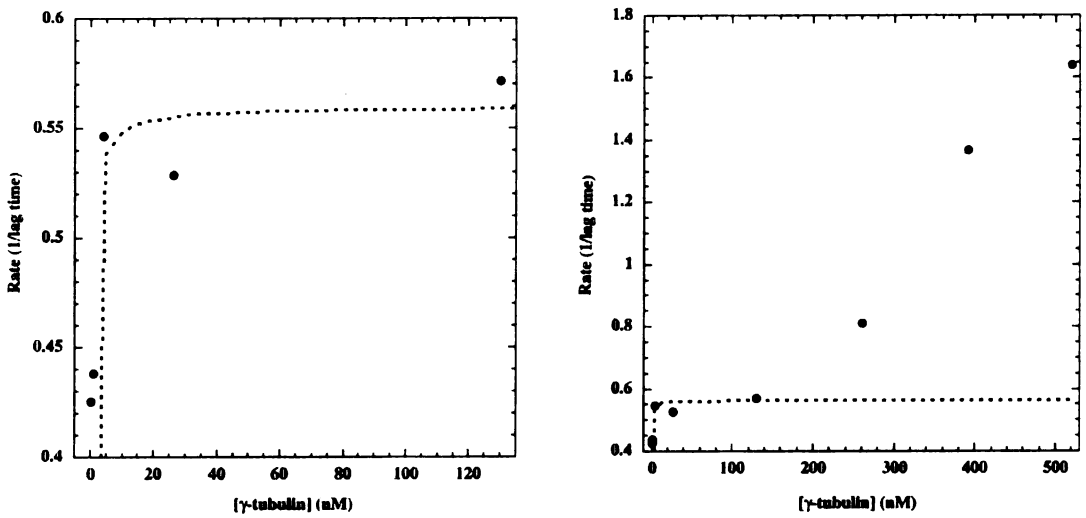

Figure 6. Pure γ-tubulin can nucleate microtubule assembly

B.) γ-Tubulin-mediated acceleration of microtubule nucleation saturates at low γ-tubulin concentration (left panel) but accelerates at higher γ-tubulin concentrations (right panel). The nucleation rate is defined as 1/lag time, where the lag time is defined as the time it takes a given curve to reach one tenth of the plateau value. Data for the lower concentrations of γ-tubulin are well modeled by simple Michaelis-Menten kinetics. The acceleration in rate at high concentrations is likely due to the presence of γ-tubulin oligomers larger than tetramers (Figure 3).

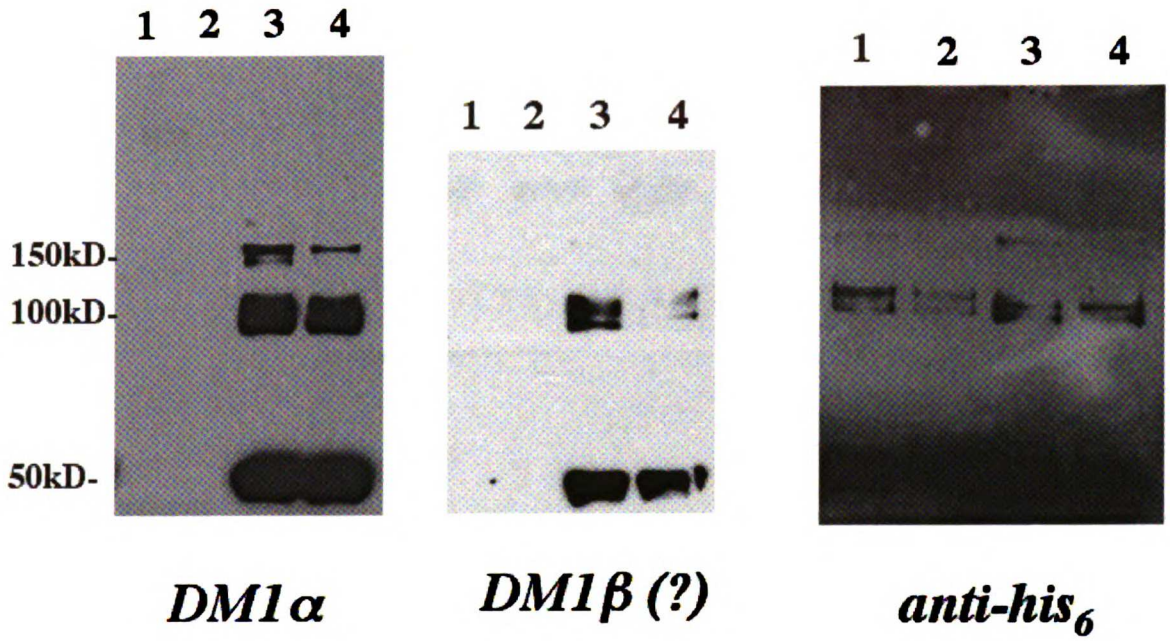

Figure 7. Chemical crosslinking of γ-tubulin to αβ-tubulin.

A.) Lane 1, 2: γ-tubulin. Lanes 3, 4: γ-tubulin+αβ-tubulin. Lanes 2, 4:+ 1mM GTP. Left panel: probed with α-tubulin-specific antibody. Midlle panel: probed with β-tubulin specific antibody. Right panel: probed with antibody specific for polyhistidine-tagged recombinant γ-tubulin. A 150kDa species is present on the α-tubulin and γ-tubulin blots, but less so on the β-tubulin blot. GTP appears to result in less crosslinking.

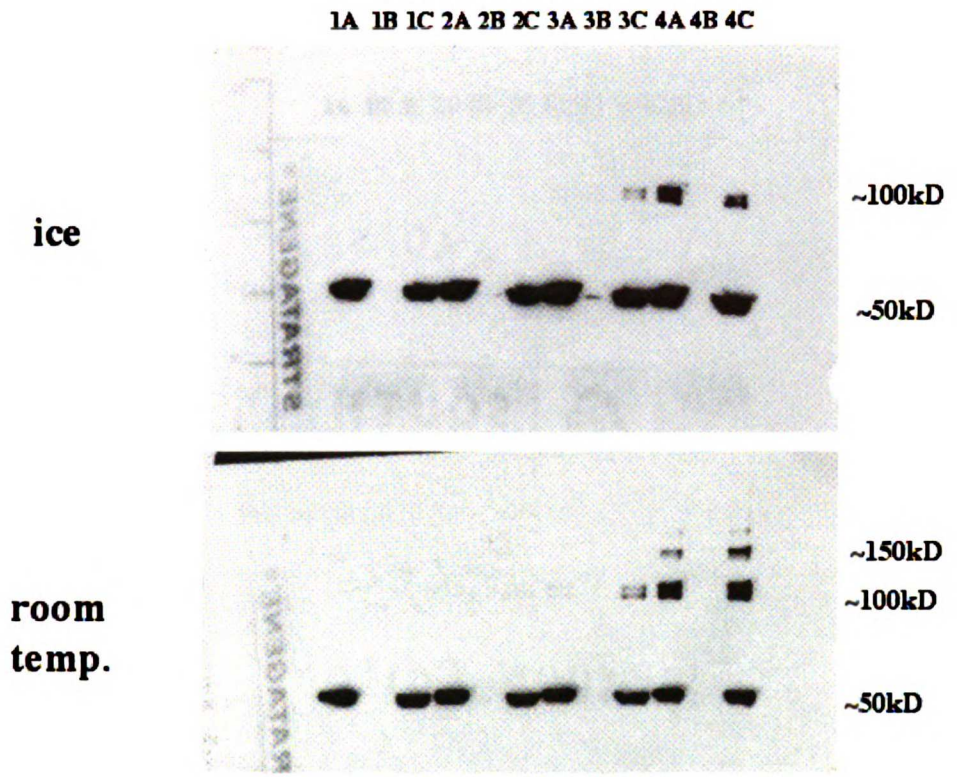

Figure 7. Chemical crosslinking of γ-tubulin to αβ-tubulin with varying temperature and crosslinker concentration.

B.) Probed with anti-his_6 antibody for recombinant γ-tubulin. Top panel: samples incubated on ice prior to quenching. Bottom panel: samples incubated at room temperature prior to quenching. A: γ-tubulin. B: αβ-tubulin. C: γ-tubulin + αβ-tubulin. [EDAC/NHS]: 1 = 0 mM, 2 = 0.37mM, 3 = 1.1mM, 4 = 3.3mM. Lane 3 indicates a condition that yields higher order complexes only in the presence of αβ-tubulin.

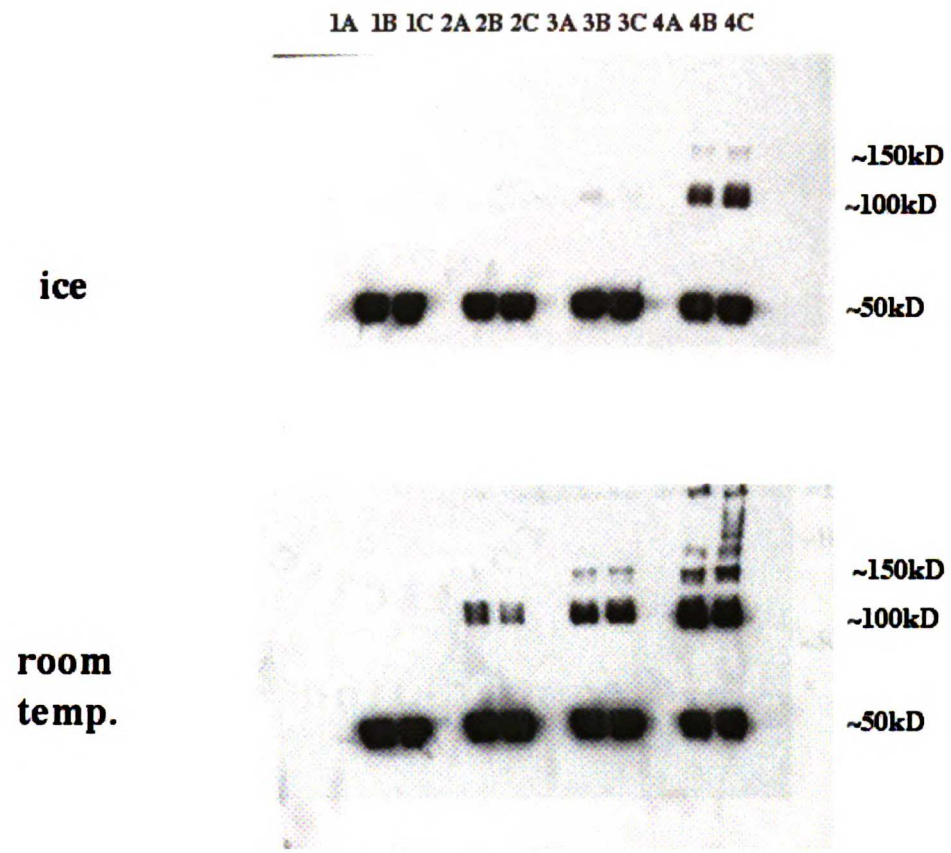

Figure 7. Chemical crosslinking of γ-tubulin to αβ-tubulin with varying temperature and crosslinker concentration.

C.) Probed with DM1α antibody for α-tubulin. See 7B for details.

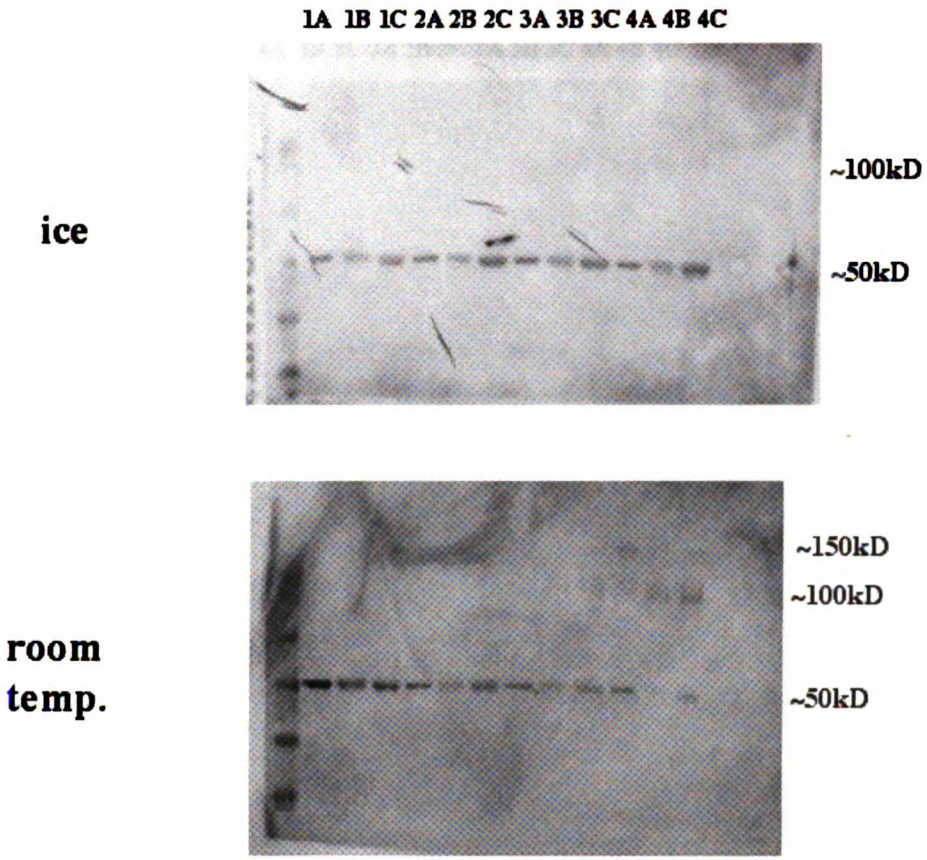

Figure 7. Chemical crosslinking of γ-tubulin to αβ-tubulin with varying temperature and crosslinker concentration.

D.) Probed with DM1β antibody for β-tubulin. See 7B for details. DM1β crossreacts with γ-tubulin.

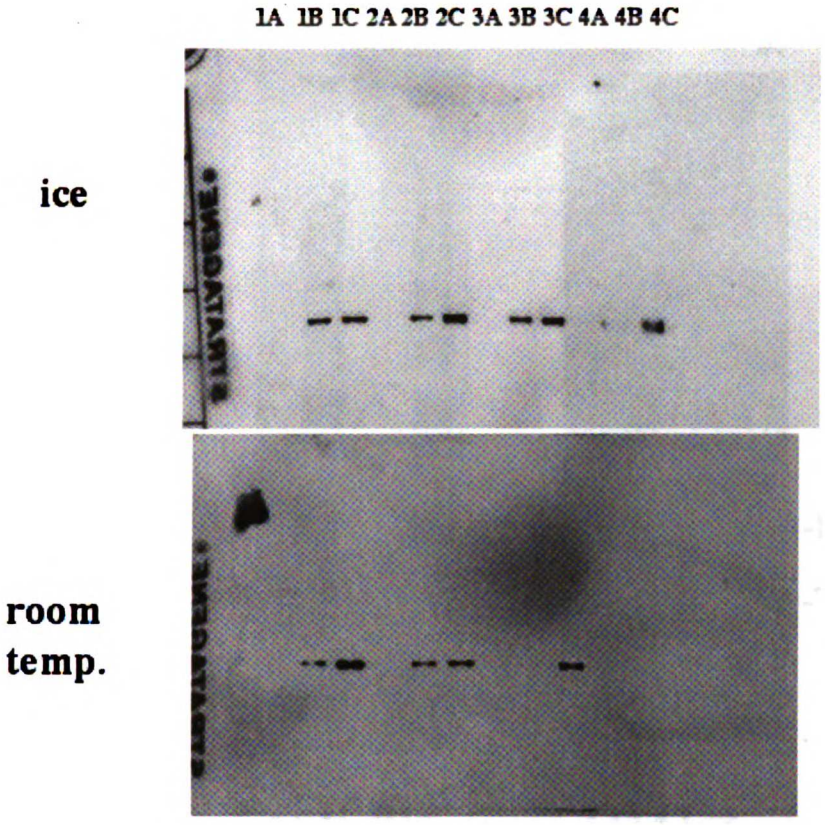

Figure 7. Chemical crosslinking of γ-tubulin to αβ-tubulin with varying temperature and crosslinker concentration.

E.) Additional Ni-NTA pulldown step included. Probed with DM1α antibody for α-tubulin.

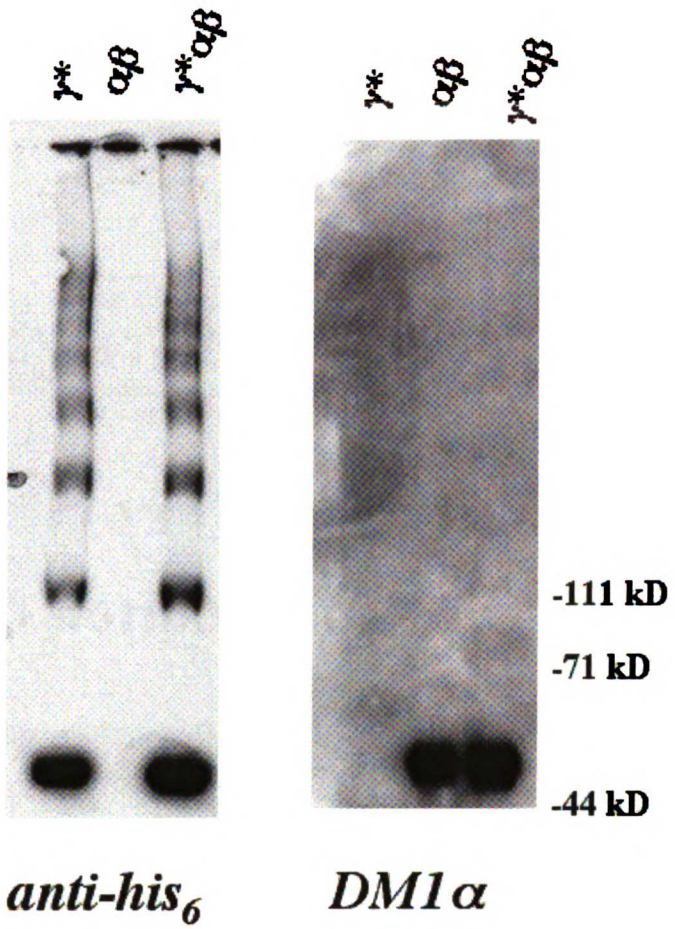

Figure 8. Photocrosslinking of γ-tubulin to αβ-tubulin.

A.) Left panel indicates γ-tubulin-γ-tubulin crosslinks. No shift in α-tubulin detected (right panel).

Figure 8. Photocrosslinking of γ-tubulin to αβ-tubulin.

B.) As in A.), but with lower γ-tubulin : α-tubulin ratio. (γ-tubulin= 100nM, αβ-tubulin = 10μM). Also has added TCA precipitation step. Higher order α-tubulin species seen even without crosslinker may be due to too much αβ-tubulin in load.

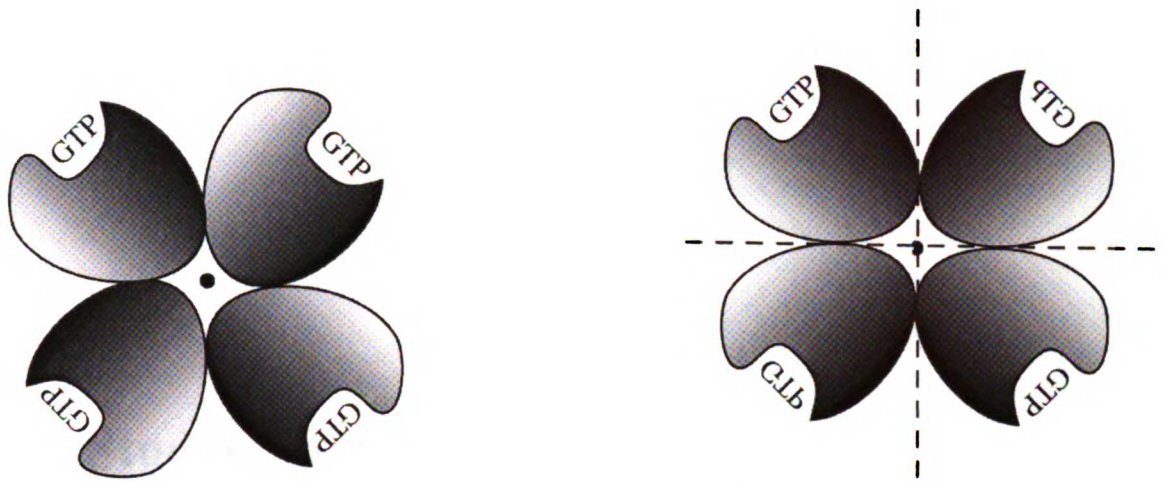

A. B.

Figure 9. Possible models for γ-tubulin organization within the tetramer

A.) γ-Tubulin tetramer with one 4-fold axis of symmetry. Axis of symmetry is perpendicular to the plane of the page and goes through the center of the tetramer, denoted by a black square.

B.) γ-Tubulin tetramer with three 2-fold axes of symmetry. Axes of symmetry are denoted by dashed lines or a single black dot. Inverted GTP emphasizes a rotation of γ-tubulin by 180° relative to the molecule next to it.

Chapter 2:

Studies on the GTP Hydrolyzing Activity of Pure Human γ-Tubulin

Synopsis

The hydrolysis of GTP by αβ-tubulin is known to form the basis of microtubule dynamic instability. Our observations that γ-tubulin has nearly identical GTP and GDP binding interactions with β-tubulin and that the nucleotide binding site is structurally equivalent to β-tubulin's suggest that there might be a role for GTP hydrolysis in γ-tubulin function. This possibility has not yet been explored. Here are described preliminary investigations into the GTP hydrolysis activity of purified recombinant human γ-tubulin. Monomeric γ-tubulin is found to be a weak GTPase. A similar activity is observed for semi-purified Drosophila γ-TuRC, though a more highly purified version of this protein complex will be required verify its GTPase activity. Experiments were also performed to develop methods that could probe the relationship between the nucleotide state of γ-tubulin and γ-tubulin/αβ-tubulin interactions. It was determined that azido-GTP could be crosslinked to γ-tubulin, providing a manner with which to follow the fate of nucleotides specifically bound to γ-tubulin during interactions with αβ-tubulin. It was also demonstrated that taxol-stabilized microtubules do not hydrolyze GTP, providing an alternate method to probe the relationship between the nucleotide state of γ-tubulin and γ-tubulin/microtubule interactions.

Introduction

Microtubules are assembled from αβ-tubulin heterodimers in a GTP-dependent manner. Biochemical studies have revealed that α-tubulin is bound non-exchangeably to GTP, while β-tubulin possesses an exchangeable nucleotide-binding site[64]. Kinetic analyses of GTP hydrolysis together with microtubule assembly have illustrated that GTP hydrolysis closely follows microtubule assembly and is approximately stoichiometric, with one GTP being hydrolyzed per heterodimer incorporated into the lattice[71], while the GTPase activity of unpolymerized αβ-tubulin is practically zero[72]. Once the microtubule population reaches a steady state length, GTP hydrolysis continues at a constant rate, suggesting the presence of dynamic instability. Structural analyses of zinc-induced tubulin sheets have revealed that β-tubulin-bound GTP becomes buried at the β-tubulin/α-tubulin longitudinal interface upon microtubule assembly[17, 21]. α-Tubulin then is allowed to donate an acidic residue to the environment surround the β-tubulin-bound GTP, completing the active site and promoting the hydrolysis of GTP to GDP, which leads to the depolymerization of the microtubule. The most widely accepted model for the molecular mechanism of GDP-induced microtubule disassembly is that guanine nucleotides induce conformational changes into the tubulin subunit, with GTP-tubulin assuming a straight conformation and GDP-tubulin assuming a curved conformation incompatible with the microtubule lattice[64]. We have proposed an alternate model in which guanine nucleotides only act to modulate the strength of longitudinal interactions (Chapter 4).

The high degree of sequence conservation between γ-tubulin and αβ-tubulin is pronounced in the region corresponding to the nucleotide-binding pocket. γ-Tubulin

nucleotide binding studies have demonstrated that guanine nucleotides can be specifically crosslinked to γ-tubulin in the γ-TuRC, the γ-TuSC[36], or to purified, recombinant γ-tubulin (Chapter 1). Structural and quantitative binding studies on pure γ-tubulin reveal that nucleotide binding is highly conserved between β-tubulin and γ-tubulin (Chapter 4), suggesting a similar functional role in regulating interactions with α-tubulin. Though there is little structural evidence for an assembly-coupled GTP hydrolysis mechanism in γ-tubulin as there is in αβ-tubulin (Chapter 4) [17, 18], monomeric γ-tubulin will allow hydrolysis studies to be carried out at higher concentrations of unpolymerized tubulin than previously possible[72]. Furthermore, a Gly-Gly insertion unique to γ-tubulins is positioned near the γ-phosphate of GTP and may confer unique catalytic properties to γ-tubulin (Chapter 4).

In order to begin exploring these possibilities, the ability of purified γ-tubulin to hydrolyze GTP was investigated. It was found that monomeric γ-tubulin possesses a weak GTPase activity. A similar activity was found in the γ-TuRC partially purified from Drosophila embryo extracts. Reagents and methods useful for studying the relationship between αβ-tubulin/γ-tubulin interactions and the nucleotide state/hydrolyzing activity of γ-tubulin were also identified.

Results and Discussion

Preliminary experiments at a γ-tubulin concentration of 3.3μM showed that GTP hydrolysis proceeds with freshly prepared γ-tubulin at 37°C (Figure1). These preliminary experiments did not reveal any detectable GTP hydrolysis products when the reaction

was monitored at 4°C or when γ-tubulin had been through a freeze/thaw cycle (data not shown).

The appearance of GTP hydrolysis products was monitored over time by thin layer chromatography (Figure 1A). GDP concentrations at each time point were determined by quantifying spots corresponding to GDP and GTP, calculating the GDP/total nucleotide ratio, and multiplying this ratio by the starting GTP concentration. Hydrolysis was monitored over a range of starting GTP concentrations and samples containing buffer alone were processed in parallel to allow for background correction (Figure 1B).

At a γ-tubulin concentration of 3.3μM, GTP concentrations greater than or equal to 50 μM yielded data that could be fit (Figure 1C,1D, Table 1). Using GTP concentrations of 50, 100, 200 and 400 μM (Figure 1D), clear plateaus, some above the concentration of γ-tubulin, were reached. The plateau values, however, were still significantly below the concentration of free nucleotide. In initial experiments using GTP concentrations of 25, 50, and 100 μM (Figure 1C), no plateau was evident. It was expected that, if γ-tubulin could hydrolyze GTP, GDP production would continue until all the free GTP was hydrolyzed. The low plateaus may reflect product inhibition and possibly a need for an as yet unidentified exchange factor. Though the structure of γ-tubulin reveals a binding pocket very similar to the exchangeable one on β-tubulin (Chapter 4), that structure is GTP- or GTPγS-bound and does not necessarily represent the structure of a γ-tubulin that has hydrolyzed GTP. Also, earlier competition experiments in which free nucleotide exchange was observed (Chapter 1) were performed at 4°C, a temperature at which hydrolysis does not occur. Further functional and

structural studies will be required to determine the extent of γ-tubulin product release after hydrolysis and the origin of the low plateaus.

A similar experiment was performed with ~100 nM Drosophila γ-TuRC (~1.3 μM γ-tubulin) (courtesy of Michelle Moritz) plus 100 μM GTP (Figure 2). A low plateau similar to that in the monomeric γ-tubulin experiments was observed. However, the γ-TuRC was purified by antibody affinity chromatography, undoubtedly leaving contaminants in the preparation. A more highly purified sample assayed over a broad range of concentrations will be required to definitively attribute any GTPase activity to the γ-TuRC.

In order to begin to investigate the effects of αβ-tubulin/γ-tubulin interactions on γ-tubulin GTP hydrolysis, a strategy had to be developed to ensure that the observed hydrolysis products are due to the action of γ-tubulin, not αβ-tubulin. One strategy involved covalently linking a γ-^{32}P-labeled GTP to γ-tubulin prior to adding αβ-tubulin. Disappearance of this label on SDS-PAGE would then indicate that GTP bound to γ-tubulin, but not αβ-tubulin, had undergone a round of hydrolysis. γ^{32}P-labeled N_3-GTP was found to photocrosslink to γ-tubulin in a nucleotide-specific manner (Figure 3). To examine the effect of αβ-tubulin on γ-tubulin GTP hydrolysis, γ^{32}P-labeled N_3-GTP was first photocrosslinked to γ-tubulin. The solution was then dialyzed to remove excess radioactive nucleotide, incubated at 37°C (with and without αβ-tubulin), and monitored for γ-phosphate release (Figure 4). Control experiments revealed that the signal from γ-tubulin alone was too weak to detect (Figure 4B), which could be remedied by simply loading a larger sample on the gel. However, UV irradiation and dialysis were not sufficient to rid the solution of active N_3-GTP, resulting in the radiolabeling of αβ-

tubulin. (Figure 4C). Hence, a better method of removing excess N_3-GTP from the reaction needs to be developed before this strategy can be implemented (see Future Directions).

Another strategy to separate the GTPase activity of γ-tubulin from that of αβ-tubulin involved the use of the natural product taxol. Taxol-stabilized microtubules are resistant to a variety of conditions which usually result in microtubule disassembly and were reasoned to possess β-tubulin GTP binding sites that are either non-exchangeable (except for the exposed plus-end) or unable to promote hydrolysis. In order to test this, taxol-stabilized microtubules were assembled from 10 μM αβ-tubulin (courtesy of John Lyle) and incubated with 100μM GTP for 30 minutes at 37°C (Figure 4). They did not possess any detectable GTP hydrolysis activity. Taxol-stabilized microtubules are known to interact with γ-tubulin[33] and are thus valuable reagents for studying the effect of microtubule interactions on the GTPase activity of γ-tubulin.

Future Directions

Monomeric γ-tubulin was found to possess a weak GTPase activity over a small range of GTP concentrations. A broader range of GTP concentrations in future experiments should provide more detail into the parameters (K_M, k_{CAT}) governing this activity. Additionally, investigating the GTPase activity of γ-tubulin under conditions where microtubule assembly is promoted and γ-tubulin oligomerizes (Chapter 1) will provide more functionally relevant insight into this phenomenon.

The use of N_3-GTP:γ-tubulin to separate the GTPase activities of γ-tubulin and αβ-tubulin requires optimization. Excess nucleotide may be more efficiently removed

through desalting in spin columns packed with G-25 gel filtration media. Pilot experiments using this method resulted in much less free nucleotide, though the ratio of free nucleotide to labeled protein did not appear to be much lower than prior to desalting (data not shown). Variations in spin times, sample loads, and fractionation will be required to identify an optimally desalted sample using this method. Furthermore, N_3-GTP:γ-tubulin did not reveal detectable phosphate release after incubation at 37°C. However, this experiment used frozen protein that had been thawed, before it was established that fresh γ-tubulin should always be used for functional assays. Future experiments should investigate the ability of N_3-GTP:γ-tubulin (freshly prepared) to undergo a round of hydrolysis.

Taxol-stabilized microtubules hold promise as reagents to study the relationship between γ-tubulin/microtubule interactions and the nucleotide state of γ-tubulin. The effects of γ-tubulin /microtubule interactions on γ-tubulin GTP hydrolysis can be explored by following the hydrolysis of α-^{32}P GTP by γ-tubulin (as above), both in the presence and absence of taxol-stabilized microtubules. The effect of different nucleotide states of γ-tubulin on γ-tubulin/microtubule interactions can be explored by incubating taxol-stabilized microtubules with γ-tubulin:GTP or γ-tubulin:GDP, separating the microtubules by centrifugation, and looking for γ-tubulin association as a function of nucleotide state. Future experiments should also explore the use of sheared or GMPCPP taxol-stabilized microtubules, to increase the number of minus ends and any signal resulting from interactions with minus ends. Based on high functional and structural conservation between γ-tubulin and β-tubulin (Chapter 4), it is predicted that GTP

hydrolysis will be facilitated by γ-tubulin/microtubule interactions and γ-tubulin/microtubule interactions will be stronger with GTP than with GDP.

The structure of recombinant γ-tubulin provides a unique opportunity to study the chemistry of GTP hydrolysis by a tubulin. Site-directed mutagenesis can be guided by the structure of the γ-tubulin:GTPγS complex in order to create mutants which can be subsequently assayed for GTP hydrolyzing activity, in an effort to understand the mechanism of hydrolysis. The structure may also be used to possibly create analog-sensitive alleles[73] in order to be able to selectively study the role of GTP binding and hydrolysis in γ-tubulin function, both in vitro and in vivo.

Materials and Methods

Protein purification. Pure human γ-tubulin was expressed and purified as described in Chapter 1. Drosophila γ-TuRC was purified by Michelle Moritz as described in [35].

GTP hydrolysis. Experiments were performed as follows: Freshly prepared γ-tubulin (see Chapter 1) in the gel filtration buffer (50mM K-MES pH6.6, 500mM KCl, 5mM $MgSO_4$, 1mM EGTA, 1mM DTT) or buffer alone was mixed with α-^{32}P-GTP (400 Ci/mmol; 10mCi/ml) on ice. This mixture was then incubated at 37° C. 1 μl time-points were removed, spotted on a TLC plate, and allowed to air dry. TLC-spotted reactions products were separated in a TLC chamber equilibrated with 0.6M KH_2PO_4, pH 3.4. Reactions products were visualized and quantified with a Phosphorimager (Storm 840, Molecular Dynamics), allowing for background correction (see text). Experiments were performed using 3.3 μM monomeric γ-tubulin and a range of initial GTP concentrations

(Figure 1). Curves were fitted via Michaelis-Menten to extract rates (Table 1). Buffer conditions for γ-TuRC GTP hydrolysis experiment was identical to that used during immuno-purification of γ-TuRC[36]. Buffer conditions for taxol-stabilized microtubule GTP hydrolysis experiments were identical to those at which microtubule assembly is monitored (Chapter 2)

γ^{32}P-labeled N_3-GTP crosslinking. Freshly prepared monomeric γ-tubulin was dialyzed to remove DTT, which reduces the crosslinking efficiency of the azido group. 2 μl 26μM γ^{32}P-labeled N_3-GTP (0.5mCi/ml) (ALT, Inc., Lexington, KY) was mixed with 2 μl 5mM competing cold nucleotide or buffer. 1 μl of this mixture was added to 15 μl of a 3μM monomeric γ-tubulin solution. The solution was incubated for 30 minutes on ice and crosslinked with a 30 second exposure to a Saran wrap-covered 312 nm UV lamp. Samples were separated by SDS-PAGE and visualized with a Phosphorimager as before.

To determine whether or not αβ-tubulin effected γ-tubulin GTP hydrolysis, an experiment similar to the previous N_3-GTP experiment was set up, with the following modifications: After mixing buffer with γ^{32}P-labeled N_3-GTP and irradiating as above, the solution was dialyzed for 1 hour at 4°C in an attempt to remove excess nucleotide. αβ-tubulin was then added to a final concentration of 11μM and the mixture was incubated at 37°C. Time points were boiled in SDS sample buffer for 5 minutes, separated by SDS-PAGE and visualized with a Phosphorimager as before.

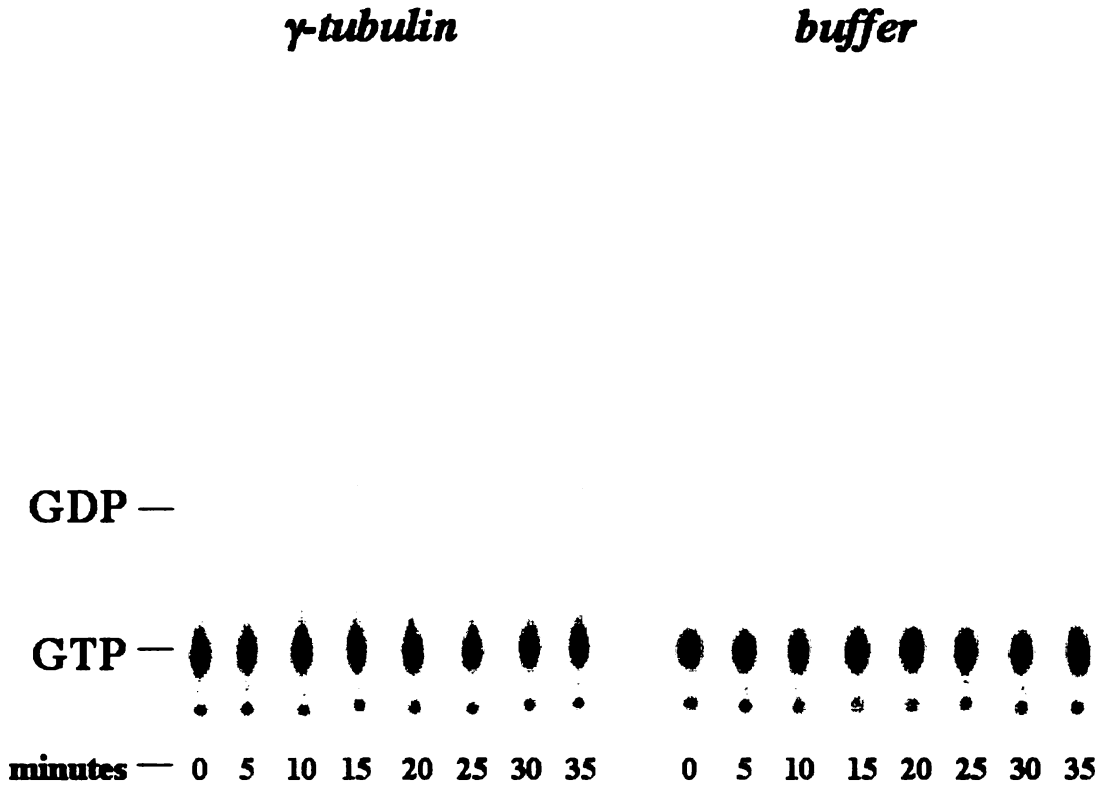

Figure 1A. Monomeric γ-tubulin can hydrolyze GTP. Example of TLC-separated α-^{32}P-labelled GTP hydrolysis products at different time points.[γ-tubulin]=3.3μM, [GTP]=300μM.

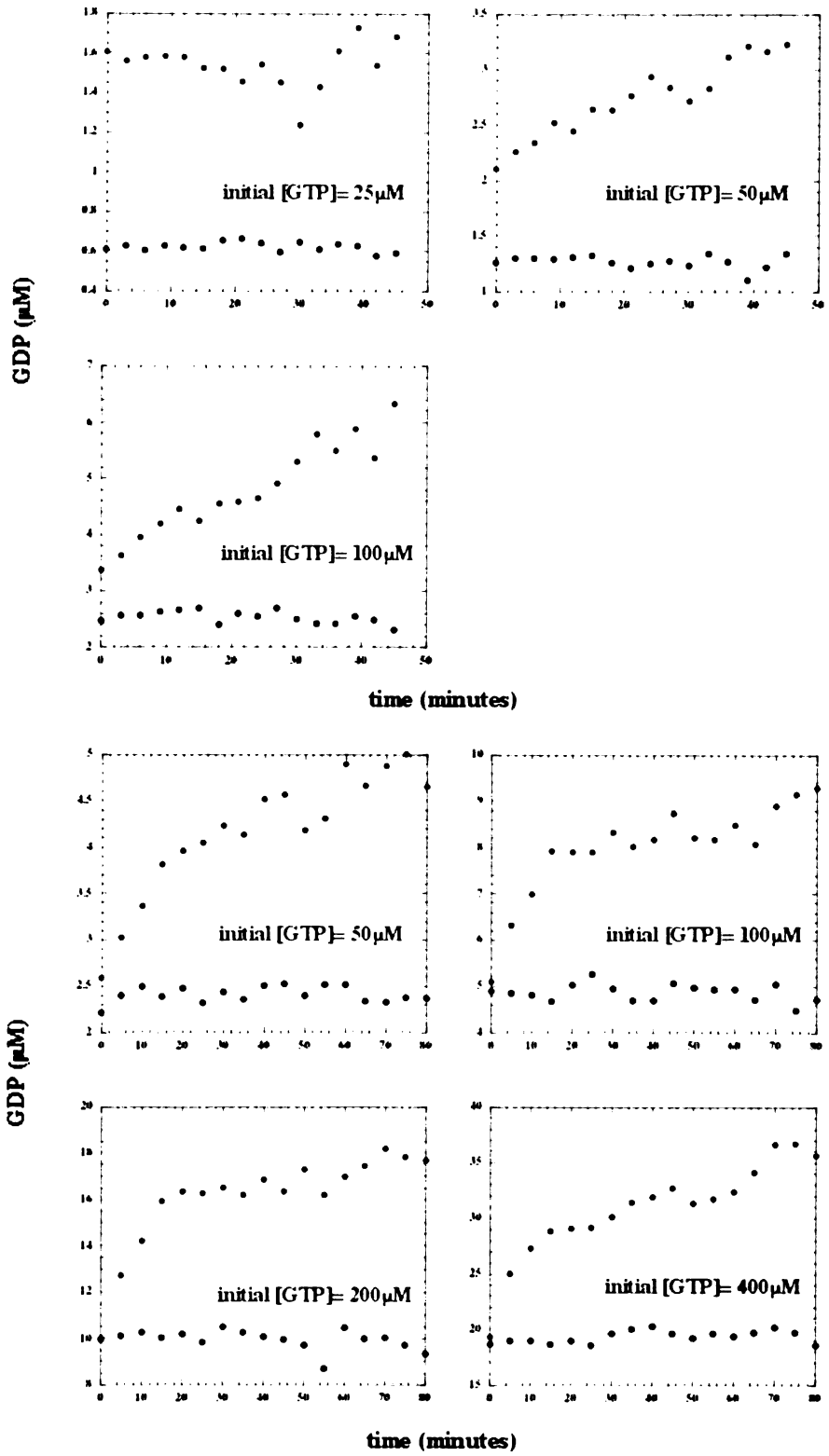

Figure 1B. 3.3μM monomeric γ-tubulin can hydrolyze GTP. Quantitation of TLC separated GTP hydrolysis products. γ-Tubulin in red, buffer alone in blue.

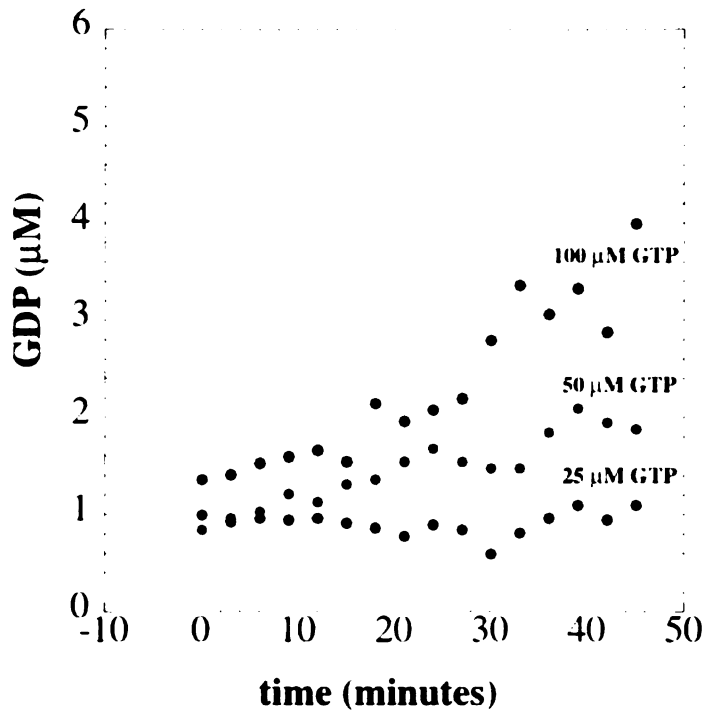

Figure 1C. Monomeric γ-tubulin can hydrolyze GTP. Background corrected plot. [γ-tubulin]=3.3 μM. [GTP]=25μM, 50μM, 100μM.

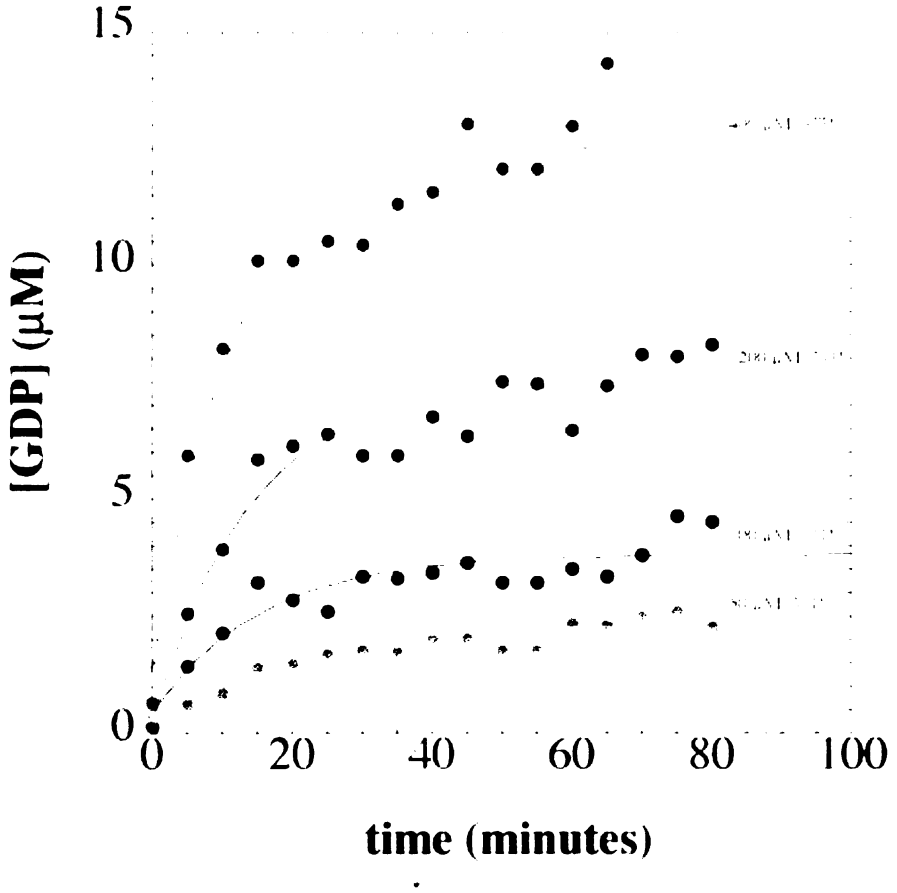

Figure 1D. Monomeric γ-tubulin can hydrolyze GTP. Background corrected plot and curve fits. [γ-tubulin]=3.3 μM. [GTP]=50μM, 100μM, 200μM, 400 μM

([γ-tubulin] = 3.3μM)

Initial [GTP] (μM)	Rate (μM/min.)
50	**0.032 (±0.008)**
100	**0.066 (±0.018)**
200	**0.073 (±0.013)**
400	**0.085 (±0.015)**

Table 1. Monomeric γ-tubulin-mediated GTP hydrolysis rates.

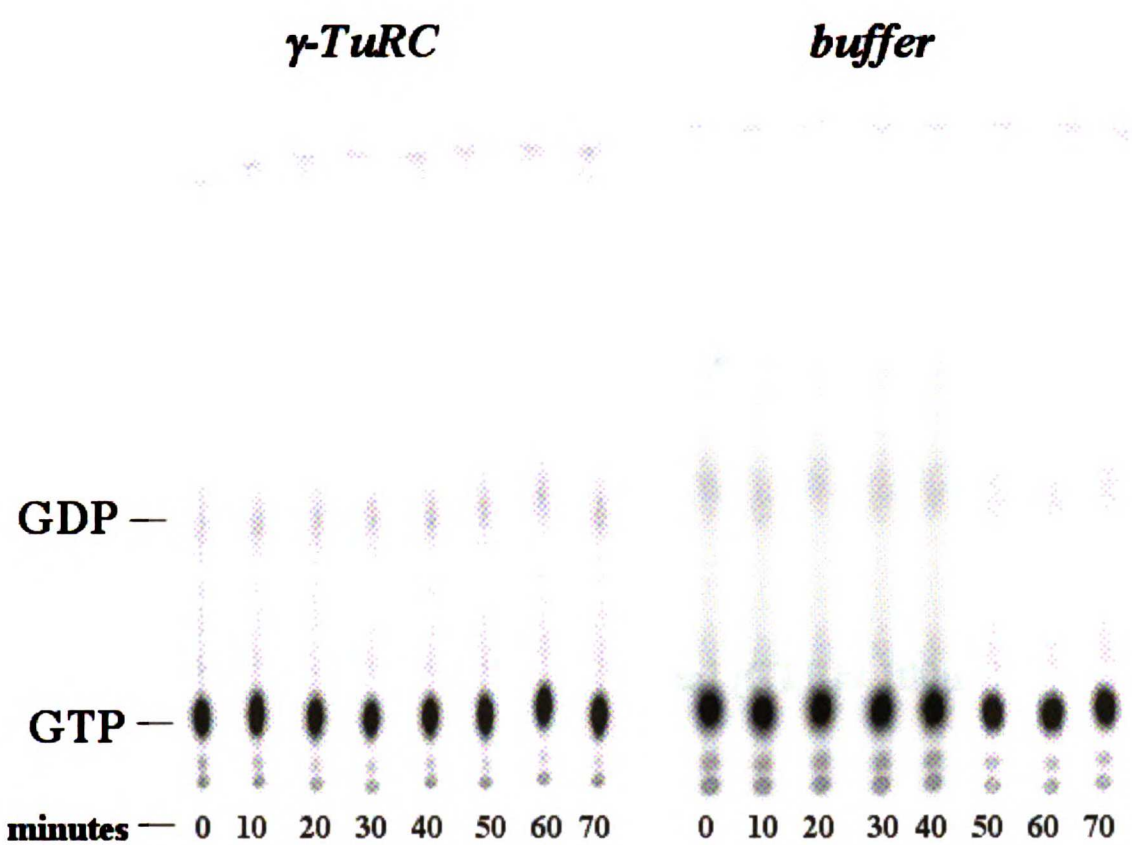

Figure 2A. Semi-purified Drosophila γ-TuRC can hydrolyze GTP.

TLC-separated α-^{32}P-labelled GTP hydrolysis products at different time points.

[γ-TuRC]=~100nM ([γ-tubulin]=~1.3 μM), [GTP] = 100 μM.

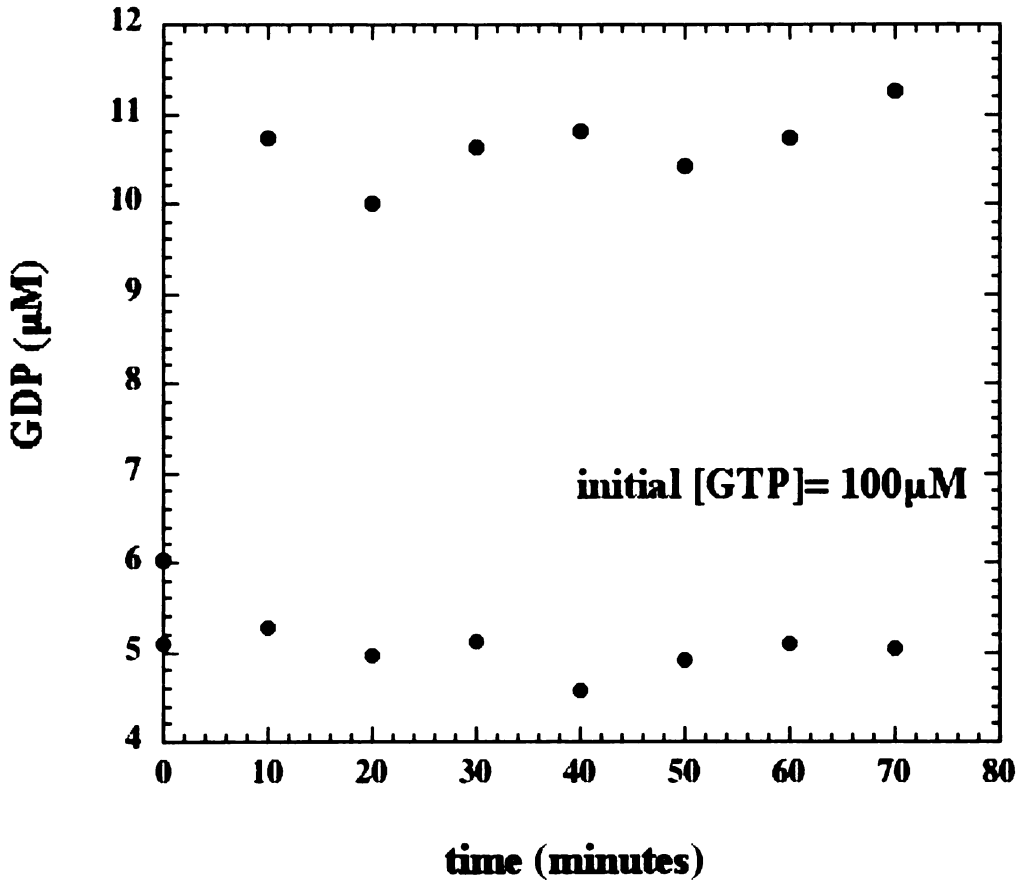

Figure 2B. Semi-purified Drosophila γ-TuRC can hydrolyze GTP.

Quantitation of γ-TuRC GTP hydrolysis products. γ-TuRC in blue, buffer alone in red. [γ-TuRC]~100nM ([γ-tubulin]~1.3μM).

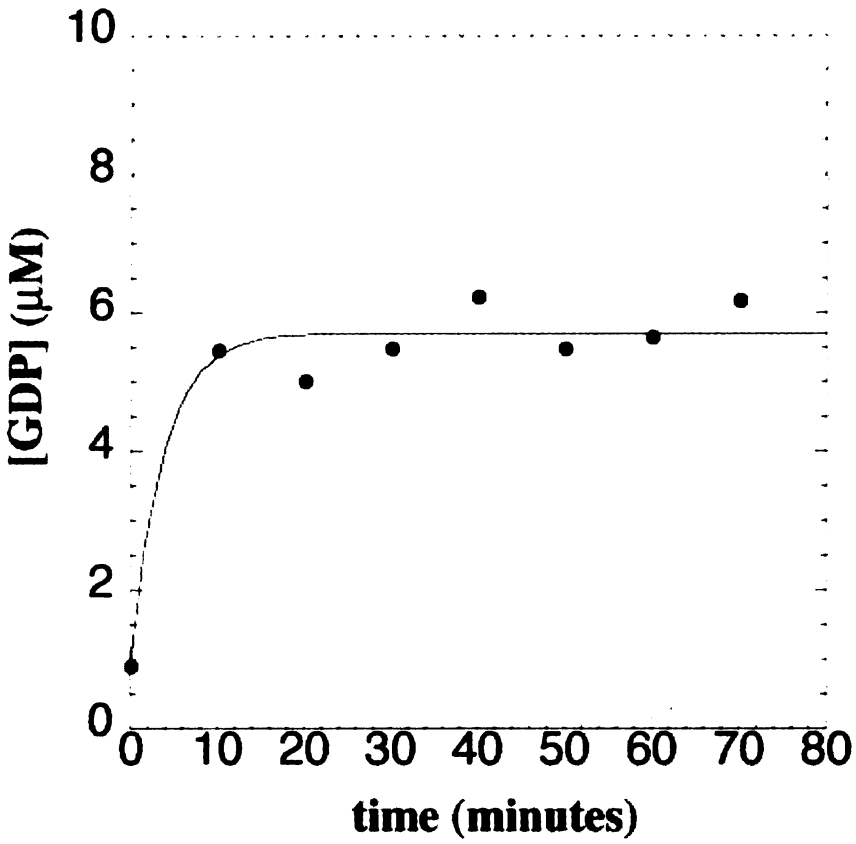

Figure 2C. Semi-purified Drosophila γ-TuRC can hydrolyze GTP.

Background corrected plot of γ-TuRC GTP hydrolysis. Curve fitting yielded a rate of 0.27 (±0.15) μM/min.

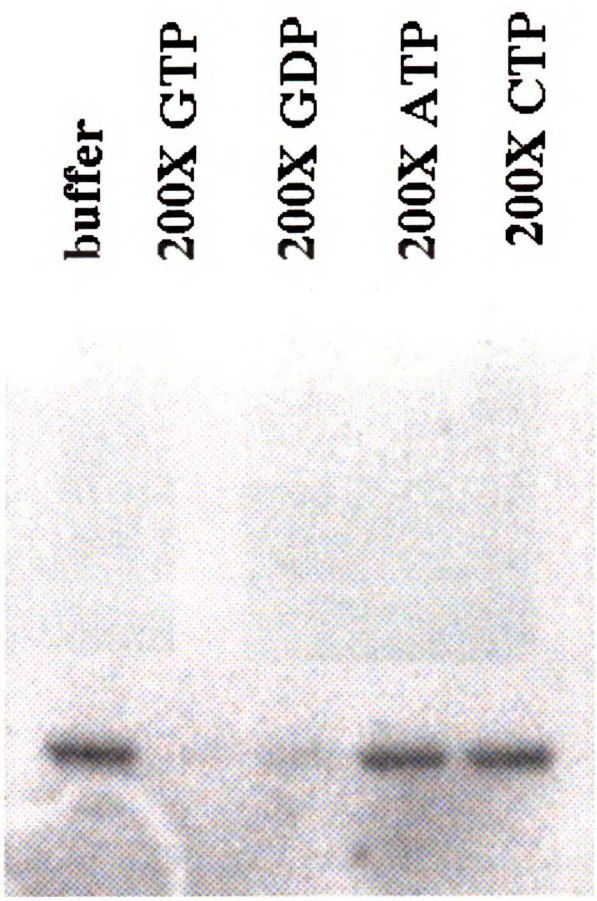

Figure 3. γ^{32}P-labeled N_3-GTP can be specifically crosslinked to monomeric γ-tubulin. Excess cold GTP or GDP, but not ATP or CTP, could compete off N_3-GTP.

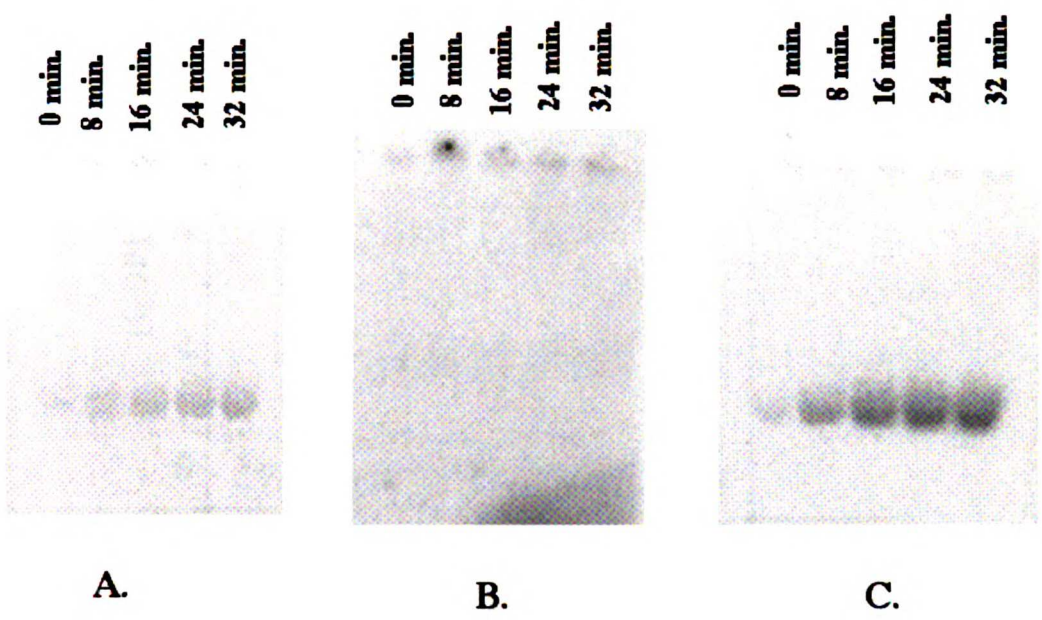

Figure 4. UV-irradiation and dialysis is not sufficient to remove excess active γ^{32}P-labeled N_3-GTP

A. γ-tubulin: N_3-GTP + αβ-tubulin

B. γ-tubulin: N_3-GTP + buffer

C. buffer: N_3-GTP + αβ-tubulin

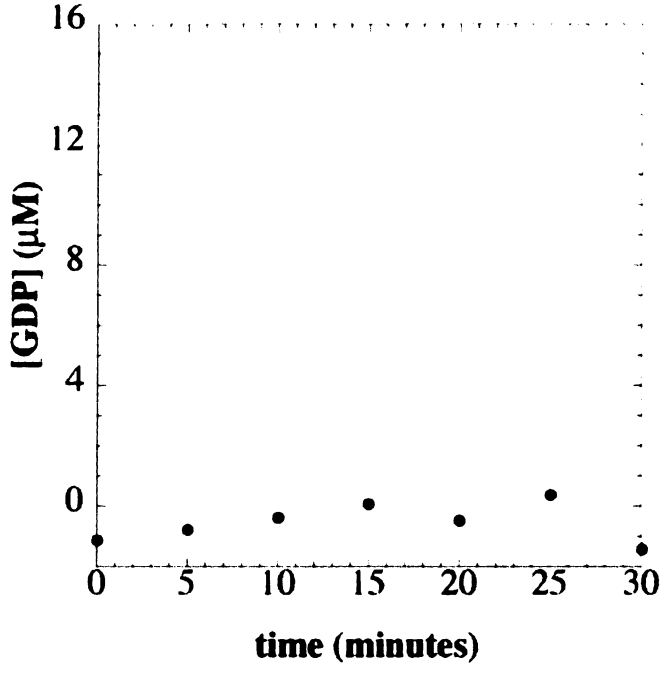

Figure 5. Taxol-stabilized microtubules do not hydrolyze GTP. Background-corrected plot. [αβ-tubulin]=10μM, [GTP]=100μM.

Chapter 3:

Mechanisms of Microtubule Nucleation by Human γ-Tubulin

Preface

The following chapter is a version of a manuscript that has been submitted for publication in PloS Biology and is currently under revision. The work represents a collaboration between Michelle Moritz, Luke Rice, and myself. I purified and characterized the recombinant γ-tubulin, Michelle carried out the nucleation assays and the subsequent analysis, and Luke Rice participated in the data analysis, both directly and through the development of software to expedite the analysis. We all participated in experimental design, troubleshooting, and developing a molecular interpretation of the kinetic model. In its presented form, Michelle and Luke share first authorship and I am second author.

Synopsis

Microtubule assembly begins with the thermodynamically unfavorable formation of small α/β-tubulin oligomers. Rapid elongation of the microtubule does not occur until a stable oligomer of a certain size, termed the nucleus, is formed. While this process can occur in vitro from pure α/β-tubulin, in vivo it appears to require γ-tubulin, which is the major constituent of the γ-tubulin ring complex (γTuRC), a ~2.2 MDa protein complex that nucleates microtubules at the centrosome. We have performed a detailed kinetic analysis of the microtubule-nucleating activity of pure, recombinant human γ-tubulin. Our results indicate that at low (60-100 nM) concentrations, γ-tubulin is tetrameric and acts as a classic enzyme catalyst, accelerating the rate of nucleus formation rather than decreasing the nucleus size. However, at higher concentrations (670 nM), γ-tubulin formed large oligomers that facilitated microtubule nucleation by decreasing the size of the nucleus. The oligomerization-state dependence of γ-tubulin's mechanism may provide insight into the mechanism of microtubule nucleation by γTuRC, which is the major higher-order γ-tubulin assembly in cells.

Introduction

Microtubule assembly involves 'nucleation-elongation' behavior, in which initiation of a new polymer depends on the thermodynamically unfavorable formation of small oligomers of α/β-tubulin heterodimers. Above a certain size, these oligomers become thermodynamically stable, and polymer growth proceeds rapidly by α/β-tubulin heterodimer addition. We refer to the smallest stable tubulin oligomer, which represents the rate-limiting species for microtubule initiation, as the nucleus. Although microtubule nucleation and polymerization can occur in vitro from pure α/β-tubulin, inside most cells the process requires a specific nucleating site, such as the centrosome. A large body of genetic and biochemical evidence indicates that the tubulin isoform γ-tubulin is the key factor required for microtubule nucleation at these specialized sites in cells (reviewed in [65, 74-76]).

γ-Tubulin is not found as a free monomer in the cell; instead, it forms two major highly conserved complexes with a group of at least six additional proteins. The smaller complex is a heterotetramer consisting of two copies of γ-tubulin and one copy each of the related accessory proteins GCP2/Dgrip84/Spc97 and GCP3/Dgrip91/Spc98. Current biochemical and electron microscopy evidence suggests that six or seven of these small complexes assemble with at least four accessory proteins to form the large, ~2.2 MDa γ-tubulin ring complex (γTuRC). The γTuRC, perhaps acting in concert with additional proteins at the centrosome, is thought to be the active protein complex for microtubule nucleation, although the γ-tubulin small complex (γTuSC) has weak activity in vitro (reviewed in [77-79]). In *Saccharomyces cerevisiae*, the smaller γ-tubulin complex (Tub4

complex) is the major species isolated from cells and also has weak nucleating activity in vitro. It is possible that it forms a higher-order complex at the spindle pole body [38, 39].

Early clues concerning the mode of action of the γTuRC came from structural and biochemical work. In the electron microscope, γTuRCs in isolation and bound to the minus end of microtubules exhibited a domed lockwasher shape with a diameter identical to that of microtubules [33, 41, 42]. Furthermore, in activity assays, the γTuRC displayed a potent ability to cap and prevent polymerization at microtubule minus ends [33, 43]. Taken together, this suggested that the γTuRC may act as a template upon which microtubules assemble [33, 41-43]. An alternative model proposes that the γTuRC may function in microtubule nucleation by unraveling and acting as the first protofilament of the microtubule, or by stabilizing the first protofilament [40, 66]. These two models differ greatly in their proposed mechanism, and in particular in the way they envision the multiple copies of γ-tubulin interacting with each other and with α/β-tubulin. The template model proposes a laterally-interacting array of γ-tubulins, analogous to the lateral interactions of α- or β-tubulins in adjacent protofilaments. In contrast, the protofilament model proposes that the γ-tubulins interact longitudinally, similarly to the longitudinal interactions of α/β-tubulins in the same protofilament.

Although evidence indicates that γ-tubulin complexes carry out microtubule nucleation in vivo, almost nothing is known about the kinetic mechanism of this process. Leguy et al [46]showed that human γ-tubulin partially-purified from a reticulocyte expression system nucleated microtubules in vitro. Their evidence suggested that γ-tubulin did so by decreasing the size of the nucleus. Leguy et al also concluded that a single molecule of γ-tubulin bound to the minus end of the microtubule was sufficient for

nucleation and also blocked this end from polymerizing. While intriguing, their studies were limited by the small amount of γ-tubulin available from reticulocyte lysates, making it impossible for them to examine the activity of γ-tubulin over a broad range of concentrations. From recently determined biochemical properties of pure γ-tubulin (Chapter 1), we know that γ-tubulin can adopt multiple oligomerization states, making it imperative to understand in detail the activity of each state. In addition, in analyzing their data Leguy et al [46] relied on a kinetic model originally developed for actin polymerization [62, 80]. Microtubules have an intrinsically more complicated structure than actin filaments, and previous work has shown that the relatively simple kinetic model used for actin cannot account for the complexity present in the microtubule assembly data. Thus, we were interested in re-examining the nucleation activity of purified γ-tubulin in different oligomerization states as a prelude to studying the activity of the γ-tubulin complexes γTuSC/Tub4 and γTuRC.

Using baculovirus-infected insect cells, it is now possible to obtain milligram quantities of very pure recombinant human γ-tubulin (Chapter 1). Here we describe how this has allowed the identification of detailed, kinetic mechanisms of γ-tubulin-mediated microtubule nucleation in vitro. Throughout our study, a kinetic model developed specifically for microtubule assembly [63, 81, 82] has been used for data interpretation. This model exploits an intrinsic property of the polymerization data, known as "scaling" (see below), to dramatically simplify the possible set of kinetic equations, thereby allowing the true kinetic pathway to be determined without having to make specific, and potentially erroneous geometric assumptions about the size or assembly pathway of the nucleus. In particular, it represents a generalization of the Oosawa model [62, 80] used to

describe actin assembly in that it allows an arbitrary number of rate-limiting steps prior to nucleus formation. The model provides a generic set of kinetic equations describing the assembly process and can be fit very well to previously published tubulin polymerization data [61, 63, 81, 82].

By applying the Flyvbjerg analysis to our own microtubule assembly data with and without low nanomolar amounts of γ-tubulin, a condition under which γ-tubulin forms a tetramer (Chapter 1), we found that γ-tubulin does not change the assembly pathway, and therefore does not alter the nucleus size. Instead, at low concentrations, γ-tubulin acts by accelerating the rate at which the nucleus is formed. At a higher concentration where γ-tubulin forms larger oligomers, significantly higher microtubule nucleation activity was observed, and a different assembly pathway was used. Under these conditions, the assembly curves showed a lower α/β-tubulin concentration dependence, indicating a smaller nucleus. We believe that the more potent nucleation activity of the γ-tubulin polymers stems from a regular, ordered array of γ-tubulin monomers in a geometry conducive to stabilizing lateral associations between small oligomers of α/β-tubulin. A similar principle may underlie the increased activity of the γTuRC compared to the γTuSC.

Results and Discussion

Pure γ-tubulin nucleates microtubules in vitro.

To work toward a detailed understanding of the kinetic mechanism of microtubule nucleation by the γTuRC, we began by exploring the activity of human γ-tubulin expressed in baculovirus and purified to homogeneity. This recombinant expression

system allowed the isolation of large quantities of fresh γ-tubulin (~1 mg from 1L of Sf9 cells), which were required to explore its nucleation activity fully over a broad range of γ- and α/β-tubulin concentrations in a single day.

The polymerization of α/β-tubulin in the presence or absence of nanomolar concentrations of γ-tubulin was followed using a light-scattering assay. The turbidity recorded is proportional to the amount of tubulin polymerized, and therefore provides a convenient way to monitor microtubule assembly as a function of time [61, 63, 81, 82]. A typical dataset illustrates that γ-tubulin consistently accelerated microtubule assembly, as evidenced by the decreased lag-time before rapid microtubule elongation occurred (Fig. 1). This was the case at all concentrations of α/β-tubulin (6-20 μM) and of γ-tubulin (60-670 nM) tested (Fig. 1, 3, 4, and data not shown). Samples of the reaction mixtures at their plateaus were fixed and examined in the electron microscope to confirm that the turbidity reflected the formation of microtubules and not other types of tubulin oligomers (data not shown). Control reactions without α/β-tubulin demonstrated that, as expected, 100 nM γ-tubulin did not in itself contribute to the turbidity (data not shown).

γ-Tubulin tetramer accelerates the rate of microtubule nucleus formation without changing the nucleus size.

We first confirmed that the analysis developed by Flyvbjerg et al [61, 63, 81, 82] for the spontaneous nucleation of microtubules from pure α/β-tubulin gave the same results in our hands as were previously published (data not shown). This analysis is based on two primary features of the microtubule assembly data: the number of rate-limiting steps (as determined by the power-law growth behavior of the curves at early

times), and the concentration dependence of the characteristic time ($T_{0.1}$), which is the time it takes to reach 10% of the final reaction. Flyvbjerg et al. (1996, 1997) found that the microtubule assembly curves of Voter and Erickson were characterized by at least two rate-limiting steps prior to forming the nucleus, and by an inverse cubic relationship between the $T_{0.1}$ and the initial concentration, which indicated that successive intermediates differed by three α/β-tubulin heterodimers.

We next applied the Flyvbjerg analysis to our γ-tubulin and control polymerization data (Fig. 1) in a semi-automated manner using a program that we developed for this purpose. For each dataset, we first had to determine whether the data from all polymerization reactions could scale together. If the data scale, this means that a single assembly mechanism is followed at all tubulin concentrations [61, 63, 81, 82], and that we can use the Flyvbjerg model to fit our data. For this analysis, the characteristic plateau value (A_∞) and $T_{0.1}$ were extracted, and the assembly curves were then plotted as A/A_∞ and $T/T_{0.1}$ (Fig. 2A). The polymerization reactions followed in the presence or absence of γ-tubulin (Fig. 1) indeed exhibited this scaling property (Fig. 2A). This phenomenon was observed in eight separate experiments done on different days and with different preparations of γ- and α/β-tubulin.

Once it was verified that the microtubule assembly data scale, it remained to extract the dependence of the characteristic time ($T_{0.1}$) on the initial concentration of α/β-tubulin, and the power-law growth of the curves at early times. Both with and without γ-tubulin, the $T_{0.1}$ was shown to have an inverse cubic relationship with the initial α/β-tubulin concentration (Fig. 2B). This result is consistent with earlier studies of the behavior of pure α/β-tubulin [61, 63, 81, 82].

The power-law growth characteristic of the curves at early times is directly related to the number of rate-limiting intermediates. As discussed by Flybjerg et al., this parameter is more difficult to extract from the raw data than the concentration dependence of the $T_{0.1}$. Thus, we chose to determine it empirically by performing global fits of kinetic models with different numbers of rate-limiting steps, selecting the model with the fewest kinetic steps that best fit the data. The γ-tubulin and control data were both best described by a model allowing two rate-limiting intermediates before the nucleus, with three α/β-tubulin heterodimers adding at each step (see fits in Fig. 2C), the latter confirming the results of the concentration-dependence plots. Thus, both data sets show a nucleus size of twelve α/β-tubulin heterodimers. The equations describing this model are as follows:

$$\frac{dc_1}{dt} = f_0 c^6 - f_1 c_1 c^3$$

$$\frac{dc_2}{dt} = f_1 c_1 c^3 - f_1 c_2 c^3$$

$$\frac{d\nu}{dt} = f_1 c_2 c^3$$

$$\frac{dc}{dt} = -f_3 \nu\, c$$

where c denotes the α/β-heterodimer concentration, c1, c2, and ν denote respectively the concentrations of the first and second rate-limiting intermediates, and of the nucleus. f_0 and f_1 are the rate constants that describe the rates at which rate-limiting intermediates are formed from their precursors, and f_3 is the rate constant describing elongation by α/β-heterodimer addition. Thus, we conclude that γ-tubulin tetramers do not act by decreasing the nucleus size, but instead accelerate the rate of nucleus formation.

Analysis of the rates of formation of the two intermediates revealed that the second rate is affected, indicating that γ-tubulin binds to the second intermediate (Table 1).

The mechanism of microtubule nucleation changes with higher concentrations and larger oligomers of γ-tubulin.

We wanted to explore the concentration dependence of γ-tubulin activity, particularly since our earlier γ-tubulin dose-response study indicated a complex mechanistic behavior (Chapter 1). At both 170 and 670 nM, γ-tubulin was a substantially more potent nucleator than it was at 100 nM (compare Figs. 1, 3, 4). Moreover, at 670 nM, in addition to tetramers, γ-tubulin formed much larger oligomers, as measured by sucrose gradient sedimentation (Chapter 1). Since tetramers are the preferred configuration of γ-tubulin at low nanomolar concentration and low ionic strength, and based on the appearance and dimensions of γ-tubulin filaments in the electron microscope, we assume that the tetramers assemble into filaments as they become more and more concentrated (Chapter 1). In order to determine the parameters of the kinetic mechanism, microtubule assembly data at a range of initial α/β-tubulin concentrations are required. This requirement rules out simple dose-response experiments performed at a single concentration of α/β-tubulin, so instead we performed an analogous experiment to that shown in Fig. 1, collecting a series of assembly curves using 670 nM γ-tubulin and a variety of α/β-tubulin concentrations.

When the microtubule assembly data sets obtained in the presence or absence of 670 nM γ-tubulin were analyzed, we found that, unlike for 100 nM γ-tubulin, microtubule nucleation activity was achieved by lowering the α/β-tubulin concentration-dependence

of the reaction (Fig. 4C). In other words the nucleus size was decreased from 9 to 6 α/β-tubulin heterodimers in the presence of 670 nM γ-tubulin. In the previous experiment the nucleus size was 12 for both buffer- and 100 nM γ-tubulin-containing reactions. In the 670 nM γ-tubulin experiment, the nucleus size was 9 for the buffer data. We believe this difference in nucleus size in the control reactions from the different experiments is due to small variations in ionic strength between the two experiments (data not shown), which affect the number of intermediates. Flyvbjerg saw similar variations in nucleus size [61, 63, 81, 82]. However, it is important to note that although nucleus size can vary slightly on different days, tetrameric γ-tubulin was always found to accelerate the rate of nucleation and not change the size of the nucleus compared to the buffer control, and large oligomers of γ-tubulin were always found to decrease the nucleus size. In contrast, the number of heterodimers added per step is less sensitive to the buffer conditions.

Nucleus formation in the presence or absence of 670 nM γ-tubulin occurred through one intermediate via the association of dimers (n=2) of α/β-tubulin heterodimers in the γ-tubulin-containing reaction and trimers (n=3) in the case of the buffer control (Fig. 4C,D). The model equations describing the behavior of the buffer-control reaction and for the reactions containing 670 nM γ-tubulin are as follows:

$$\frac{dc_1}{dt} = f_0 c^{2n} - f_1 c_1 c^n$$

$$\frac{d\nu}{dt} = f_1 c_1 c^n$$

$$\frac{dc}{dt} = -f_3 \nu c$$

where c denotes the α/β-heterodimer concentration, c_1 and ν denote respectively the concentrations of rate-limiting intermediates, and of the nucleus. f_0 and f_1 are the rate constants that describe the rates at which rate-limiting intermediates are formed from their precursors, and f_3 is the rate constant describing elongation by α/β-heterodimer addition (Table 2).

Thus, large polymers of γ-tubulin act as potent microtubule nucleators by decreasing the nucleus size. Based on our kinetic analysis, we believe that this occurs via the stabilization of smaller oligomers of α/β-tubulin as well as through a decrease in the number of intermediates that must form prior to the nucleus.

Molecular interpretations of how different oligomers of γ-tubulin may facilitate microtubule nucleation via different mechanisms.

Our analysis of microtubule nucleation kinetics revealed that γ-tubulin acts by different mechanisms at different concentrations, most likely due to changes in its oligomerization state. As a tetramer it has moderate nucleation activity, achieved by accelerating the rate of nucleus formation, but as a large polymer it displays potent nucleation activity, achieved by decreasing the nucleus size. Given the known physical properties of pure γ-tubulin in vitro (Chapter 1), and structural evidence for a likely mode of γ-tubulin assembly (Chapter 4), we can begin to model how it might interact with α/β-tubulin to facilitate microtubule nucleation. If we take into account the thermodynamic arguments for the likely configurations of α/β-tubulin oligomers [83, 84]we can limit further the number of models to consider.

The best-fitting model to the tetrameric γ-tubulin nucleation data indicated that γ-tubulin binds to the second intermediate before the nucleus, which is likely to consist of three trimers of α/β-tubulin heterodimers. Based on thermodynamic arguments [83, 84], a reasonable arrangement of these heterodimers is in three, short protofilaments that are laterally associated (Figure 5).

In order to speculate how γ-tubulin might stabilize such an intermediate, the architecture and relevance of the tetramer should be considered. A tetramer of γ-tubulin could recognize such a structure by interacting with the two interprotofilament spaces (Figure 6, left), a type of interaction not previously considered which has interesting biological consequences (see below). However, the functional relevance of tetramerization is unknown, making it possible that a single γ-tubulin molecule of a given tetramer is responsible for its microtubule nucleating activity. A single γ-tubulin could interact with a modified model of the second intermediate, composed of two short protofilaments and a third L-shaped trimer (Figure 6, right).

These models can be extended to explain how larger oligomers of γ-tubulin might facilitate microtubule nucleation as well. The best fits to our data obtained using 670 nM γ-tubulin indicated one pre-nucleus rate-limiting intermediate assembled from dimers of α/β-tubulin heterodimers. The large γ-tubulin oligomers that form under these conditions may stabilize lateral interactions between α/β-tubulins, which are known to be weak [83, 84](Figure 7). In comparison, smaller oligomers of γ-tubulin presumably do not bind sufficiently tightly to stabilize dimers of α/β-tubulin heterodimers, and so trimers must co-assemble to form the pre-nuclear intermediates.

Crystallographic analyses of human γ-tubulin reveal lateral crystal packing interactions which are likely to be physiologically relevant (Chapter 4). It is therefore possible that tetramerization is not functionally relevant, since such lateral interactions are difficult to reconcile with the architecture of a closed homo-tetramer (Chapter 1). If this is so, then a speculative model for higher-order oligomers in which tetramers interact with one another through lateral interactions is possible (Figure 8). A definitive model for the γ-tubulin filament, however, awaits a detailed structural analysis (see Postscript).

The interprotofilament-binding model for γ-tubulin/αβ-tubulin interactions has interesting biological consequences. Assuming a template mode of action, interprotofilament interactions would solve the problem of how the γ-TuRC, which most likely contains an even number of γ-tubulins (12 or 14), nucleates microtubules with an odd number of protofilaments, plus a seam. However, high-resolution crystallographic analysis of human γ-tubulin reveals that many structural features of α-, and β-tubulin are conserved (Chapter 4). Among these is a lateral mode of recognition, as mentioned above, suggesting γ-tubulin is also capable of microtubule-like longitudinal interactions. Such an interaction could also potentially make use of GTP binding and hydrolysis as a means to regulate longitudinal contacts, as in a microtubule (Chapter 4). It has also been shown that γ-tubulin can bind to γ-TuRC components other than the γ-TuSC[50]. This led to a model in which not all γ-tubulins are γ-TuSC bound, allowing for an odd number of γ-tubulins within the γ-TuRC and way to specify the assembly of a 13-protofilament microtubule while maintaining longitudinal-like contacts between γ-tubulin and the microtubule.

Our ability to purify relatively large quantities of γ-tubulin should allow a more detailed cross-linking study to be performed so that we can directly test whether γ-tubulin interacts with α/β-tubulin in microtubules in an interprotofilament or a longitudinal-like manner. High-resolution electron tomographic studies should also provide structural evidence of the nature of the interaction between γ-tubulin and microtubule protofilaments.

In a previous study in which the nucleation potential of sub-nanomolar concentrations of partially-purified γ-tubulin was explored, Leguy et al [46] concluded that monomeric γ-tubulin binds with high affinity to microtubule minus ends and nucleates microtubules by decreasing the nucleus size. Unlike Leguy et al, we did not observe nucleating activity for γ-tubulin at sub-nanomolar concentrations. In our hands, low (~3-10) nanomolar γ-tubulin was the lowest concentration for which activity was consistently measurable. Given the imprecision of determining γ-tubulin concentration by Bradford assays (this study) or gel-band intensity [46] however, it is difficult to compare the exact amounts of γ-tubulin used in the two studies. They may in fact be the same at the lower concentrations we tested. More importantly, however, we found that γ-tubulin only exists as a monomer if kept at high ionic strength (0.5 M KCl) (Chapter 1), and so we were not able to test its nucleating capacity due to limitations with the microtubule assembly assay. Considering this, and the fact that the sizing column used by Leguy et al (Superose 6) was not optimal for resolving a monomer of ~50 kDa, it is possible that the γ-tubulin in their study was not in fact monomeric, and was instead in a complex with itself or other proteins. The oligomerization properties of γ-tubulin certainly seem to be complex and very sensitive to ionic strength and pH.

Another potential inconsistency between our study and that of Leguy et al involves their conclusion that low nanomolar γ-tubulin acts by decreasing the nucleus size. The current study shows that this change in assembly mechanism is not evident until large polymers of γ-tubulin form at higher concentrations. This discrepancy does not arise from the very different nucleation models that were employed to explain the turbidity data. Leguy et al relied on a now classic theory of actin nucleation [62, 80], which does not adequately describe microtubule nucleation [61], while we chose a model that was specifically developed for this purpose [63, 81, 82]. When we model our low-concentration γ-tubulin data using the Leguy (Oosawa) approach, however, we still find no difference in mechanism or nucleus size between the γ-tubulin and control data (not shown). Interestingly, the nucleation mechanism we arrived at for our γ-tubulin filament data does agree with the mechanism Leguy et al concluded was operating for their γ-tubulin. Alternatively, it is also possible that the γ-tubulin in the Leguy experiment was associated with accessory proteins from the reticulocyte lysate that enhanced its activity, bringing it into agreement with our results with large γ-tubulin polymers. In any case, both studies show that γ-tubulin can be a potent nucleator of microtubules in vitro. Comparisons of this activity with that of γ-TuRC isolated from Drosophila embryos has shown that this active concentration range is relevant to γ-TuRC function (data not shown).

Our studies of the oligomerization and microtubule nucleation behavior of pure γ-tubulin in vitro have provided valuable working models for pursuing the mechanisms of the γTuRC and γTuSC/Tub4 complexes, and ultimately the centrosome/spindle pole body. Important questions such as the roles of GTP binding and hydrolysis in these

processes and their more complicated counterparts in vivo must also be answered. Furthermore, the molecular origin of the complex assembly kinetics remains unknown. Nevertheless, the basic understanding of γ-tubulin-mediated microtubule nucleation we have gained here gives a first glimpse of the molecular basis of the process, and allows us to work toward a more detailed understanding of the detailed kinetic mechanisms used by the macromolecular machines and modulators that govern the microtubule cytoskeleton in vivo.

Materials and Methods

Purification of γ-tubulin and determination of its oligomerization state

Human γ-tubulin C-terminally tagged with Myc and His_6 epitopes [68] was generated in Sf9 insect cells using a baculovirus expression system and purified on Ni-NTA Superflow resin (Qiagen) followed by Superdex 200 gel filtration as described previously (Chapter 1). The oligomerization state of γ-tubulin under nucleation assay conditions (100 nM γ-tubulin in 50 mM K-MES, pH 6.6, 5 mM $MgSO_4$, 1 mM EGTA, 1mM GTP) was determined by gel filtration on Superdex 200 and sucrose gradient (2-16%) sedimentation as described (Chapter 1).

Microtubule nucleation assays

To study the microtubule-nucleating activity of pure, recombinant human γ-tubulin *in vitro*, polymerization of phosphocellulose-purified bovine-brain tubulin in the presence or absence of γ-tubulin or γTuRC was followed by turbidity at 350 nm basically as described previously [61, 70]. Care was taken to remove microtubule seeds and inactive protein from the tubulin to be used for nucleation assays by cycling it through an

additional polymerization/depolymerization step. Immediately prior to performing assays, tubulin was taken from –80°C storage and rapidly thawed in a 37°C water bath. After thawing, it was placed on an ice-water slurry (0°C), the buffer was adjusted to 80 mM K-PIPES, pH 6.8, 1mM EGTA, 4 mM $MgCl_2$ and 1 mM GTP. After 5 min incubation, a half-volume of 37°C glycerol was mixed in and the tubulin was allowed to polymerize at 37°C for 20 min. Microtubules were pelleted through a 37°C, 60% glycerol cushion in 50 mM K-MES, pH 6.6, 5 mM $MgSO_4$, 1 mM EGTA, 1 mM GTP in a TLA110 rotor (Beckman, Palo Alto, CA) at 80,000 rpm, 20 min. The pellets were resuspended at 37°C in assembly buffer (AB: 50 mM K-MES, pH6.6, 3.4 M glycerol, 5 mM $MgSO_4$, 1 mM EGTA, 1 mM GTP) using a warm Potter homogenizer. The tubulin was then deploymerized on an ice-water slurry for 20 min and centrifuged in a TLA100.3 rotor at 100,000 rpm for 35 min at 2°C to remove any polymerized tubulin remaining. The tubulin was kept at 0°C as reaction mixtures were prepared. Dilution series (6-20 μM tubulin) were made in AB.

Freshly-purified γ-tubulin in 50 mM K-MES, pH6.6, 0.5 M KCL, 5 mM $MgSO_4$, 1 mM EGTA, 1 μM GTP (γ-buffer) or γ-buffer alone was mixed with the cycled tubulin at 0°C in thin-walled, 0.5 ml plastic tubes (Stratagene, Cedar Creek, TX), and rapidly heated to 37°C (30 sec in a 37°C water bath). Experimental and control reactions were performed in pairs at each α/β-tubulin concentration. The mixtures were transferred within 10 sec after warming to pre-warmed cuvettes in a 37°C Peltier cell changer in a Perkin Elmer Lambda 20 spectrometer (Perkin Elmer Instruments, Norwalk, CT) and the A_{350nm} was recorded approximately every 4 sec until plateaus were reached. The final concentration of γ-tubulin in the experimental reactions ranged from 60 to 670 nM,

depending on the day. The final salt concentration in the reactions was found to have a great influence on the reaction kinetics (Rice, L.M, unpublished data), so care was taken to dilute the γ-buffer component into the reaction mixture so that the final KCl concentration was the same in all reactions, which in our experiments was 16.7 mM.

Data analysis

The raw polymerization time and absorbance datasets were normalized and plotted using either Kaleidagraph (Synergy Software) or a program that we developed specifically for the analysis of turbidity data. Our program automatically determines the plateau (A_∞) values and the characteristic times (T_{10}) required for determining the kinetic model for microtubule nucleation as described by Flyvbjerg et al [63, 81]. Briefly, the program first determines an approximate A_∞ by averaging the last five timepoints for each dataset. An approximate T_{10} is then determined by choosing, for each dataset, the timepoint with a plateau value closest to one-tenth of the A_∞. Once initial guesses have been obtained for all datasets, they are simultaneously optimized by a grid search to find (A_∞,T_{10}) pairs for each dataset that give optimal scaling. The concentration dependence of the T_{10} values thus obtained was confirmed indepently by the simple algorithm described in Flyvbjerg et al. [63, 81]. Kinetic models describing microtubule assembly through 0 - 4 intermediate steps involving the addition of 2 - 4 α/β-tubulin heterodimers at each step were tested for fitting to the raw or scaled turbidity data using Berkeley Madonna (www.berkeleymadonna.com) software. Rate constants presented in the text were obtained by performing a global fit of the appropriate Flyvbjerg model (as

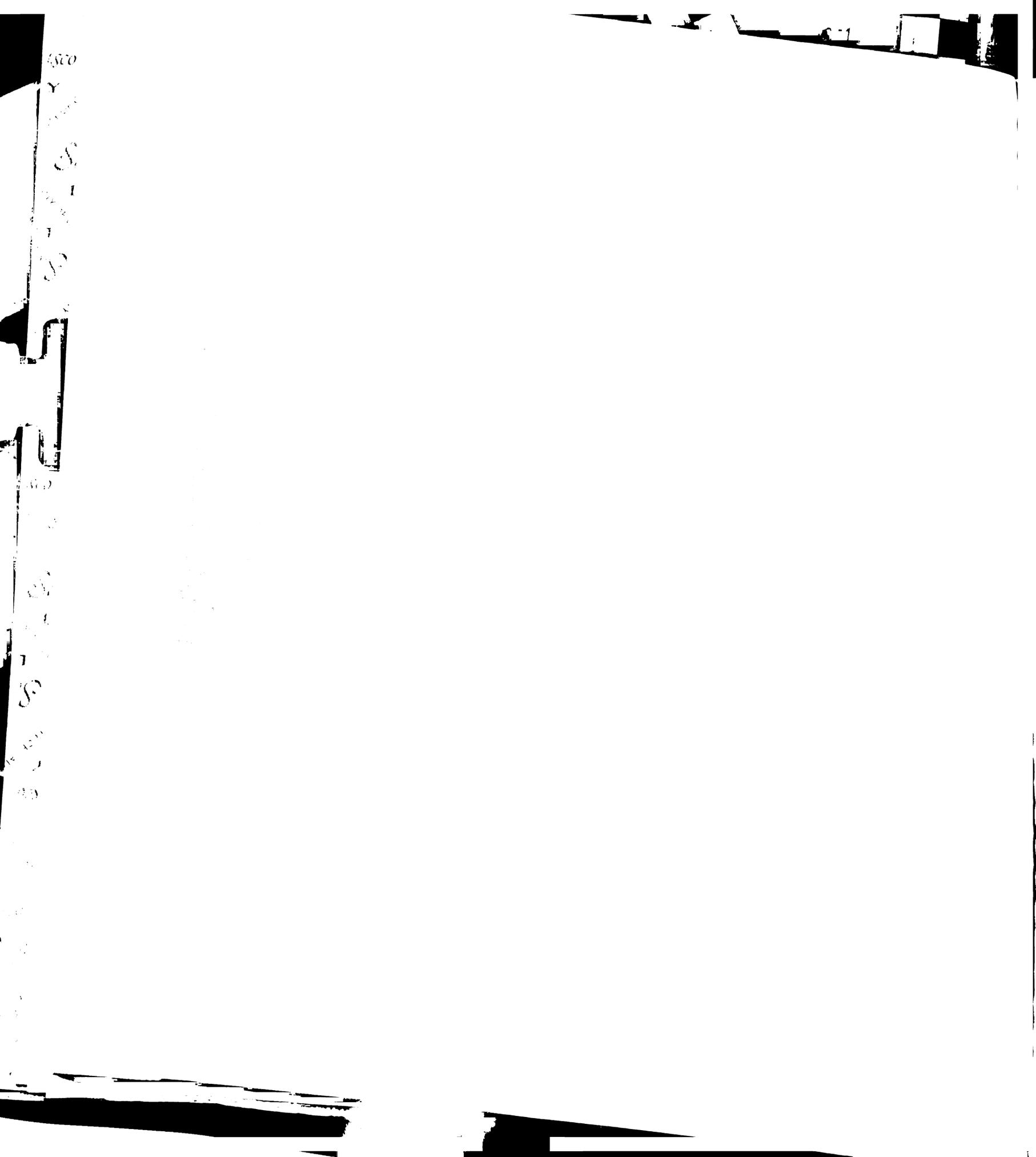

determined by the number of rate-limiting intermediates and by the concentration dependence of the characteristic times) to an entire set of raw microtubule assembly data.

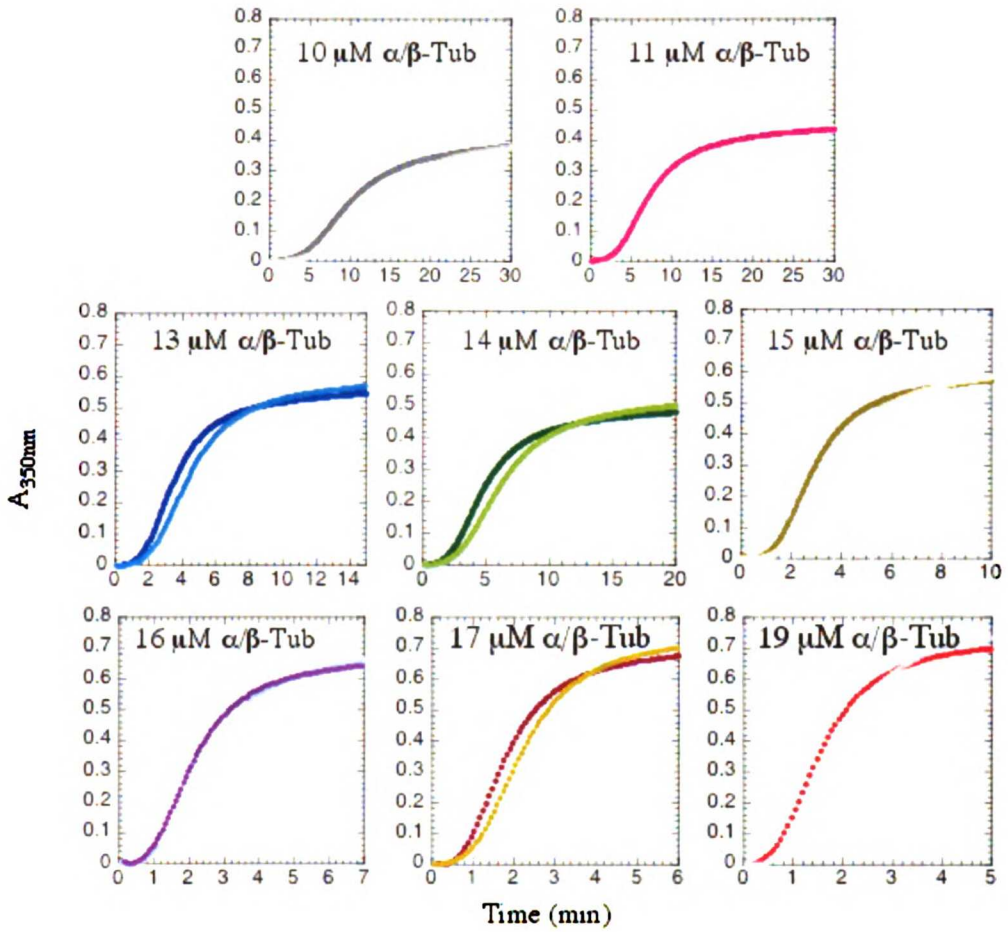

Figure 1

γ-Tubulin decreases the lag time before microtubule polymerization reactions enter their rapid elongation phase. Paired reactions containing 10-19 µM α/β-tubulin and 100 nM γ-tubulin (dark color) or buffer (light color) were rapidly warmed to 37°C, transferred to a spectrometer, and their A_{350nm} was followed over time.

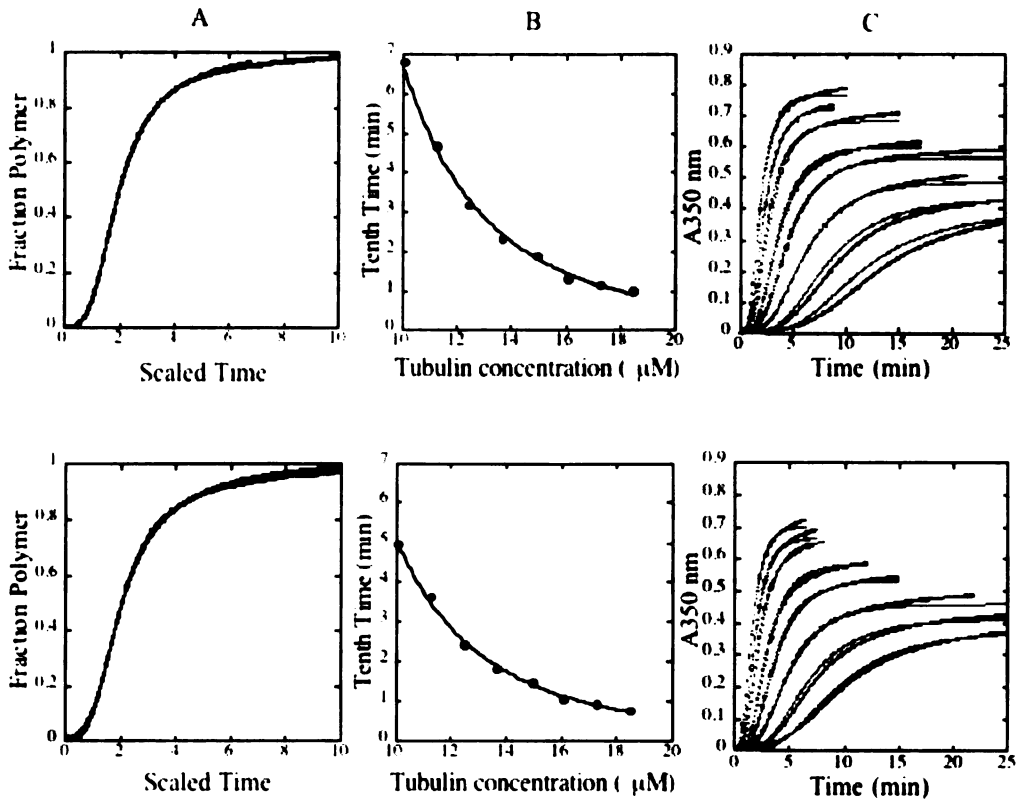

Figure 2

γ-Tubulin tetramers increase the rate of microtubule nucleus formation and do not affect the size of the nucleus. Under these reaction conditions (50 mM K-MES, pH6.6, 3.4 M glycerol, 16.7 mM KCl, 5 mM $MgSO_4$, 1 mM EGTA, 1 mM GTP) the nucleus consists of 12 α/β-tubulin heterodimers. A) Buffer control (top) and γ-tubulin-mediated (bottom) polymerization data shown in Fig. 1 were plotted as fraction polymer (A_{350nm}/plateau) vs. scaled time ($T/T_{0.1}$), revealing that the data scale. This indicates that microtubule nucleation occurs by the same mechanism at all α/β-tubulin concentrations in the presence or absence of nucleator. B) Concentration dependence of the tenth times

($T_{0.1}$) of the buffer control (top) and γ-tubulin-mediated (bottom) polymerization data. Curve fits to both data sets indicate that trimers of α/β-tubulin are added at each step before the nucleus in the presence or absence of γ-tubulin. Equations: $y = 12580x^{-3.276}$, $R = 0.998$ (top), $y = 7301.9x^{-3.172}$, $R = 0.998$ (bottom), where the exponent indicates the number of α/β-tubulin heterodimers added per step [63, 81]. C) Empirical fits to tubulin assembly data. The mechanism of microtubule nucleation in the presence (bottom) or absence (top) of γ-tubulin under these reaction conditions involves the assembly of trimers of α/β-tubulin heterodimers in two steps before the nucleus. The experimental data are shown in gray and the model in red. See text for equations describing this model. Comparing the rates of formation of the intermediates before the nucleus in the presence or absence of γ-tubulin indicates that this nucleator accelerates the rate of formation of the second intermediate.

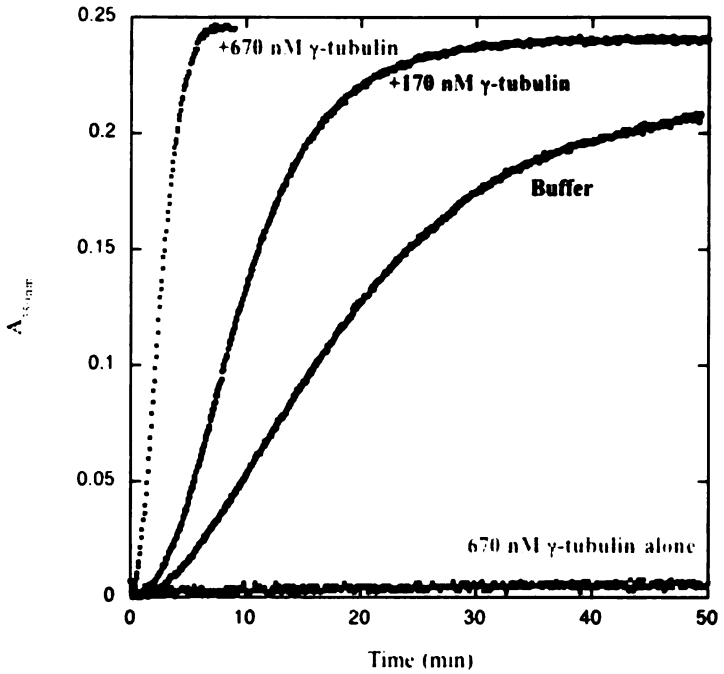

Figure 3

Dose-response of microtubule nucleation to γ-tubulin concentration. Microtubule assembly occurs much faster in the presence of 170 (green curve) or 670 nM (purple curve) γ-tubulin. 670 nM γ-tubulin alone (red curve) contributes negligibly to turbidity.

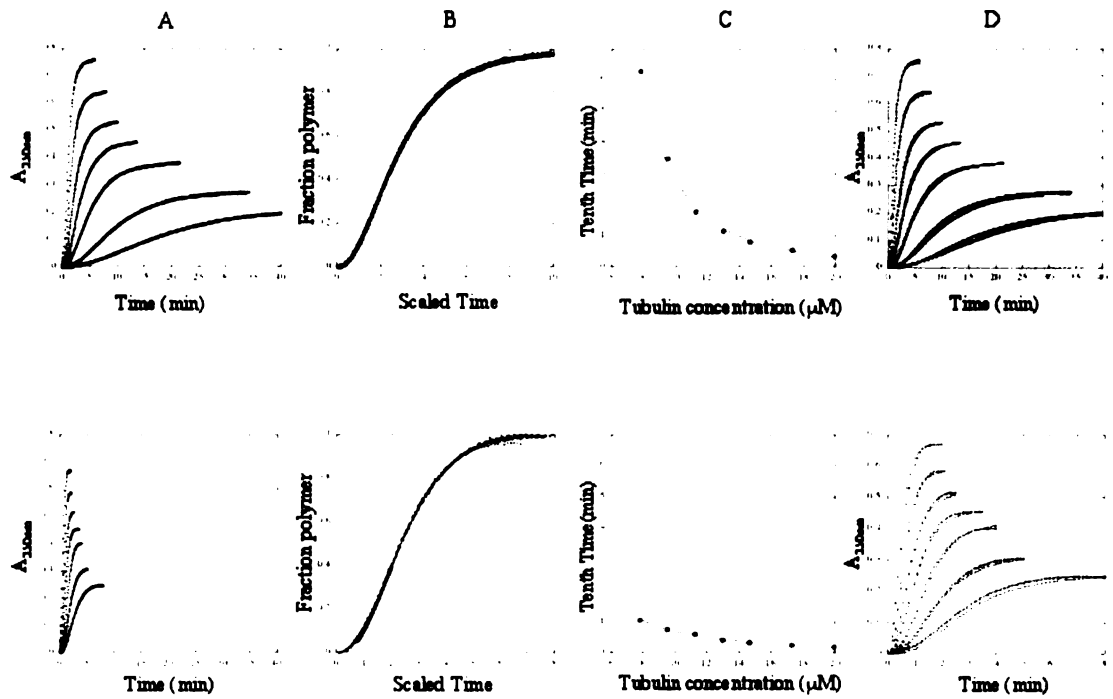

Figure 4

Filaments formed at 670 nM γ-tubulin efficiently promote microtubule formation by decreasing the size of the nucleus from 9 to 6 α/β-tubulin heterodimers. A) Buffer control (top) and 670 nM γ-tubulin-mediated (bottom) turbidity data show that γ-tubulin filaments decrease strikingly the lag time before rapid elongation occurs. B) The buffer control (top) and γ-tubulin (bottom) data scale when plotted as fraction polymer (A_{350nm}/plateau) vs. scaled time ($T/T_{0.1}$). For each condition, this indicates that microtubule nucleation occurs by the same mechanism at all α/β-tubulin concentrations. C) Concentration dependence of the tenth times ($T_{0.1}$) of the buffer control (top) and γ-tubulin-mediated (bottom) polymerization data. Curve fits to both data sets indicate that

trimers of α/β-tubulin are added at each step before the nucleus in the absence of γ-tubulin (top). Equation: $y = 3512.6x^{(-3.0982)}$, R=0.99856, where the exponent indicates the number of α/β-tubulin heterodimers added per step [63, 81]. However, in the presence of 670 nM γ-tubulin, dimers of α/β-tubulin are added at each step before the nucleus (bottom). Equation: $y= 47.498x^{(-1.8368)}$, R=0.99721. D) Empirical fits to tubulin assembly data. The mechanism of microtubule nucleation in the absence (top) of γ-tubulin under these reaction conditions involves the assembly of trimers of α/β-tubulin heterodimers in one step before the nucleus. The experimental data are shown in gray and the model in red. However, in the presence (bottom) of γ-tubulin, the best-fitting model indicates that dimers of α/β-tubulin assemble in one step before the nucleus. See text for equations describing these models.

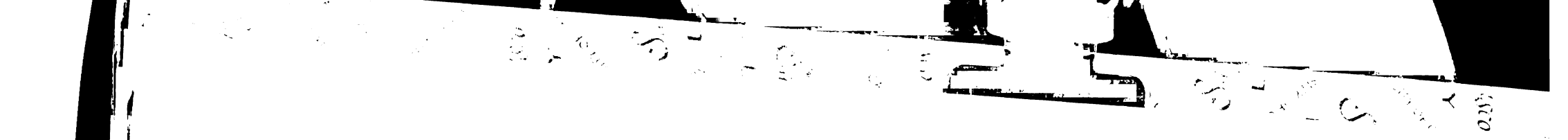

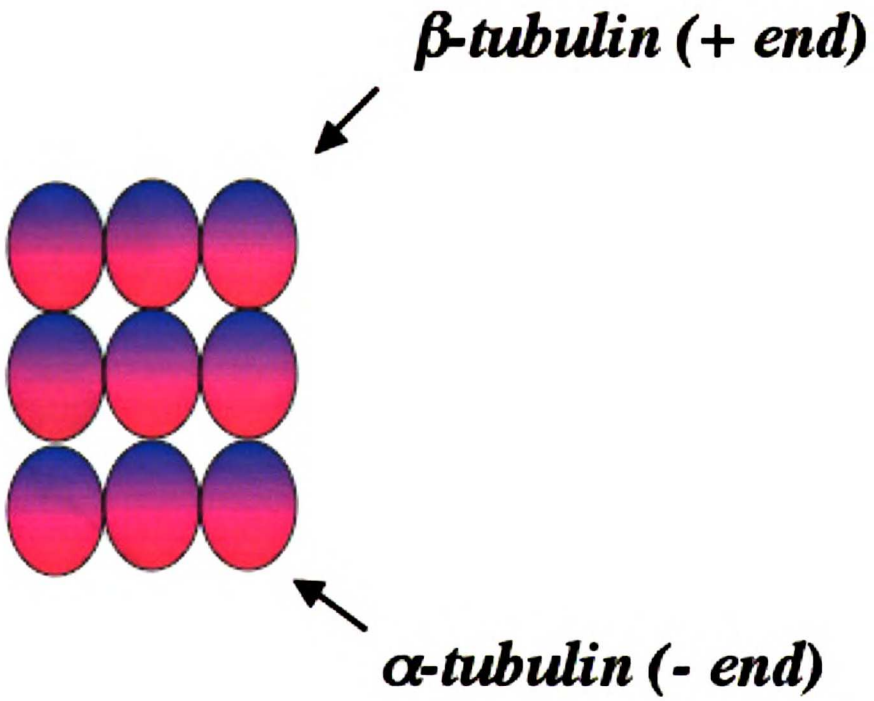

Figure 5

A model for the second intermediate whose stability is enhanced by low concentrations of γ-tubulin. Assembly would proceed through the sequential addition of three short protofilaments.

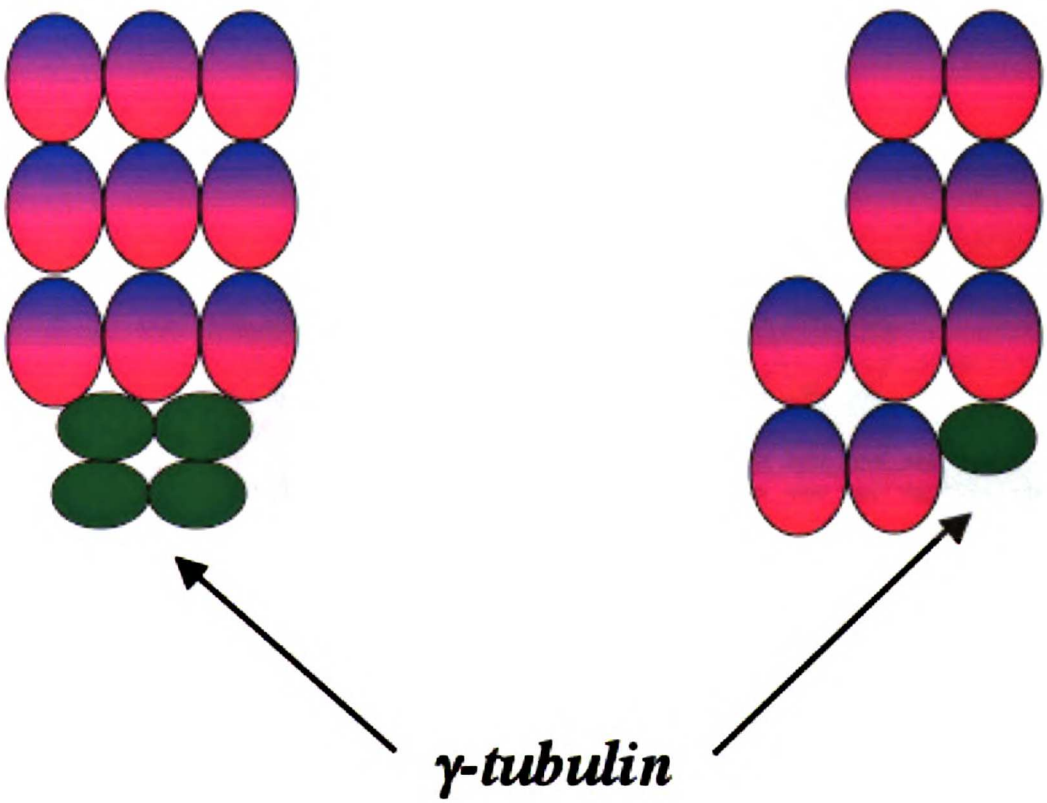

Figure 6

Models for how γ-tubulin might stabilize the second intermediate. Left: A tetramer of γ-tubulin interacts with the interprotofilament spaces of the second intermediate. Right: Tetramerization is not required for γ-tubulin's nucleating activity and a single γ-tubulin molecule could interact with a modified model of the second intermediate.

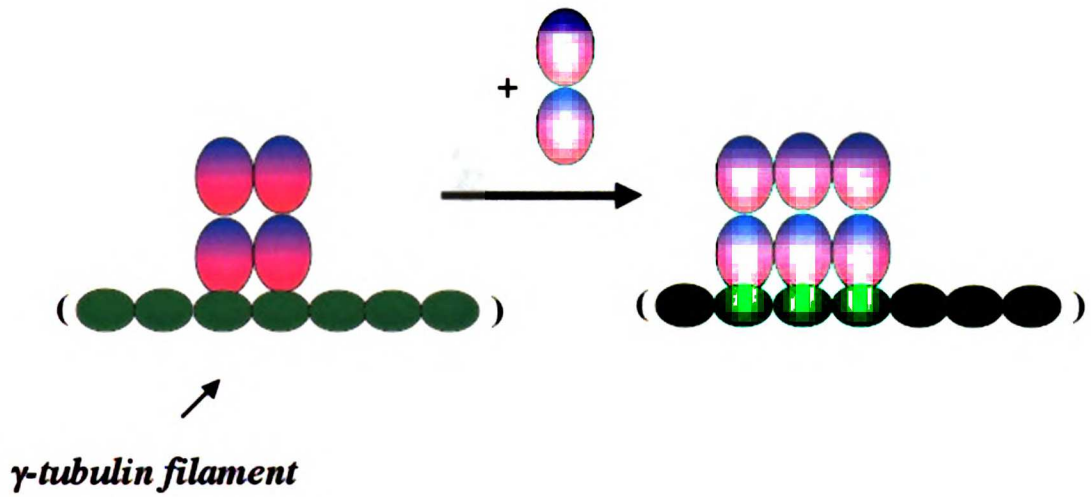

Figure 7

Model depicting how γ-tubulin filaments could stabilize an intermediate composed of dimers of αβ-tubulin heterodimers. γ-tubulin/α-tubulin interactions depicted as longitudinal contacts, though interprotofilament binding by a γ-tubulin filament could provide a similar amount of stabilization.

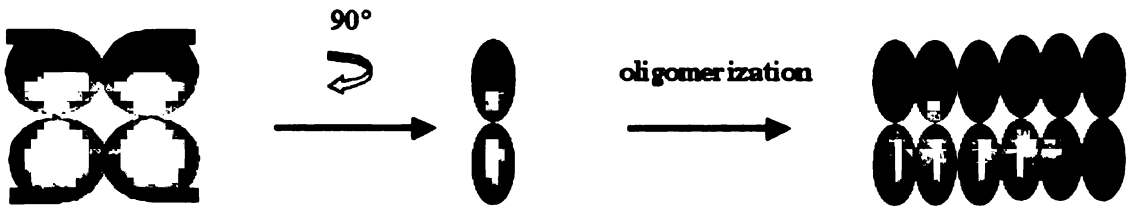

Figure 8

Speculative model for γ-tubulin filament organization. Tetramers interact with one another through lateral contacts, yielding a functional nucleation surface upon which γ-tubulins are related to one another by translation. The depicted tetramer has three two-fold symmetry axes, though this assembly model would work just as well for tetramers possessing a single four-fold symmetry axis.

Table 1: Rate constants describing microtubule assembly in the absence or presence of tetrameric (100 nM) γ-tubulin.

	Buffer rates	γ-tubulin rates	Ratio (γ-tubulin/buffer)
f_0 ($\mu M^{-5}s^{-1}$)	2.03×10^{-11}	1.73×10^{-11}	0.85
f_1($\mu M^{-3}s^{-1}$)	1.54×10^{-6}	2.82×10^{-6}	1.83
f_3 ($\mu M^{-1}s^{-1}$)	4	4	1

Legend: Rate constants for the Flyvbjerg model were obtained by global fits to the assembly data assuming an elongation rate constant of 4 $\mu M^{-1}s^{-1}$ [84-86].

Table 2: Rate constants describing microtubule assembly in the absence or presence of large oligomers (670 nM) of γ-tubulin.

	Buffer rates	γ-tubulin rates
f_0	4.22×10^{-12} ($\mu M^{-5}s^{-1}$)	1.21×10^{-8} ($\mu M^{-3}s^{-1}$)
f_1	1.28×10^{-5}($\mu M^{-3}s^{-1}$)	1.83×10^{-4} ($\mu M^{-2}s^{-1}$)
f_3 ($\mu M^{-1}s^{-1}$)	4	4

Legend: Rate constants for the Flyvbjerg model were obtained by global fits to the assembly data assuming an elongation rate constant of 4 $\mu M^{-1}s^{-1}$ [84-86]. Ratios of rate constants are not indicated because the buffer and γ-tubulin reactions have different concentration dependence.

Postscript

A precise molecular model for the second intermediate and how γ-tubulin might stabilize it is lacking. It is possible that the numbers extracted from the analysis for calculating the nucleus size represent an average and are not sufficient to generate a precise physical model. Data from kinetic analyses will likely need to be coupled to structural and biochemical data to understand the molecular details of how γ-tubulin stabilizes the second intermediate.

EM structural analysis of γ-tubulin filaments, both in isolation and in the presence of nucleated microtubules, has been initiated by Michelle Moritz. Surprisingly, γ-tubulin filament formation appears to be sensitive to the presence of αβ-tubulin. γ-Tubulin filaments form in low salt buffers on their own and if assembled prior to adding αβ-tubulin, as described in Chapter 1. Mixing γ-tubulin with αβ-tubulin, however, yields no detectable filaments, though microtubule assembly is clearly accelerated relative to controls without γ-tubulin. Indeed, this was precisely how nucleation experiments were performed in this chapter. This phenomenon is being explored by Michelle Moritz. Preliminary work also suggests that EM image analysis techniques can lead to a higher resolution understanding of γ-tubulin filaments. This work is being carried out by Michelle Moritz with the help of Koji Yonekura.

Future kinetic analyses should focus on the microtubule nucleating activities of the γ-Tubulin Small Complex (γ-TuSC) and the γ-Tubulin Ring Complex (γ-TuRC). Kinetic analysis of γ-TuRC nucleating activity has also been preliminarily explored by Michelle Moritz.

Chapter 4:

Crystal Structure of Human γ-Tubulin: Implications for the Mechanism of Microtubule Assembly

Preface

The following chapter is a version of a manuscript that has been submitted for publication as a Letter to Nature. The work represents a collaboration between Luke Rice and myself. I grew the crystals of γ-tubulin and collected the diffraction data. Luke and I together processed the data, found a molecular replacement solution, refined the model, interpreted the model, and wrote the paper. We will share first authorship on the publication.

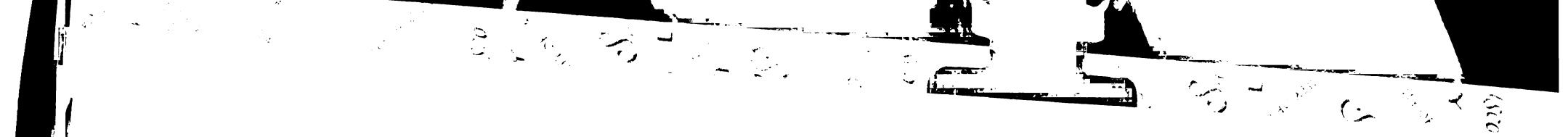

Synopsis

Microtubules are hollow polymers of αβ-tubulin that exhibit GTP-dependent assembly dynamics and comprise a critical part of the eukaryotic cytoskeleton. Initiation of new microtubules *in vivo* requires γ-tubulin, organized as an oligomer within the γ-Tubulin Ring Complex (γ-TuRC) of higher eukaryotes. While much has been learned about the structure of αβ tubulin, structural insight into γ-tubulin, its oligomerization, and how it promotes microtubule assembly remains lacking. Here we report the 2.7Å crystal structure of human γ-tubulin bound to GTPγS. One of the crystal packing interactions recapitulates the lateral contacts between tubulins in the microtubule lattice and is proposed to form the basis for γ-tubulin oligomerization within the γ-TuRC. Unexpectedly, γ-tubulin:GTPγS adopts a curved conformation very similar to that seen in GDP-bound microtubule depolymerization products. This suggests that, unlike signaling GTPases, tubulins do not undergo nucleotide dependent conformation switching. This has significant implications for αβ-tubulin assembly. We propose a model for microtubule assembly in which guanine nucleotides do not regulate curved-to-straight transitions, but instead only modulate the strength of longitudinal interactions within the microtubule lattice.

Introduction

γ-Tubulin is the principal component of the γ-TuRC, the 2.2 MDa multi-protein machine responsible for initiating microtubule assembly at the centrosome[31, 33, 35]. The γ-TuRC contains 12-14 γ-tubulins and forms a capped lock-washer shaped structure partly composed of repeating subunits[41]. The open rim of the γ-TuRC is likely lined with the γ-tubulins, leading to the hypothesis that the γ-TuRC provides a template upon which initiation of αβ-tubulin polymerization proceeds efficiently[41-43]. However, many important mechanistic details remain elusive. How is γ-tubulin organized within the γ-TuRC? How does γ-tubulin promote microtubule assembly? Is the role of GTP in γ-tubulin function similar to its role in microtubule assembly?

Results and Discussion

To begin addressing these questions from a structural perspective, we report the x-ray crystal structure of a human γ-tubulin:GTPγS complex determined by molecular replacement at 2.7Å resolution (Materials and Methods) (Fig. 1a,b, Table 1). This is the first structure of a monomeric tubulin, and the highest resolution structure of any tubulin to date. We also determined the essentially identical structure of a γ-tubulin:GTP complex at somewhat lower resolution, providing strong evidence that the γ-tubulin:GTPγS structure represents the bona fide GTP conformation of γ-tubulin.

As expected from the high sequence conservation within the tubulin superfamily, the overall structure of γ-tubulin is similar to the previously reported α- and β-tubulin structures. Comparative sequence analysis reveals several sites where γ-tubulin has highly-conserved insertions or deletions relative to α- and β-tubulin (Fig. 1d,e and Sup.

Fig. 1). Two of these, the Gly-Gly insertion at position 99 in the T3 loop and the Asp insertion at 175, are disordered in the γ-tubulin structure but are located on the presumptive longitudinal contact surface and may therefore help determine γ-tubulin-specific longitudinal interaction properties (longitudinal and lateral surfaces are defined as in [7,8]). γ-Tubulins also lack His107, a deletion that restores a more ideal α-helical register to helix H3' and removes a bulge from this region of the structure (nomenclature from [18]). In α- and β-tubulin, this bulge participates indirectly in longitudinal associations by interacting with the T3 loop ([18, 24] and Supp. Fig. 1). Our structure reveals that this deletion also changes the shape of a lateral interaction surface of γ-tubulin by causing the N-terminal end of H3 to protrude (Sup. Fig. 1). Several of the other features unique to γ-tubulin sequences are located on surfaces equivalent to those that make longitudinal or lateral contacts between α- and β-tubulin in microtubules (Fig. 1d,e). In particular, Asp56 and Asp57 (in the extended loop between H1 and S2), and Asp117 (in H3) all represent sites where γ-tubulins contain a negative charge at a lateral interaction site that is neutral in α- and β-tubulin. On the opposite face of the molecule, γ-tubulins have an accumulation of unique residues in H9 (γ: mRRIlQ, α: tNAcfE, β: tQQvfD) that changes the charge carried on this helix by +3. The molecular interactions underlying lateral interactions in microtubules have yet to be visualized in atomic detail, so it is difficult to determine the relative importance of the γ-tubulin-specific features mentioned above. Nevertheless, it is striking that these and other unique features of the γ-tubulin family map to known tubulin:tubulin interaction surfaces, and suggests that these residues may collectively dictate γ-tubulin interaction strengths distinct from those of α- or β-tubulin.

In contrast to these local surface differences, many of the elements responsible for GTP binding are shared between α-, β-, and γ-tubulin[17, 18, 24]. In particular, as in β-tubulin, the guanine base is sandwiched between Phe225 and Cys13, with Asn229 and Asn207 contributing important hydrogen bonds (Fig. 1b). With the exception of Ser140 and Thr145, most of the phosphate contacts are made by backbone amides: Cys13 to O1a, Gln12, Gly144, Gly146, and Thr145 to O1b, and Gly144 and Thr145 to O3g. We have modelled a Mg^{++} ion in electron density near the β- and γ-phosphates, making contacts with phosphate oxygens O2b and O3b, and with Asp68, Glu70, and a water molecule.

Not all features of the nucleotide binding pockets are identical between γ- and β-tubulin, however. In addition to the disordered T3 loop mentioned above, the T5 loop is also disordered in γ-tubulin. These two loops participate in longitudinal αβ-tubulin contacts so it is possible that they only become ordered upon formation of longitudinal tubulin associations. The Gly-Gly insertion in the T3 loop could in principle impart unique GTP binding properties to γ-tubulin. We therefore performed comparative nucleotide binding studies to determine the degree to which structural similarity between the nucleotide binding pockets of γ- and β-tubulin extended to shared GTP-binding properties (Fig. 1c). Both γ- and β-tubulin bind GTP with similar affinity (~60 nM). Competition experiments using GDP revealed that both also display a similar preference for GTP over GDP. Together with a strong conservation of sequence and structure, the similar nucleotide binding affinities of γ-tubulin and β-tubulin indicates that they share a common nucleotide binding mechanism that is largely unaffected by structural differences in the T3 and T5 loops. Furthermore, this makes it likely that, analogous to its

action on β-tubulin, α-tubulin can stimulate the GTPase activity of γ-tubulin upon longitudinal association.

αβ-Tubulin has been shown to adopt two distinct conformations characterized by domain re-arrangements within both tubulin subunits. The 'straight' αβ-tubulin conformation has only been observed in microtubules and zinc sheets[18, 22]. The 'curved' conformation has been observed in unpolymerized αβ-tubulin and is consistent with the geometry of GDP-tubulin rings[24]. The relative orientation between the structurally conserved rigid N-terminal domain and the more variable intermediate domain is a primary distinguishing characteristic of these two tubulin conformations[24]. Surprisingly, the arrangement of N-terminal and intermediate domains in the γ-tubulin:GTPγS structure is typical of the curved conformation. This is contrary to expectation, because current models suggest that the curved-to-straight transition is regulated by nucleotide state. Superposition using only the rigid N-terminal domain confirms that the γ-tubulin:GTPγS structure adopts the curved conformation, highlighted by conserved positions of key secondary structural elements (e.g. helices H6, H7, H10 and the orientation of the β-sheet) (Fig. 2).

One of the observed crystal packing interactions bears a striking similarity to the homotypic lateral interactions previously only seen to occur in the microtubule lattice [22](Fig. 3). While the γ-tubulin interaction lacks the lateral curvature of the microtubule lattice, the two different lateral interactions use virtually identical contact regions, and bury comparable surface areas (Fig. 3). The γ-tubulin structure thus shows that, at the level of a tubulin monomer, the straight-to-curved transition does not affect the intrinsic ability to form lateral interactions. These lateral interactions must be sufficiently flexible

to permit microtubules formed *in vitro* to contain between 9 and 16 protofilaments, and to allow the formation of flat sheets that have been observed as intermediates in microtubule elongation[87]. The intrinsic flexibility of the structurally conserved lateral interaction, together with local sequence conservation (Fig. 1d,e), makes it likely that the lateral interaction observed in the crystal also forms the basis for curved arrays of γ-tubulin such as those found in the γ-TuRC.

Current models of αβ-tubulin polymerization propose that GDP-bound αβ-tubulin adopts a curved conformation in both the α and β-subunits, and that GTP binding to β-tubulin drives microtubule assembly by promoting the straight, microtubule-compatible conformation[88, 89]. According to this model, binding of GTP to the exchangeable site of β-tubulin triggers a remarkably long-range allosteric conformational change in which both α- and β- subunits adopt the straight conformation. Hydrolysis of GTP to GDP on an αβ-tubulin heterodimer within the microtubule lattice is thought to generate conformational strain because GDP-bound αβ-tubulin heterodimers favor a microtubule-incompatible, bent conformation. This ultimately leads to catastrophic depolymerization as part of a process known as dynamic instability. In support of this model, curved GDP-tubulin protofilaments are readily observed in depolymerizing microtubules[14].

However, our structure reveals that when bound to either GTPγS or GTP, γ-tubulin adopts a curved conformation similar to that seen for both α-tubulin:GTP and β-tubulin:GDP in the unpolymerized state. This is the first tubulin structure with GTP bound at an exchangeable site. Given the high degree of sequence conservation and the nearly identical nucleotide binding properties of β- and γ-tubulin (Fig. 1bc), we believe

that the observed structural similarities between all unpolymerized tubulins strongly indicate that a curved conformation is the default one regardless of nucleotide state (Fig. 4a). This is supported by the fact that colchicine, which binds in a pocket unique to the curved conformation[24], has an identical affinity for GTP- or GDP-bound αβ-tubulin [12].

Our proposal that tubulin conformation is not primarily regulated by nucleotide state has important consequences for αβ-tubulin and the mechanism of microtubule assembly. We postulate that both GTP- and GDP-bound αβ-tubulin adopt a similar, relaxed conformation with intermediate domains (including H6 and H10) organized such that longitudinal αβ-tubulin interactions would lead to curved structures (Fig 2) similar to those found in GDP-protofilaments or the stathmin:αβ-tubulin complex [24]. This relaxed conformation is incompatible with the straight microtubule lattice because the curvature within the αβ-tubulin heterodimer disrupts the parallel presentation of equivalent α- and β-tubulin lateral binding surfaces (Fig. 4b). αβ-Tubulin heterodimers can associate longitudinally without straightening, but not laterally, so it must be the intrinsically weak lateral interactions that drive the curved-to-straight conformational transition (Fig. 4b). Thus, the re-orientation of the intermediate domain characteristic of the straight conformation represents a strained state stabilized only by the longitudinal and lateral interactions in the microtubule lattice. We therefore propose that lattice strain is an inherent feature of microtubules, and not just a function of the GDP state. In this model, the primary role of the GTP γ-phosphate is to strengthen longitudinal associations by making favorable contacts with the adjacent αβ-tubulin. During microtubule assembly, GTP bound at the exposed, plus-end of β-tubulin directly facilitates the

recruitment and straightening of a curved αβ-tubulin heterodimer (Fig. 4c). Subsequent hydrolysis of GTP to GDP greatly enhances lattice strain by weakening longitudinal interactions, not by favoring a curved conformation as previously believed. This provides an alternate explanation of how GTP hydrolysis leads to microtubule disassembly.

The proposal that the default conformation of αβ-tubulin:GTP is curved rather than straight, based on our structure of γ-tubulin:GTP, is consistent with several independent biochemical observations. These include (a) colchicine binds equally well to GTP- and GDP-bound αβ-tubulin, (b) GTP-bound α-tubulin is in the curved conformation in the unpolymerized state[24], (c) depolymerization products of microtubules containing the hydrolysis-resistant nucleotide GMPCPP form curved protofilaments[14], and (d) GTP- or GTP-analog bound αβ-tubulin can form rings similar to those formed by GDP-bound heterodimers[13, 61]. Our model also implies that at sufficiently high concentration it should be possible for GDP-bound αβ-tubulin to be incorporated into microtubules; at least two studies show this to be the case[90, 91]. Finally, our proposal that lattice strain is intrinsic to microtubule structure predicts that stronger lateral interactions should compensate for weaker longitudinal ones. This is strikingly confirmed by the fact that equimolar taxol, which stabilizes lateral contacts, eliminates the requirement for a γ-phosphate and allows GDP-bound αβ-tubulin to assemble into microtubules[92].

Our model has important implications for microtubule nucleation. Whereas microtubule elongation involves the addition of a single curved αβ-tubulin to straight ones already in the lattice (Figure 4c), nucleation requires the lateral association between two curved αβ-tubulins (Figure 4b). By doubling the energetic penalty required to form

the first lateral interaction, the probability of spontaneous nucleation becomes dramatically reduced, making *in vivo* microtubule growth critically dependent on an exogeneous nucleator such as γ-TuRC.

How might γ-tubulin complexes promote microtubule assembly? Appropriately spaced lateral assemblies of γ-tubulin, such as we propose exist within the γ-TuRC, could make strong longitudinal contacts with multiple αβ-tubulins. Presumably, these assemblies would utilize the unique propensity of γ-tubulin to form lateral interactions without strain, as observed in the crystal structure (Fig 3, 4b). This would stabilize lateral interactions between adjacent γ-TuRC-bound αβ-tubulins, and thereby promote microtubule assembly by driving curved-to-straight transitions. Whether γ-tubulin within the γ-TuRC is present as a curved or straight conformer remains to be determined. It is possible that γ-tubulin is capable of switching conformations like αβ-tubulin, either in response to α-tubulin binding or through the action of the other γ-TuRC components. Conformational strain and GTP binding/hydrolysis may both represent mechanisms for tuning the microtubule nucleating activity of the γ-TuRC. By analogy to β-tubulin, GTP binding and hydrolysis on γ-tubulin might regulate its affinity for α-tubulin, potentially providing a mechanism for the observed release of microtubules from the centrosome[93].

Our proposal that nucleotide state does not regulate the essential conformational change in tubulin is consistent with a simple mechanical model of the microtubule[94], and also with the original observation that tubulins represent a distinct class of GTP binding proteins [20]. In particular, tubulins lack several features typical of signaling G-proteins that clearly show γ-phosphate dependent conformational switching. These

include the phosphate-binding P-loop and obvious cognates for the switch I and II loops [95]. Furthermore, several recent structures of the prokaryotic tubulin homolog FtsZ in different nucleotide states all show essentially the same conformation [96]. An unrelated GTPase also shows analogous behavior. The signal recognition particle and its receptor change conformation in response to heterodimerization, not nucleotide state [97] and the γ-phosophate directly enhances dimerization. Thus, the structure of monomeric γ-tubulin has provided unique insight into the role of nucleotide binding and conformational change in microtubule assembly. This structural insight will inform future efforts to understand in detail the molecular mechanisms underlying this complex process.

Materials and Methods

Protein expression, purification, crystallization, and nucleotide crosslinking. Protein was expressed and purified in GF2 buffer (50 mM K-MES pH 6.6, 500 mM KCl, 5 mM $MgSO_4$, 1 mM K-EGTA, 1 μM GTP, 1 mM DTT) as described in Chapter 1. For crystallization, GTP or GTPγS (final concentration: 0.5mM) was added to the top three gel filtration fractions. These fractions were pooled and concentrated to ~2.5 mg/ml. γ-Tubulin was crystallized by mixing protein 1:2 with well solution (83.3mM Tris pH 8.2, 500mM KCl, 20% PEG6000, 0.1mM GTP) and equilibrating against 500 ml well solution. After 4 days, thin rods were harvested into cryoprotectant (83.3mM Tris pH 8.2, 500mM KCl, 23% PEG6000, 0.1mM GTPγS, 1mM $MgCl_2$, and 17% glycerol) and frozen in liquid N_2. Nucleotide crosslinking experiments were performed as in Chapter 1. The discrepancy between our calculated GDP/β-tubulin affinity and the previously reported value [67] may be explained if the γ-phosphate helps to better orient the purine

ring for more efficient photocrosslinking or if the γ-phosphate becomes crosslinked to His139.

Structure determination. Crystal diffraction data was collected at beamline 8.2.1 (HHMI) at the Advanced Light Source (Berkeley, CA). Thin, radiation sensitive crystals required the merging of two data sets in order to obtain a complete data set beyond 3.1Å resolution. Data processing and reduction were carried out with the HKL2000 package[98]. Molecular replacement searches and refinement were carried out with CNS[99] and model building was carried out with O[100]. Initial phases were determined by molecular replacement using a β-tubulin search model (Ravelli, et al; PDB 1SA0) with all sidechains truncated to alanine and all cofactors (GDP, Mg++, colchicine, and waters) removed. Regions of the search model not confirmed by the initial electron density map were deleted, and sidechains with clear electron density in the initial map were added. As the model phases improved, additional sidechains and loops were added when there was interpretable electron density. GTP was added only after the electron density clearly indicated the presence of the γ-phosphate. Over the course of refinement and rebuilding, complete annealed-omit maps were used extensively to help avoid model bias. Figures made with PyMOL[101].

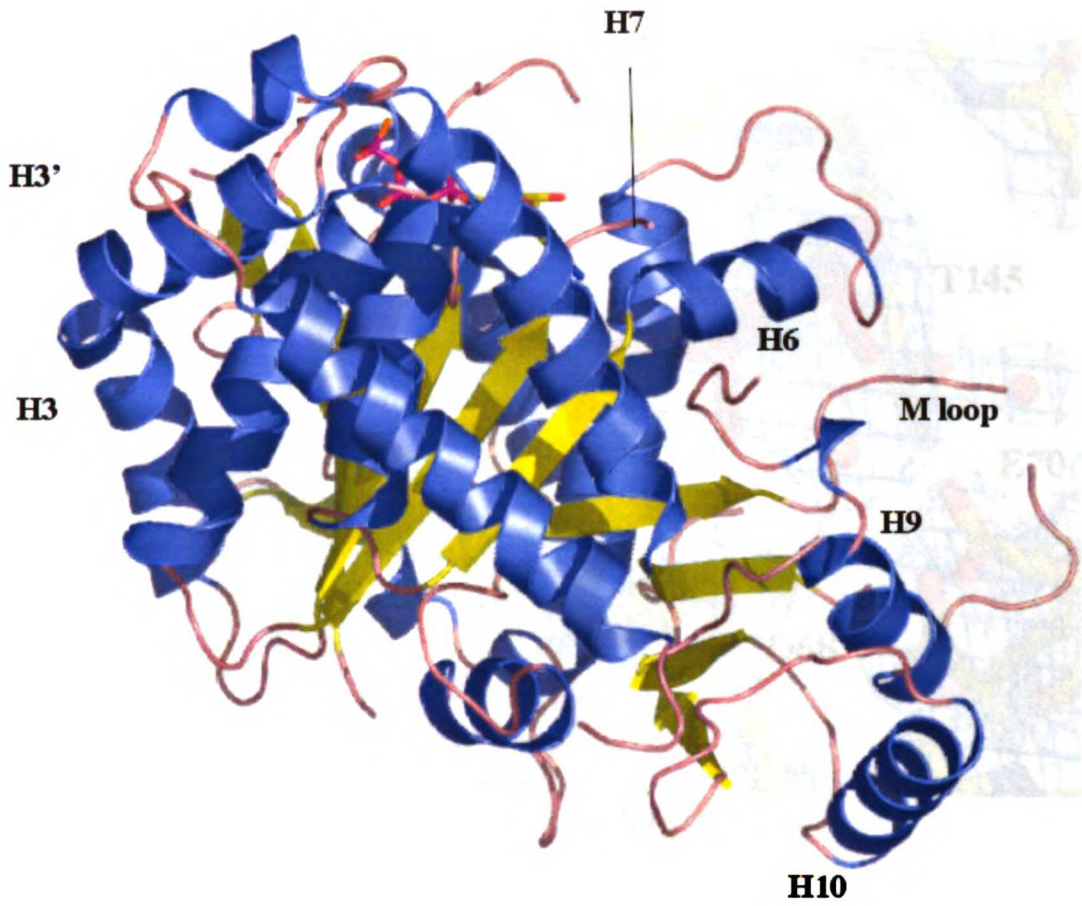

Figure 1

a). Cartoon representation of the γ-tubulin structure, with some secondary structure elements mentioned in the text labelled.

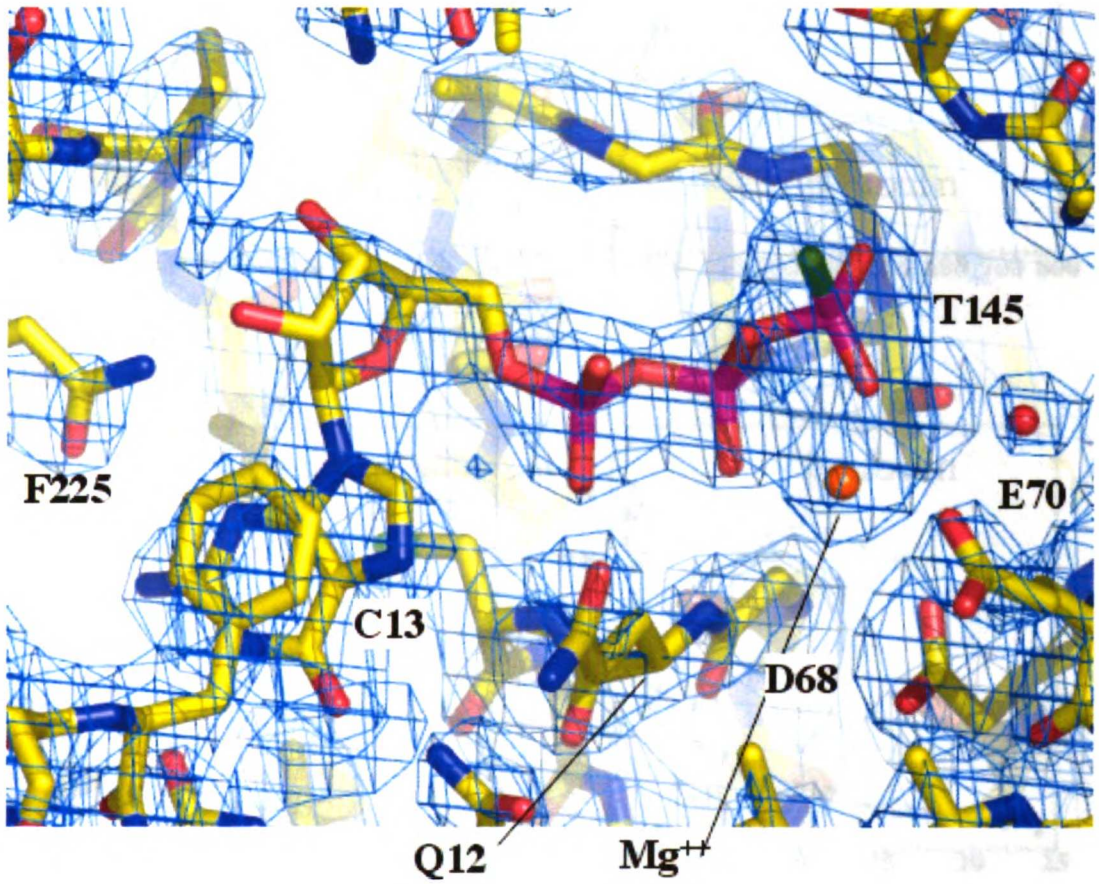

Figure 1

b). Representative electron density from a complete, annealed σ_A-weighted $2mF_o$-DF_c map computed from the final model. Some key residues interacting with the GTPγS are shown.

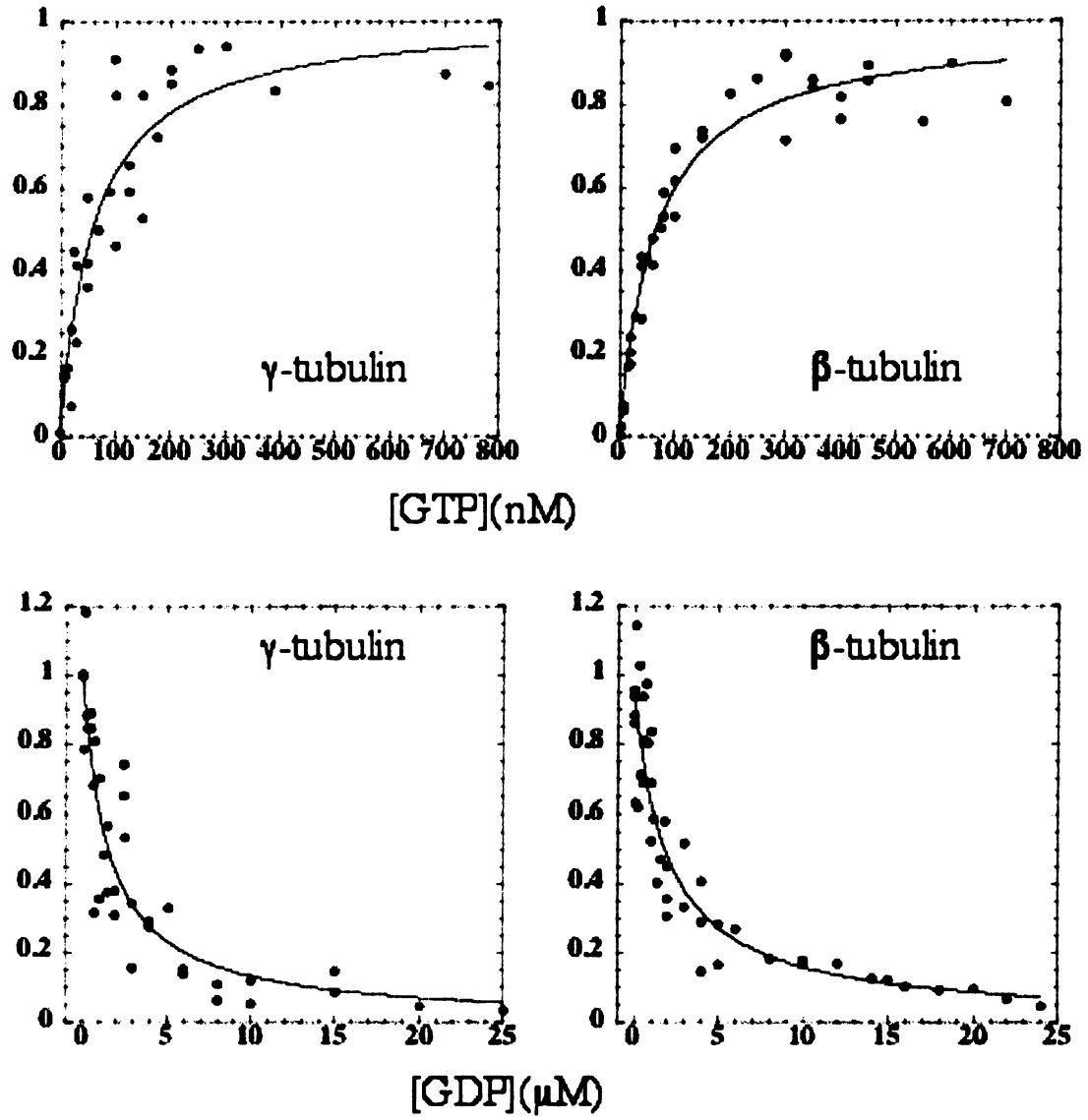

Figure 1

c). γ-Tubulin (left panels/Chapter 1) and the exchangeable site on β-tubulin (right panels) have similar GTP/GDP (top/bottom panels) binding properties. GTP affinities were determined by photocrosslinking α-^{32}P-GTP to tubulin, and GDP affinities were determined by competitive inhibition of α-^{32}P-GTP crosslinking with unlabeled GDP (see Chapter 1, Materials and Methods). The affinities of γ-tubulin and β-tubulin for GTP are 58.4 ± 12.6 nM and 64.5 ± 6.3 nM, respectively. The affinities of γ-tubulin and β-tubulin for GDP are 1.13 ± 0.2 μM and 1.55 ± 0.25 μM, respectively.

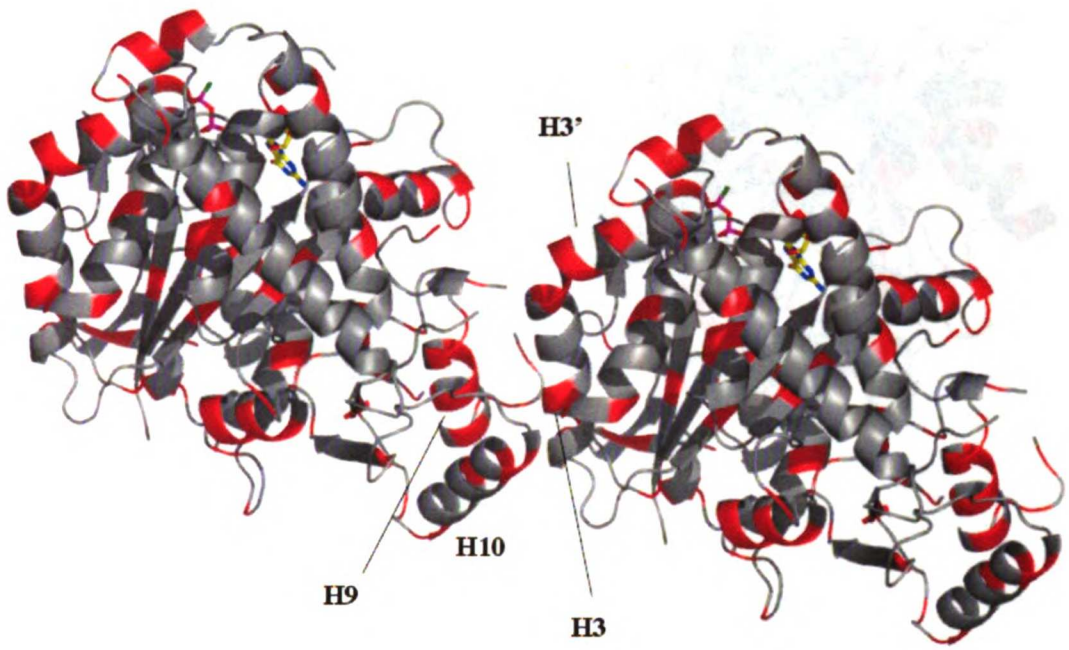

Figure 1

d). Face-on view of laterally interacting γ-tubulins (see Fig. 3), colored red at sites where γ-tubulin sequences differ significantly from α- and β-tubulin sequences. Helices H3 and H9 both contain a number of γ-tubulin-specific residues.

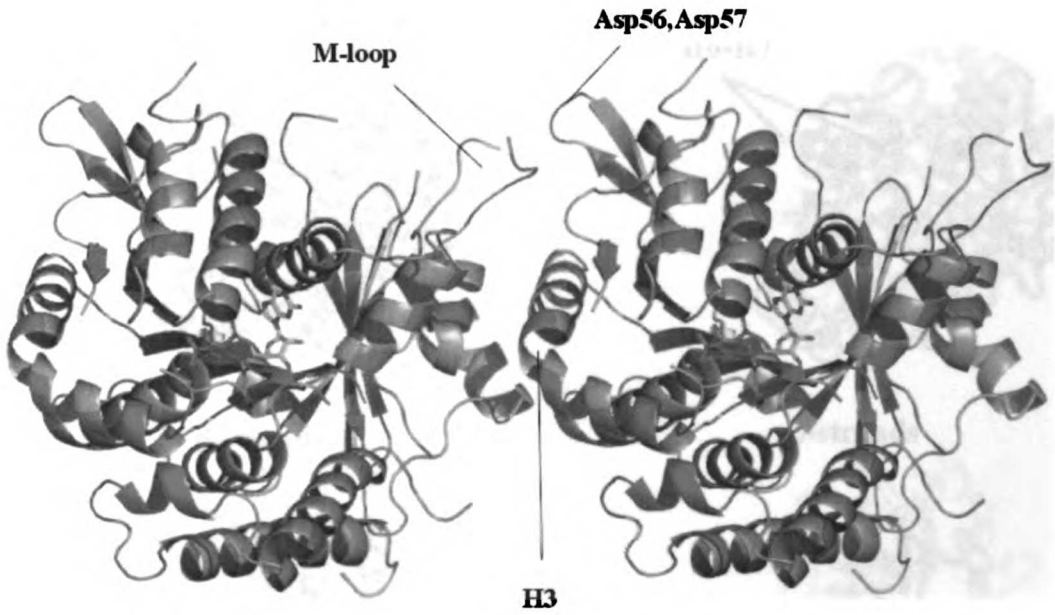

Figure 1

e). Top-down view of laterally interacting γ-tubulins (see Fig. 3), colored as in (d) and highlighting other γ-tubulin-specific residues. The lateral curvature of the microtubule lattice would bring the M-loop and the loop containing Asp56 and Asp57 into closer proximity, suggesting that this unique feature of γ-tubulins may contribute to distinctive lateral interaction patterns.

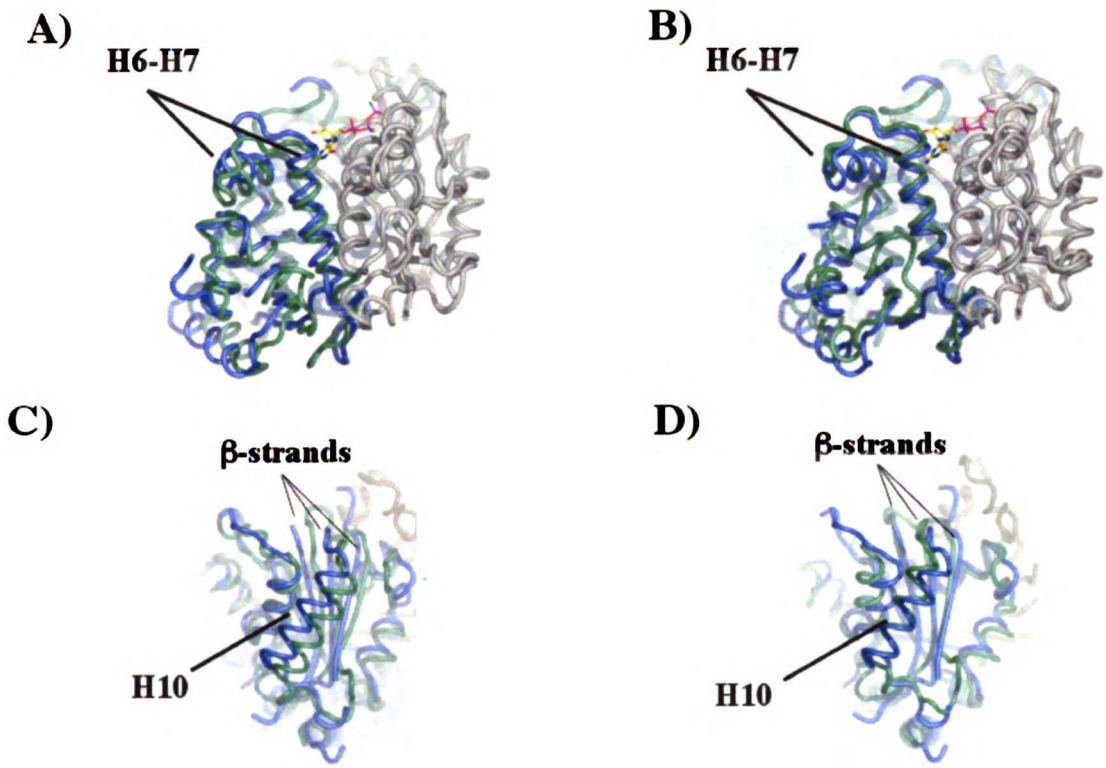

Figure 2

Structural alignment indicates that γ-tubulin is in a curved conformation. Alignments were performed using the rigid N-terminal domain, colored grey. Root mean squared coordinate deviations calculated from the two alignments confirm that the conformation of γ-tubulin is more similar to the curved one (1.5Å) than to the straight one (1.7Å).

(a) and (b). Comparative views of the γ-tubulin structure (blue) aligned to the straight (a) and curved (b) β-tubulin structures (green). Secondary structural elements (helices H6 and H7) diagnostic of the two conformations are indicated.

(c) and (d). Different views of the same alignments, illustrating that the position of helix H10 and the orientation of the β-sheet in the straight conformation (c) are different from those observed in γ-tubulin (d).

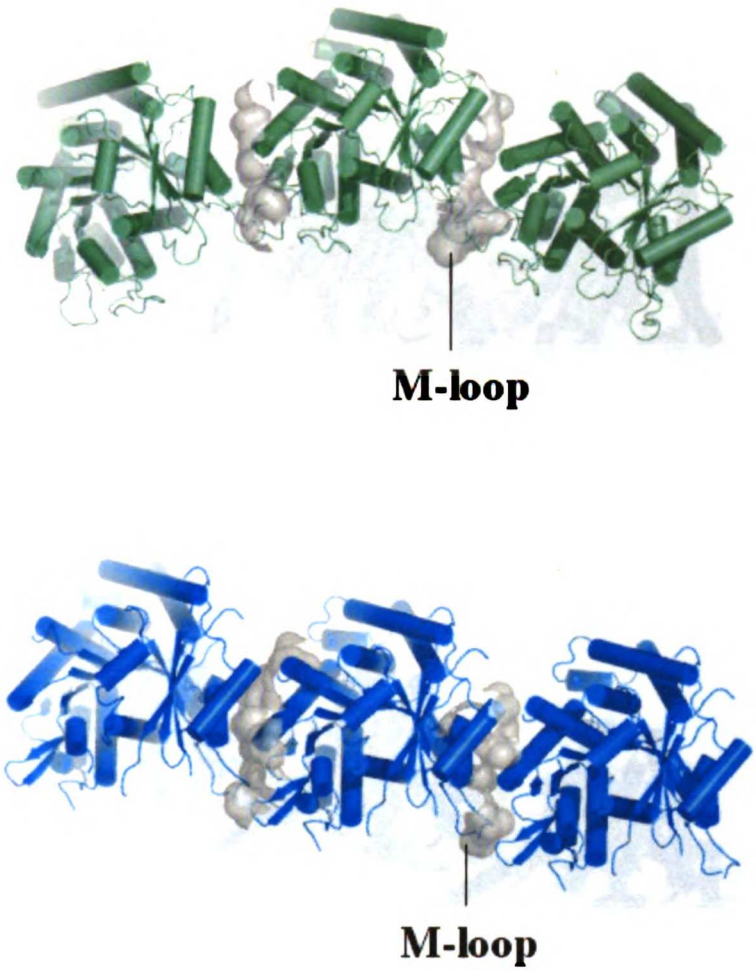

Figure 3

Lateral interactions between γ-tubulins resemble lateral interactions between β-tubulins in the microtubule lattice.

a). Comparative views of laterally interacting β-tubulins in the microtubule lattice (Ken Downing, personal communication) (green), and laterally interacting γ-tubulins in the crystal (blue). Both arrays were aligned using the central monomer, and are shown as viewed from the 'minus end'. The lateral contact regions are indicated by the grey surfaces on the central monomer. The γ-tubulin lateral interaction lacks the curvature of the microtubule one, but otherwise uses very similar regions of the structure.

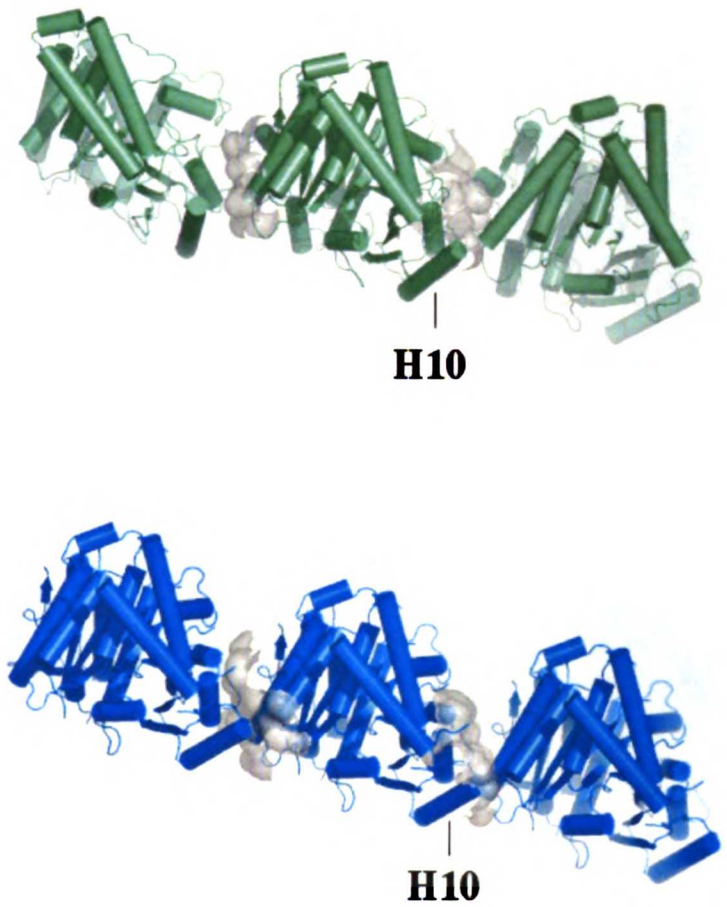

Figure 3

Lateral interactions between γ-tubulins resemble lateral interactions between β-tubulins in the microtubule lattice.

b). The same comparison, rotated 90° to be viewed from what would be the outside of the microtubule, with the minus end surface toward the bottom of the figure. Both lateral interactions display a similar pitch.

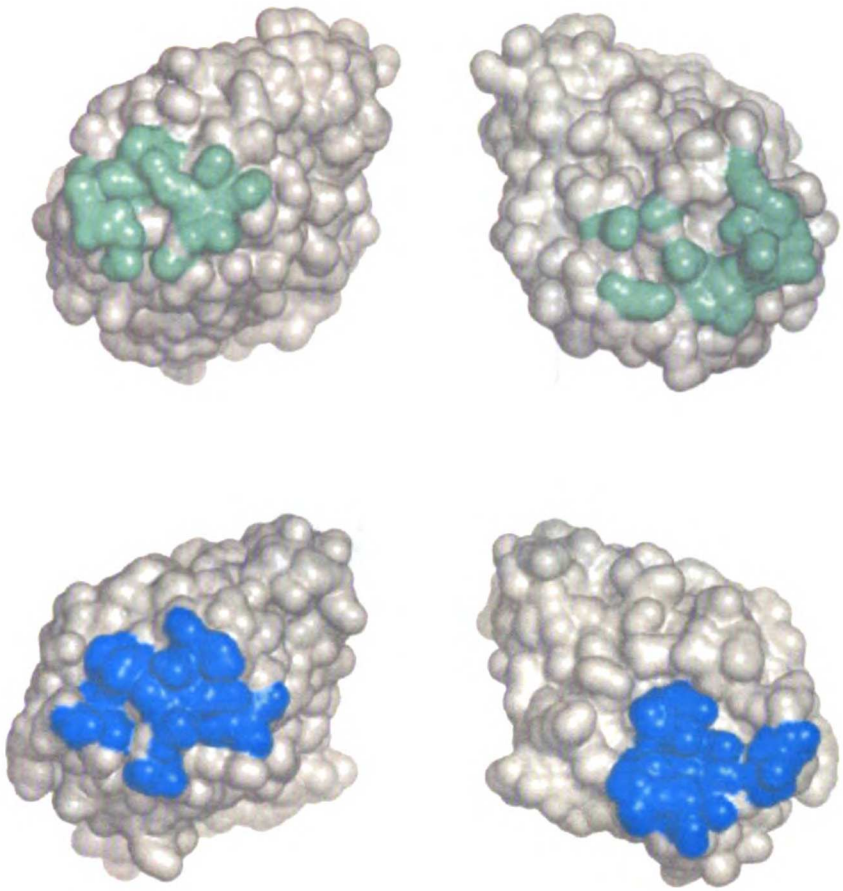

Figure 3

Lateral interactions between γ-tubulins resemble lateral interactions between β-tubulins in the microtubule lattice.

c). Molecular surfaces, with the lateral interaction regions indicated in color. The footprints of the microtubule and γ-tubulin crystal interactions are very similar.

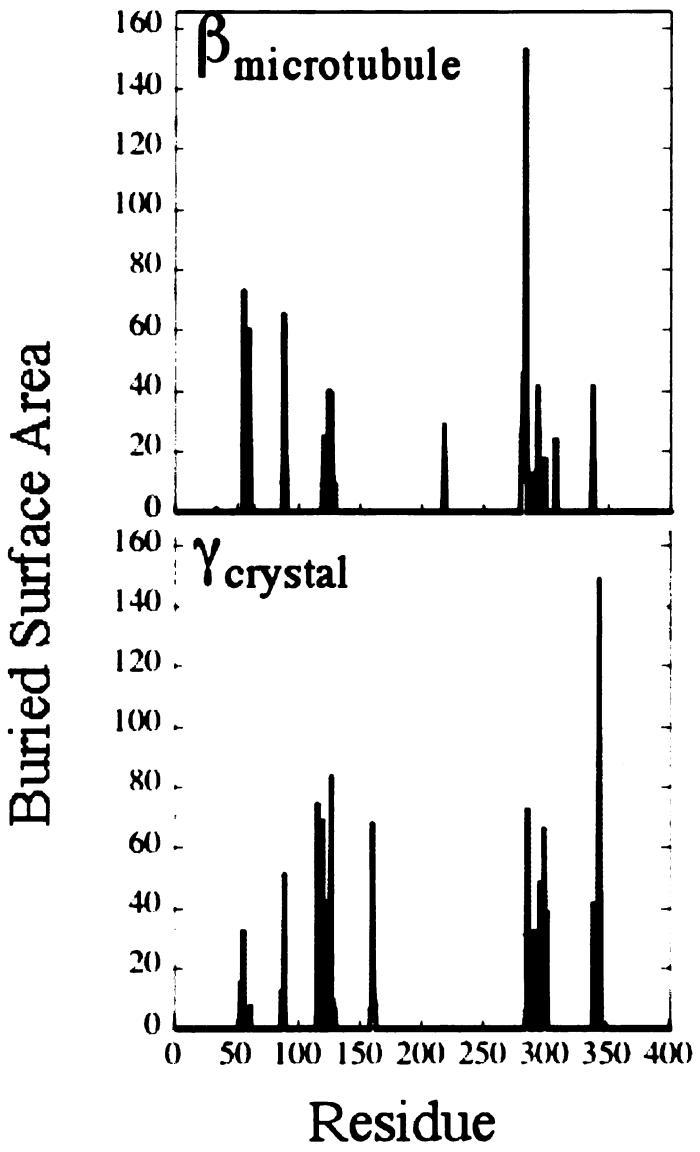

Figure 3

Lateral interactions between γ-tubulins resemble lateral interactions between β-tubulins in the microtubule lattice.

d). Comparison of the buried surface area at each position for β-tubulin lateral interactions (top) and γ-tubulin crystal interactions (bottom). Virtually identical regions of the structure are involved in both interactions.

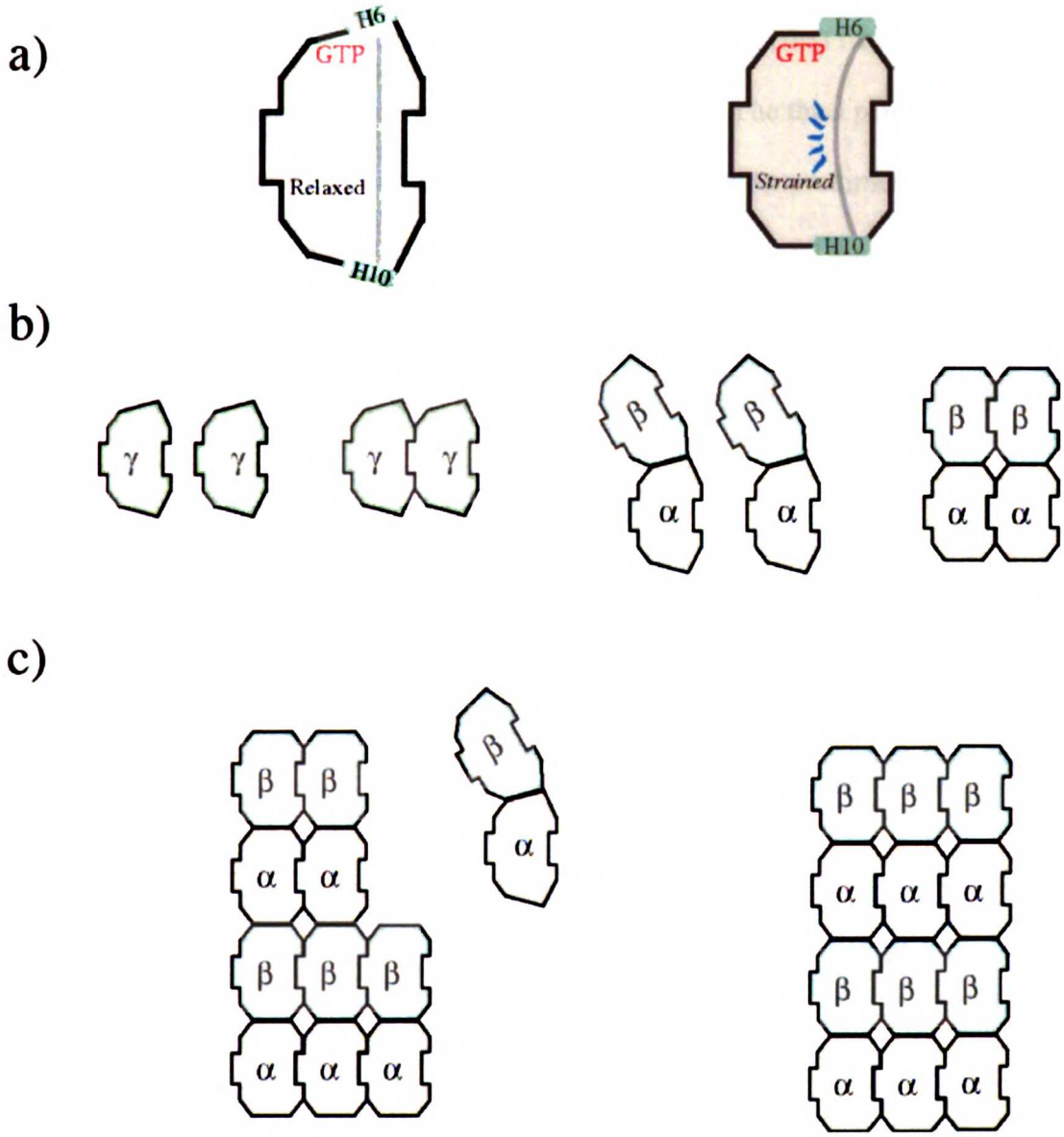

Figure 4

The curved-to-straight conformational change and its consequences for αβ-tubulin assembly.

a). Cartoon illustrating the two known conformational states of tubulins. The default conformation is proposed to be the 'curved', or relaxed, one (left) regardless of

nucleotide state. The straight conformation is strained, and is proposed only to occur only in the microtubule.

b). Cartoon illustrating that, at the level of a tubulin monomer (first two panels), the curved conformation is permissive for lateral interactions. The third panel illustrates the consequences of the curved conformation for the αβ-tubulin heterodimer: the presentation of α- and β-tubulin lateral surfaces is misaligned, and thus the heterodimers cannot interact in the parallel manner required by the microtubule lattice. The rightmost panel shows how these binding sites become aligned in the straight conformation. A lateral interaction between two relaxed αβ-tubulins requires that both of them undergo the unfavorable curved-to-straight transition.

c). Lateral interaction with an αβ-tubulin pre-straightened in the microtubule lattice requires that only the incoming αβ-tubulin undergo the unfavorable conformational change. Thus, lateral interactions during microtubule elongation are more favorable than those that occur during nucleation.

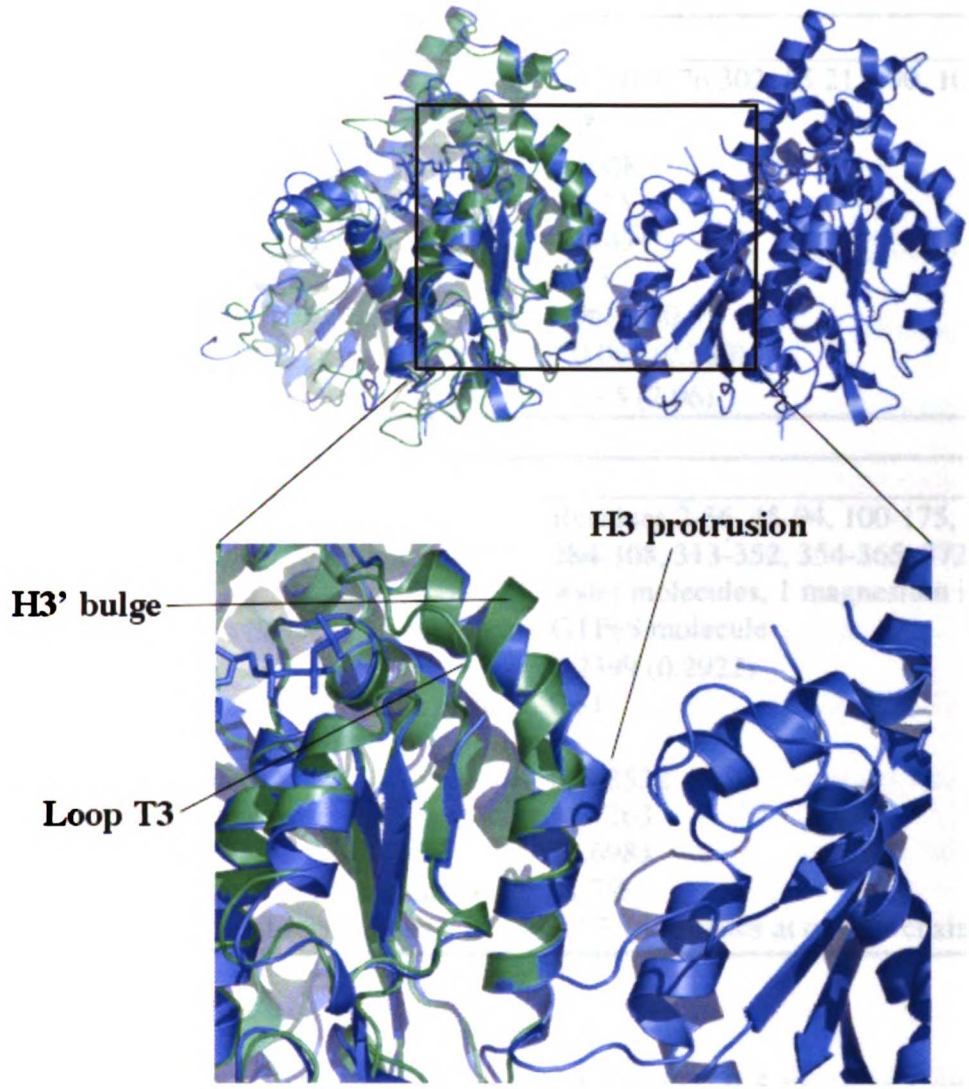

Supplementary figure 1

Structural differences between γ- and β-tubulin resulting from the deletion of His107 in helix H3' of γ-tubulins. Laterally interacting γ-tubulins are shown in blue, with β-tubulin (in green) superimposed on one monomer. The bulge in helix H3' of β-tubulin interacts with the T3-loop, which is disordered in the γ-tubulin structure. In γ-tubulin, helix H3' adopts a more ideal α-helical geometry that causes the N-terminal end of helix H3 to protrude, giving rise to a lateral interaction surface with altered shape.

Data collection	
Unit cell dimensions (a, b, c, a, b, g)	52.419, 76.302, 65.211, 90, 101.931, 90
Space group	$P2_1$
Temperature	100K
Minimum Bragg Spacing	2.7Å
Unique observations	12471
Redundancy	3.3
Completeness	96.1 (80.5)
R_{merge}	0.061 (0.380)
I/s	13.5 (2.96)

Refinement	
Model	Residues 2-36, 45-94, 100-175, 179-280, 284-308, 313-352, 354-365, 372-440, 22 water molecules, 1 magnesium ion, 1 GTPγS molecule
R (R_{free})	0.2399 (0.2922)
Cross-validated Luzzati coordinate error (Å)	0.51
Bond rms deviation (Å)	0.008532
Angle rms deviation (°):	1.67263
Average B factor (Å^2):	52.6983
Residues in most favored f/y regions	81.7%
Residues in disallowed ϕ/ψ regions	1.1% (4 residues at or near chain breaks)

Table 1

Crystallographic data and refinement for the γ-tubulin:GTPγS structure. Completeness, R_{merge}, and I/σ values in parentheses are for data in the highest resolution shell. R_{free} was calculated using a test set consisting of 10% of the data.

Postscript

The human γ-tubulin:GTP structure.

The structure of a human γ-tubulin:GTP complex was also solved and partially refined. Data processing involved merging the first sections of two different data sets to improve the resolution, R_{merge} and I/σ (see Table below), as was done for the γ-tubulin:GTPγS structure. Using the γ-tubulin:GTPγS structure(without waters, GTPγS, or magnesium) as a search model, a molecular replacement solution was found. Rigid body refinement and map calculations revealed electron density consistent with a guanosine triphosphate and possibly a metal ion in the binding pocket. Inclusion of GTP and a magnesium ion in a subsequent round of refinement (minimization) resulted in an R (Rfree)= 25% (29.64%). No major differences in the two structures were observed.

Data collection	
Unit cell dimensions (a, b, c, a, b, g)	52.159, 76.159, 64.665, 90, 102.433, 90
Space group	$P2_1$
Temperature	100K
Minimum Bragg Spacing	3.0Å
Unique observations	8608
Redundancy	2.7
Completeness	92.8 (84.5)
R_{merge}	0.088 (0.329)
I/s	7.18 (2.32)

Table 2

Crystallographic data statistics for the γ-tubulin:GTP structure.

Future Directions

The present structure provides a basis for the generation of site-directed mutants followed by functional characterization. Mutants can be assessed for their ability to oligomerize, bind nucleotide, hydrolyze GTP, and nucleate microtubule assembly.

Future structural work should include determining the structure of a γ-tubulin:GDP complex. Preliminary work indicates that the species is as well-behaved as the GTP- and GTPγS-bound complexes in a similar buffer, though crystal trials on γ-tubulin:GDP revealed no hits under conditions similar to those which yielded both γ-tubulin:GTP and γ-tubulin:GTPγS crystals. Crystallization of this complex will therefore require screening a broader range of conditions. Soaking GDP into γ-tubulin:GTP or GTPγS crystals could reveal whether or not this crystal form is compatible with GDP. Determining this structure could serve to test the hypothesis that γ-tubulin:GDP, like γ-tubulin:GTP and γ-tubulin:GTPγS, assumes a curved conformation. Structural characterization of larger γ-tubulin complexes, such as a γ-tubulin/αβ-tubulin complex or the γ-Tubulin Small Complex, would also provide much insight into γ-tubulin mechanism (Chapter 5).

Chapter 5:

Summary and Future Directions

Summary

The characterization of purified γ-tubulin has provided important molecular insight into the functional and structural properties of this essential protein. Unexpectedly, findings about γ-tubulin ran counter to what was expected from a member of the tubulin superfamily, thus informing about the role of GTP in microtubule assembly as well. The knowledge gained from these studies will aid in the design of future experiments directed at a detailed molecular understanding of microtubule nucleation by the centrosome and microtubule assembly in general.

Biochemical analyses of purified γ-tubulin suggested that it possesses qualities distinct from those of αβ-tubulin (Chapter 1). It was found that high concentrations of salt were required to keep the protein monomeric. At lower salt concentrations, tetramers and higher order oligomers were observed, the latter of which appeared as filaments with a 24nm diameter by negative stain electron microscopy. The occurrence of these higher-order oligomers appeared to occur in a concentration-dependent manner. Though GTP and heat was not required for their formation, as is the case for microtubules, it was not ruled out that these factors could favor their formation. High pH was also found to be a way to promote filament formation. Inspection of these structures by negative stain electron microscopy indicated an enhanced thickness along the edges, suggesting that these structures were in facts tubes, though no microtubule-like protofilaments were observed. Nucleotide binding studies, however, showed that γ-tubulin is very similar to β-tubulin in its GTP/GDP binding properties.

Light scattering assays have revealed that pure human γ-tubulin can promote microtubule assembly. Using an approach developed by Flyvbjerg, et al, we developed a model for microtubule nucleation both with and without γ-tubulin that fits the data very well (Chapter 3). The results indicate that, at low concentrations, γ-tubulin promotes assembly by accelerating the rate of nucleus formation. At higher concentrations, where γ-tubulin filaments are formed, γ-tubulin acts by decreasing the nucleus size. Based on thermodynamic arguments regarding αβ-tubulin assembly, and structural information on γ-tubulin, a physical model for γ-tubulin-mediated microtubule nucleation has been developed.

Structural analysis of human γ-tubulin was made possible by solving the structure of human γ-tubulin bound to GTPγS by x-ray crystallography (Chapter 4). A structure of γ-tubulin bound to GTP was also solved, though to lower resolution (Chapter 4 Postscript) in which the salient features of the GTPγS-bound structure were conserved. Despite some differences in the biochemical behavior of γ-tubulin, the major structural elements of α- and β-tubulin are conserved in γ-tubulin, with structural differences mostly found in loops and other smaller regions. The structure, however, gave two major insights: 1.) γ-Tubulin:GTPγS is in a bent conformation. This is surprising because this conformer was thought to be promoted by GDP. 2.) One of the γ-tubulin:GTPγS crystal structure contacts is very similar to the lateral contacts observed within microtubules. This is also surprising because it was previously thought that the bent conformer was incompatible with the microtubule lattice, forming the basis for microtubule disassembly. This high sequence conservation at this site gave strength to the argument that this is a

physiologically relevant interaction and that it may form the basis of γ-tubulin organization within the γ-TuRC.

The similarities between γ-tubulin and αβ-tubulin led us to generalize these observations, leading to important insights into microtubule assembly (Chapter 4). We proposed that the bent conformer is the preferred conformer for tubulins, regardless of nucleotide state. Since it was observed that bent conformers can make lateral contacts, a new model of microtubule assembly was proposed. In this model, αβ-tubulin is bent in solution and, because of the dimeric nature of αβ-tubulin, only becomes straightened upon the formation of lateral interactions. GTP then serves the role of trapping these straightened conformers by stabilizing longitudinal contacts, implying that tubulin is unlike other GTP binding proteins in that it does not possess nucleotide-dependent switching when unpolymerized.

Future Directions

γ-Tubulin Assembly Models

The manner in which γ-tubulin is organized within the γ-TuRC is not yet known, though there is strong evidence that it forms lateral interactions with itself. Because oligomerization of tetramers into higher order filaments is coincident with greater nucleation activity, structural analysis of these filaments, via electron microscopy and image analysis, may be telling about the relevant organization of γ-tubulin in higher order complexes. This line of investigation is being pursued by Michelle Moritz. Given than γ-tubulin can be produced recombinantly, mutagenesis followed by functional assays provides a means to identify which interfaces are important for assembly. Such studies

can be guided by the lateral packing observed in the crystal structure. Chemical crosslinking (Chapter 1) may also provide insight into the architecture of γ-tubulin oligomers, through mass spectroscopic identification of chemically crosslinked peptides. Finally, higher resolution tomographic or single particle reconstructions of the γ-TuRC may allow docking experiments with the crystal structure to determine the orientation that γ-tubulin assumes in the large complex.

The role of GTP in microtubule nucleation

The central role of GTP in regulating microtubule assembly demands that similar phenomenon be investigated in γ-tubulin-mediated microtubule nucleation. Questions to ask include: Are the affinities of filamentous γ-tubulin for guanine nucleotide the same as those for the tetramer? Does GDP:γ-tubulin nucleate microtubule assembly as well as GTP:γ-tubulin? Does GDP:γ-tubulin bind to microtubules or αβ-tubulin as well as GTP:γ-tubulin? Does γ-tubulin hydrolyze GTP? Do γ-tubulin/αβ-tubulin interactions affect the ability of γ-tubulin to hydrolyze GTP? Is GTP hydrolysis by γ-tubulin coupled to microtubule release?

If the affinity of filamentous γ-tubulin for guanine nucleotides is found to be the same as that of tetrameric γ-tubulin, then it could be safely assumed that these binding sites are not buried upon assembly and may constitute microtubule-interacting sites. The questions regarding potential differences between γ-tubulin-GTP and γ-tubulin-GDP in microtubule affinity or microtubule nucleation activity can be addressed by first photocrosslinking GTP or GDP to γ-tubulin and then performing the experiments. The efficiency of crosslinking can be greatly improved by using azido-derivatized

nucleotides. If γ-tubulin interacts with α-tubulin in a manner similar to β-tubulin, it is likely that GTP-bound γ-tubulin forms stronger contacts with α-tubulin than does GDP-bound γ-tubulin.

Preliminary investigations into GTP hydrolysis by monomeric γ-tubulin indicate that it can hydrolyze GTP, albeit weakly (Chapter 2). A similar activity was found in the γ-TuRC, though a more purified preparation of γ-TuRC will be required before GTPase activity can definitively attributed to this complex. The experiment with recombinant γ-tubulin will need to be repeated at a more physiological salt concentration, where microtubule assembly is known to take place. Mutagenesis of key residues in the active site of recombinant γ-tubulin will be required to fully understand the chemistry of hydrolysis.

Investigations concerning the effect of microtubule nucleation on γ-tubulin hydrolysis can be performed by first photocrosslinking γ-tubulin to γ-^{32}P azido-GTP and following the appearance of radioactive phosphate over the time course of a microtubule assembly reaction. Similarly, taxol-stabilized-microtubules, which do not hydrolyze GTP (Chapter 2), can be mixed with γ-tubulin and γ-^{32}P GTP to test whether microtubules affect the turnover rate of γ-tubulin's GTPase activity. Taxol-stabilized microtubules can also be used to determine the relative binding affinities of azido-GTP-γ-tubulin and azido-GDP-γ-tubulin through spin-down experiments. The results of these experiments can be used to determine how similar that γ-tubulin/α-tubulin interaction is to the GTP-regulated interaction of β-tubulin and α-tubulin.

Once suitable preparations are available, these experiments can be performed again with γ-TuSC and γ-TuRC, to investigate the roles of the other γ-TuRC /γ-TuSC

components on the GTP dependent activities of γ-tubulin. It is possible that the γ-TuSC can be produced recombinantly in a manner similar to γ-tubulin, opening the realm of site-directed mutagenesis studies to the small complex (Tim Stearns, personal communication).

Models of microtubule nucleation

Though the literature has reports of γ-tubulin, γ-TuSC, and γ-TuRC nucleation, a study that carefully compares the activities of all three is lacking. Just as the biochemical characterization of γ-tubulin mediated MT nucleation needs to be extended to larger complexes, the optimization of methods to collect and analyze microtubule assembly data now calls for a parallel analysis of the nucleating activities of the γ-TuSC and the γ-TuRC. The use of affinity tags in purifying these complexes from extracts promises to increase preparation yields to make these experiments possible (Tim Stearns, personal communication), which would give great molecular insight into potentially different ways to initiate microtubule assembly.

Structural analysis of microtubule nucleation

The crystal structure of human γ-tubulin at 2.7Å resolution has yielded the highest resolution image of any tubulin to date. However, many loops were disordered. In particular, the so-called M-loop, which participates in lateral interactions, was disordered. Future crystallographic experiments on γ-tubulin may include efforts to soak taxol into the crystals, in an attempt to order this loop and to see if taxol-binding is conserved between γ-tubulin and β-tubulin. Other disordered loops include loops T3 and T5, located

at the putative longitudinal interface. A crystal structure of γ-tubulin bound to αβ-tubulin may be enough to order these loops, as well as provide tremendous insight into this critical interaction, illustrating exactly how conserved the ability to form a longitudinal bond is in γ-tubulin. Such a structure may also reveal whether or not γ-tubulin undergoes a curved-to straight transition when interacting with αβ-tubulin, though such a transition may also only occur when more lateral αβ-tubulin contacts are made, such as in the proposed model of how γ-TuRC nucleates microtubule assembly. Though challenging, the purification of a γ-tubulin/αβ-tubulin complex for crystal trials may be possible, based on preliminary biochemical analyses: 1.) Native gel analysis of γ-tubulin/αβ-tubulin shows the disruption of higher order γ-tubulin and αβ-tubulin assemblies in favor of complex formation (Chapter 1, Figure 4). 2.) Preliminary gel filtration experiments on a γ-tubulin/αβ-tubulin mixture indicate complex formation (Michelle Moritz, personal communication). Low temperature would minimize αβ-tubulin associating with itself, as would the inclusion of known tubulin-sequestering factors such as colchicine or stathmin.

A crystal structure of the γ-TuSC or its budding yeast homolog, the Tub4 complex , would also provide valuable insight. High-resolution analysis of the Tub4 complex, both with crystallographic and electron microscopic methods, is being pursued by Luke Rice in collaboration with Trisha Davis (U. Washington). The results of these studies could provide information as to how γ-tubulin assembles in these complexes, as well provide insight into the role of the other two components of these complexes. Finally, cryo-electron microscopic analysis of the γ-TuRC, with and without microtubules, is being pursued by John Lyle. Together with gold labeling of the different γ-TuRC components, this study could provide a map of where in the complex the different polypeptides reside.

EM analysis of the γ-TuRC, together with higher resolution studies of the smaller components and possibly chemical crosslinking studies (Chapter 1), could lead to an atomic resolution understanding of this protein machine.

The role of GTP in microtubule assembly

The proposal that curved is the preferred conformer for αβ-tubulin and that microtubule assembly is driven by lateral interactions is difficult to test. Ideally, one would design, express, and purify mutant αβ-tubulins from a higher order heterologous expression system. The resulting mutant proteins would then be subjected to extensive functional and structural characterization. For example, mutants that are predicted to block lateral and/or longitudinal interactions could potentially be crystallized to reveal whether or not GTP actually promotes a straight conformation in the absence of assembly. Such mutants could also be subjected to small angle x-ray scattering studies, which could provide information on any differences in the overall shape between GDP-bound αβ-tubulin and GTP-bound αβ-tubulin, though these studies may be possible with lower concentrations of wild-type αβ-tubulin at 4° C.

αβ-Tubulin, however, has thus far proven difficult to express and purify in large quantities from heterologous expression systems, most likely due to the complex chaperone system αβ-tubulin requires to fold and assemble properly (reviewed in [102, 103]). It is possible, however, that enough tubulin could be purified from a genetically amenable eukaryote such as Pichia pastoris, which can be grown in large amounts to compensate for low expression yields. Such a system would have the added advantage of being able to test function in vivo for subsequent validation of in vitro results.

Computational modeling of microtubule assembly processes has also met some success (Luke Rice, personal communication). It is possible that inclusion of parameters to account for curved-to-straight transitions could yield a model that more accurately describes the experimental data.

The described results and proposed experiments promise to reveal a great deal about the molecular nature of the microtubule cytoskeleton. However, as a more sophisticated understanding of in vitro processes becomes accessible, various in vivo components must be added to the system. For example, a mutation that disrupts a conserved phosphorylation site on γ-tubulin does not affect γ-tubulin localization but does affect microtubule organization in budding yeast[104]. The phosphorylation of γ-tubulin could act indirectly by recruiting other factors to the microtubule-organizing center to effect microtubule nucleation, or it could act more directly influence the activity of the Tub4 complex. By identifying the responsible kinases, the latter could be tested by looking at the kinase effect on the nucleating activity of γ-tubulin or γ-tubulin complexes in vitro. This study may reveal a new level of molecular complexity that will require additional functional and structural analyses to fully understand. If, however, the kinase is found to play a more complex, indirect role in regulating γ-tubulin function, we may begin to dissect the process genetically and biochemically in a model organism such as budding yeast, paving the way toward an even deeper understanding of γ-tubulin and microtubule function.

References

1. Weisenberg, R.C., G.G. Borisy, and E.W. Taylor, *The colchicine-binding protein of mammalian brain and its relation to microtubules.* Biochemistry, 1968. **7**: p. 4466-4479.
2. Weisenberg, R.C., *Microtubule formation in vitro in solutions containing low calcium concentrations.* Science, 1972. **177**: p. 1104-1105.
3. Amos, L.A. and A. Klug, *Arrangement of subunits in flagellar microtubules.* Journal of Cell Science, 1974. **14**: p. 523-549.
4. Weisenberg, R.C., W.J. Deery, and P.J. Dickinson, *Tubulin-nucleotide interactions during the polymerization and depolymerization of microtubules.* Biochemistry, 1976. **15**: p. 4248-4254.
5. Mitchison, T.J. and M.W. Kirschner, *Dynamic instability of microtubule growth.* Nature, 1984. **312**: p. 237-242.
6. Holy, T.E. and S. Leibler, *Dynamic instability of microtubules as an efficient way to search space.* PNAS, 1994. **91**: p. 5682-5685.
7. Mitchison, T.J., *Localization of an exchangeable GTP binding site at the plus ends of microtubules.* Science, 1993. **261**: p. 1044-1047.
8. Fan, J., et al., *Microtubule minus ends can be labelled with a phage display antibody specific to α-tubulin.* Journal of Molecular Biology, 1996. **259**: p. 325-330.
9. Chretien, D. and R.H. Wade, *New data on the microtubule surface lattice.* Biol. Cell, 1991. **71**: p. 161-174.

10. Mandelkow, E.M., E. Mandelkow, and R.A. Miiligan, *Microtubule dynamics and microtubule caps: a time-resolved cryo-electron microscopic study.* Journal of Cell Biology, 1991. **114**: p. 977-991.

11. Howard, W.D. and S.N. Timasheff, *GDP state of tubulin: stabilization of double rings.* Biochemistry, 1986. **25**: p. 8292-8300.

12. Shearwin, K.E. and S.N. Timasheff, *Effect of Colchicine Analogues on the Dissociation of αβ-Tubulin into Subunit: The Locus of Colchicine Binding.* Biochemistry, 1994. **33**: p. 894-901.

13. Shearwin, K.E. and S.N. Timasheff, *Linkage Between Ligand Binding and Control of Tubulin Conformation.* Biochemistry, 1992. **31**: p. 8080-8089.

14. Muller-Reichert, T., et al., *Structural changes at microtubule ends accompanying GTP hydrolysis: Information from a slowly hydrolyzable analogue pf GTP, guanylyl (α, β) methylenediphosphonate.* PNAS, 1998. **95**: p. 3661-3666.

15. Gaskin, F. and Y. Kress, *Zinc ion-induced assembly of tubulin.* Journal of Biological Chemistry, 1977. **252**: p. 6918-6924.

16. Unwin, P.N. and R. Henderson, *Molecular structure determination by electron microscopy of unstained crystalline specimens.* Journal of Molecular Biology, 1975. **94**: p. 425-440.

17. Nogales, E., S.G. Wolf, and K.H. Downing, *Structure of the alpha beta tubulin dimer by electron crystallography.* Nature, 1998. **391**(6663): p. 199-203.

18. Lowe, J., et al., *Refined structure of alpha beta-tubulin at 3.5 A resolution.* J Mol Biol, 2001. **313**(5): p. 1045-57.

19. Lowe, J. and L.A. Amos, *Crystal structure of the bacterial cell-division protein FtsZ.* Nature, 1998. **391**: p. 203-206.

20. Nogales, E., et al., *Tubulin and FtsZ form a distinct class of GTPases.* Nature Structural Biology, 1998. **5**: p. 451-458.

21. Nogales, E., et al., *High resolution structure of the microtubule.* Cell, 1999. **96**: p. 79-88.

22. Li, H., et al., *Microtubule structure at 8 A resolution.* Structure (Camb), 2002. **10**(10): p. 1317-28.

23. Gigant, B., et al., *The 4A X-Ray Structure of a Tubulin:Stathmin-like Domain Complex.* Cell, 2000. **102**: p. 809-816.

24. Ravelli, R.B.G., et al., *Insight into tubulin regulation from a complex with colchicine and a stathmin-like domain.* Nature, 2004. **378**: p. 198-202.

25. Oakley, C.E., Oakley, B.R., *Identification of γ-tubulin, a new member of the tubulin superfamily encoded by mipA gene of Aspergillus nidulans.* Nature, 1989. **338**: p. 662-664.

26. Oakley, B.R., et al., *γ-Tubulin is a component of the spindle pole body that is essential for microtubule function in Asperilligus nidulans.* Cell, 1990. **61**: p. 1289-1301.

27. Stearns, T., Evans, L., Kirschner, M., *γ-Tubulin Is A Highly Conserved Component of the Centrosome.* Cell, 1991. **65**: p. 825-836.

28. Zheng, Y., Jung, M.K., Oakley, B.R., *γ-Tubulin Is Present in Drosophila melanogaster and Homo sapiens and Is Associated with the Centrosome.* Cell, 1991. **65**: p. 817-823.

29. Burns, R.G., *Analysis of the gamma-tubulin sequences: implications for the functional properties of gamma-tubulin.* Journal of Cell Science, 1995. **108**: p. 2123-2130.

30. Mitchison, T.J. and M.W. Kirschner, *Microtubule assemby nucleated by isolated centrosomes.* Nature, 1984. **312**: p. 232-237.

31. Stearns, T., Kirschner, M., *In Vitro Reconstitution of Centrosome Assembly and Function: The Central Role of γ-Tubulin.* Cell, 1994. **76**: p. 623-637.

32. Shu, H.B. and H.C. Joshi, *γ-Tubulin can both nucleate microtubule assembly and self-assemble into novel tubular structures in mammalian cells.* J Cell Biol, 1995. **130**(5): p. 1137-47.

33. Zheng, Y., et al., *Nucleation of microtubule assembly by a γ-tubulin-containing ring complex.* Nature, 1995. **378**: p. 578-583.

34. Moritz, M., et al., *Microtubule nucleation by γ-tubulin-containing rings in the centrosome.* Nature, 1995. **378**: p. 638-640.

35. Moritz, M., et al., *Recruitment of the gamma-tubulin ring complex to Drosophila salt-stripped centrosome scaffolds.* J Cell Biol, 1998. **142**(3): p. 775-86.

36. Oegema, K., et al., *Characterization of two related Drosophila γ-tubulin complexes that differ in their ability to nucleate microtubules.* J Cell Biol, 1999. **144**(4): p. 721-33.

37. Gunawardane, R.N., et al., *Characterization and reconstitution of Drosophila γ-tubulin ring complex subunits.* J Cell Biol, 2000. **151**(7): p. 1513-24.

38. Knop, M. and E. Schiebel, *Spc98p and Spc97p of the yeast γ-tubulin complex mediate binding to the spindle pole body via their interaction with Spc110p.* Embo J, 1997. **16**(23): p. 6985-95.

39. Vinh, D.B., et al., *Reconstitution and characterization of budding yeast γ-tubulin complex.* Mol Biol Cell, 2002. **13**(4): p. 1144-57.

40. Erickson, H.P. and D. Stoffler, *Protofilaments and rings, two conformations of the tubulin family conserved from bacterial FtsZ to alpha/beta and gamma tubulin.* J Cell Biol, 1996. **135**(1): p. 5-8.

41. Moritz, M., et al., *Structure of the γ-tubulin ring complex: a template for microtubule nucleation.* Nature Cell Biology, 2000. **2**: p. 365-370.

42. Keating, T.J. and G.G. Borisy, *Immunostructural evidence for the template mechanism of microtubule nucleation.* Nat Cell Biol, 2000. **2**(6): p. 352-7.

43. Wiese, C. and Y. Zheng, *A new function for the γ-tubulin ring complex as a microtubule minus-end cap.* Nature Cell Biology, 2000. **2**: p. 358-364.

44. Gunawardane, R.N., et al., *γ-Tubulin complexes and their role in microtubule nucleation.* Curr Top Dev Biol, 2000. **49**: p. 55-73.

45. Melki, R., Vainberg, I.E., Chow, R.L., Cowan, N.J., *Chaperonin-mediated Folding of Vertebrate Actin-Related Protein and γ-Tubulin.* Journal of Cell Biology, 1993. **122**: p. 1301-1310.

46. Leguy, R., et al., *Monomeric γ-tubulin nucleates microtubules.* J Biol Chem, 2000. **275**(29): p. 21975-80.

47. Llanos, R., et al., *Tubulin binding sites on γ-tubulin: identification and molecular characterization.* Biochemistry, 1999. **38**(48): p. 15712-20.

48. Inclan, Y.F. and E. Nogales, *Structural models for the self-assembly and microtubule interactions of γ-, δ- and ε-tubulin.* J Cell Sci, 2001. **114**(Pt 2): p. 413-22.

49. Tange, Y., et al., *Functional Dissection of the γ-Tubulin Complex by Suppressor Analysis of gtb1 and alp4 Mutations in Schizosaccharomyces pombe.* Genetics, 2004. **167**: p. 1095-1107.

50. Gunawardane, R.N., O.C. Martin, and Y. Zheng, *Characterization of a new gammaTuRC subunit with WD repeats.* Molecular Biology of the Cell, 2003. **14**: p. 1017-1026.

51. Rios, R.M., et al., *GMAP-210 Recruits γ-Tubulin Complexes to cis-Golgi Membranes and Is Required for Golgi Ribbon Formation.* Cell, 2004. **118**: p. 323-335.

52. Jung, M.K., et al., *Alanine-scanning mutagenesis of Aspergillus gamma-tubulin yields diverse and novel phenotypes.* Mol Biol Cell, 2001. **12**(7): p. 2119-36.

53. Hendrickson, T.W., Yao, J., Bhadury, S., Corbett, A.H., Joshi, H.C., *Conditional Mutations in γ-Tubulin Reveal Its Involvement in Chromosome Segregation and Cytokinesis.* Molecular Biology of the Cell, 2001. **12**: p. 2469-2481.

54. Prigozhina, N.L., et al., *γ-Tubulin Plays an Essential Role in the Coordination of Mitotic Events.* Molecular Biology of the Cell, 2004. **15**: p. 1374-1386.

55. Lajoie-Mazenc, I., et al., *Recruitment of antigenic gamma-tubulin during mitosis in animal cells: presence of gamma-tubulin in the mitotic spindle.* J Cell Sci, 1994. **107 (Pt 10)**: p. 2825-37.

56. Julian, M., Tollon, Y., Lajoie-Mazenc, I., Moisand, A., Mazarguil, H., Puget, A., Wright, M., *γ-Tubulin participates in the formation of the midbody during cytokinesis in mammalian cells.* Journal of Cell Science, 1993. **105**: p. 145-156.

57. Fuller, S.D., Gowen, B.E., Reinisch, S., Sawyer, A., Buendia, B., Wepf, R., Karsenti, E., *The core of the mammalian centriole contains γ-tubulin.* Current Biology, 1995. **5**: p. 1384-1393.

58. Liu, B., Marc, J., Joshi, H.C., Palevitz, B.A., *A γ-tubulin-related protein associated with the microtubule arrays of higher plants in a cell cycle-dependent manner.* Journal of Cell Science, 1993. **104**: p. 1217-1228.

59. Erickson, H.P., *Microtubule surface lattice and subunit structure and observations on reassembly.* Journal of Cell Biology, 1974. **60**: p. 153-167.

60. Alberts, B., et al., *The cytoskeleton*, in *Molecular Biology of the Cell.* 1994, Garland: New York. p. 805.

61. Voter, W.A. and H.P. Erickson, *The kinetics of microtubule assembly.* J Biol Chem, 1984. **259**: p. 10430-10438.

62. Oosawa, F. and S. Asakura, *Thermodynamics of the polymerization of protein.* 1975, New York: Academic Press.

63. Flyvbjerg, H., E. Jobs, and S. Leibler, *Kinetics of self-assembling microtubules: an "inverse problem" in biochemistry.* Proc Natl Acad Sci U S A, 1996. **93**(12): p. 5975-9.

64. Desai, A. and T.J. Mitchison, *Microtubule Polymerization Dynamics*, in *Annual Review of Cell and Developmental Biology.* 1997. p. 83-117.

65. Nogales, E., *Structural insights into microtubule function*, in *Ann Rev Biochem.* 2000. p. 277-302.

66. Erickson, H.P., *Gamma-tubulin nucleation: template or protofilament?* Nat Cell Biol, 2000. **2**(6): p. E93-6.

67. Zeeberg, B., Caplow, M., *Determination of free and bound microtubular protein and guanine nucleotide under equilibrium conditions.* Biochemistry, 1979. **18**: p. 3880-3886.

68. Murphy, S.M., L. Urbani, and T. Stearns, *The mammalian γ-tubulin complex contains homologues of the yeast spindle pole body components spc97p and spc98p.* J Cell Biol, 1998. **141**(3): p. 663-74.

69. Vassilev, A., et al., *Identification of intrinsic dimer and overexpressed monomeric forms of gamma-tubulin in Sf9 cells infected with baculovirus containing the Chlamydomonas gamma-tubulin sequence.* Journal of Cell Science, 1995. **108**: p. 1083-1092.

70. Gaskin, F. and C.R. Cantor, *Turbidimetric studies of the in vitro assembly and disassembly of porcine neurotubules.* J Mol Biol, 1974. **89**: p. 737-758.

71. Erickson, H.P. and E.T. O'Brien, *Microtubule Dynamic Instability and GTP Hydrolysis.* Annual Review of Biophysics and Biomolecular Structure, 1992. **21**: p. 145-166.

72. David-Pfeuty, T., H.P. Erickson, and D. Pantaloni, *Guanosine triphosphatase activity of tubulin associated with microtubule assembly.* PNAS, 1977. **74**: p. 5372-5376.

73. Bishop, A., et al., *Unnatural ligands for engineered proteins: new tools for chemical genetics.* Annual Review of Biophysics and Biomolecular Structure, 2000. **29**: p. 577-606.

74. Oakley, B.R., *γ-Tubulin*, in *The centrosome in cell replication and early development.*, R.E. Palazzo and G.P. Schatten, Editors. 2000, Academic Press: San Diego. p. 27-54.

75. Job, D., O. Valiron, and B. Oakley, *Microtubule nucleation.* Curr Opin Cell Biol, 2003. **15**(1): p. 111-7.

76. Moritz, M., L.M. Rice, and D. Agard, *Microtubule nucleation*, in *Centrosomes in Disease and Development*, E.A. Nigg, Editor. 2004, Wiley-VCH: Weinheim.

77. Schiebel, E., *γ-tubulin complexes: binding to the centrosome, regulation and microtubule nucleation.* Curr Opin Cell Biol, 2000. **12**(1): p. 113-8.

78. Wiese, C. and Y. Zheng, *γ-Tubulin complexes and their interaction with microtubule-organizing centers.* Curr Opin Struct Biol, 1999. **9**(2): p. 250-9.

79. Moritz, M. and D.A. Agard, *γ-Tubulin complexes and microtubule nucleation.* Curr Opin Struct Biol, 2001. **11**(2): p. 174-81.

80. Oosawa, F. and M. Kasai, *A theory of linear and helical aggregations of macromolecules.* J Mol Biol, 1962. **4**: p. 10-21.

81. Flyvbjerg, H. and E. Jobs, *Microtubule dynamics. II. Kinetics of self assembly.* Phys. Rev. E., 1997. **56**(6): p. 7083-7099.

82. Fygenson, D.K., et al., *Spontaneous nucleation of microtubules.* Phys. Rev. E., 1995. **51**: p. 5058-5063.

83. Sept, D., N.A. Baker, and J.A. McCammon, *The physical basis of microtubule structure and stability.* Protein Sci, 2003. **12**(10): p. 2257-61.

84. VanBuren, V., D.J. Odde, and L. Cassimeris, *Estimates of lateral and longitudinal bond energies within the microtubule lattice.* Proc Natl Acad Sci U S A, 2002. **99**(9): p. 6035-40.

85. Northrup, S.H. and H.P. Erickson, *Kinetics of protein-protein association explained by Brownian dynamics computer simulation.* Proc Natl Acad Sci U S A, 1992. **89**(8): p. 3338-42.

86. Koren, R. and G.G. Hammes, *A kinetic study of protein-protein interactions.* Biochemistry, 1976. **15**(5): p. 1165-71.

87. Chretien, D., S.D. Fuller, and E. Karsenti, *Structure of growing microtubule ends: two-dimensional sheets close into tubes at variable rates.* J Cell Biol, 1995. **129**(5): p. 1311-28.

88. Melki, R., et al., *Cold depolymerization of microtubules to double rings: geometric stabilization of assemblies.* Biochemistry, 1989. **28**: p. 9143-9152.

89. Nogales, E., H.W. Wang, and H. Niederstrasser, *Tubulin rings: which way do they curve?* Current Opinion in Structural Biology, 2003. **13**: p. 256-261.

90. Lin, C.M. and E. Hamel, *Interrelationships of Tubulin-GDP and Tubulin-GTP in Microtubule Assembly.* Biochemistry, 1987. **26**: p. 7173-7182.

91. Caplow, M., R.L. Ruhlen, and J. Shanks, *The Free Energy for Hydrolysis of a Microtubule-Bound Nucleotide Triphosphate Is Near Zero: All of the Free Energy for Hydrolysis Is Stored in the Microtubule Lattice.* Journal of Cell Biology, 1994. **127**: p. 779-788.

92. Diaz, J.F., M. Menendez, and J.M. Andreu, *Thermodynamics of Ligand-Induced Assembly of Tubulin.* Biochemistry, 1993. **32**: p. 10067-10077.

93. Keating, T.J., et al., *Microtubule release from the centrosome.* Proc Natl Acad Sci U S A, 1997. **94**(10): p. 5078-83.

94. Janosi, I.M., D. Chretien, and H. Flyvbjerg, *Modeling elastic properties of microtubule tips and walls.* Eur Biophys Journal, 1998. **27**: p. 501-513.

95. Vetter, I.R. and A. Wittinghofer, *The Guanine Nucleotide-Binding Switch in Three Dimensions.* Science, 2001. **294**: p. 1299-1304.

96. Oliva, M.A., S.C. Cordell, and J. Lowe, *Structural insights into FtsZ protofilament formation.* Nature Structural and Molecular Biology, 2004. **11**: p. 1243-1250.

97. Egea, P.F., et al., *Substrate twinning activates the signal recognition particle and its receptor.* Nature, 2004. **427**: p. 215-221.

98. Otwinowski, Z., Minor, W., *Processing of X-ray Diffraction Data Collected in Oscillation Mode*, in *Methods in Enzymology: Macromolecular Crystallography, part A*, C.W. Carter and R.M. Sweet, Editors. 1997, Academic Press: New York. p. 307-326.

99. Brunger, A.T., et al., *Crystallography & NMR system: A new software suite for macromolecular structure determination.* Acta Crystallogr D Biol Crystallogr., 1998. **54**: p. 905-921.

100. Jones, T.A., et al., *Improved methods for building protein models in electron density maps and the location of errors in these models.* Acta Crystallogr A., 1991. **47 (Part 2)**: p. 110-119.

101. Delano, W.L., *The PyMOL Molecular Graphics System.* 2002.

102. Lopez-Fanarraga, M., et al., *Postchaperonin tubulin folding cofactors and their role in microtubule dynamics.* Journal of Structural Biology, 2001. **135**: p. 219-229.

103. Dunn, A.Y., M.W. Melville, and J. Frydman, *Cellular substrates of the eukaryotic chaperonin TriC/CCT.* Journal of Structural Biology, 2001. **135**: p. 176-184.

104. Vogel, J., et al., *Phosphorylation of γ-tubulin regulates microtubule organization in budding yeast.* Dev Cell, 2001. **1**(5): p. 621-31.

(2) 3 2